

STUDIES ON ANCIENT DNA AND STABLE ISOTOPE PROFILING OF FOSSILS

Ph.D THESIS

by

SONAL JAIN



DEPARTMENT OF BIOTECHNOLOGY
INDIAN INSTITUTE OF TECHNOLOGY ROORKEE
ROORKEE - 247667, INDIA
MAY, 2016

STUDIES ON ANCIENT DNA AND STABLE ISOTOPE PROFILING OF FOSSILS

A THESIS

*Submitted in partial fulfilment of the
requirements for the award of the degree*

of

DOCTOR OF PHILOSOPHY

in

BIOTECHNOLOGY

by

SONAL JAIN



DEPARTMENT OF BIOTECHNOLOGY
INDIAN INSTITUTE OF TECHNOLOGY ROORKEE
ROORKEE – 247 667 (INDIA)
MAY, 2016

**©INDIAN INSTITUTE OF TECHNOLOGY ROORKEE, ROORKEE- 2016
ALL RIGHTS RESERVED**



INDIAN INSTITUTE OF TECHNOLOGY ROORKEE ROORKEE

CANDIDATE'S DECLARATION

I hereby certify that the work which is being presented in the thesis entitled “**STUDIES ON ANCIENT DNA AND STABLE ISOTOPE PROFILING OF FOSSILS**” in partial fulfillment of the requirements for the award of the Degree of Doctor of Philosophy and submitted in the Department of Biotechnology of the Indian Institute of Technology, Roorkee is an authentic record of my own work carried out during a period from December, 2010 to May, 2016 under the supervision of Dr. V. Pruthi, Professor, Department of Biotechnology and Dr. S. Bajpai, Director, Birbal Sahni Institute of Paleobotany, Lucknow.

The matter presented in this thesis has not been submitted by me for the award of any other degree of this or any other Institute.

(SONAL JAIN)

This is to certify that the above statement made by the candidate is correct to the best of our knowledge.

(V. Pruthi)
Supervisor

(S. Bajpai)
Supervisor

Date: _____

ABSTRACT

Ancient DNA (aDNA) analysis of extinct ratite species is of considerable interest as it provides important insights into their origin, evolution, palaeogeographical distribution and vicariant speciation in congruence with continental drift theory. Recent discoveries and methodological advancement in molecular biology, and in particular in sequencing techniques, have rendered successful analysis of ancient DNA (aDNA) from Pleistocene populations and fossil sediments. This genetic information from ancient specimens is invaluable to reconstruct the evolutionary path adopted by species.

In contrast to ancient DNA analyses from subfossil bones and teeth, as well as ancient sediments, recovery, and characterization of aDNA from fossil eggshell has been performed recently by Oskam et al. 2010. These eggshells are found frequently in archaeological deposits and are an important source for paleoecology, paleodietary, zooarchaeology and geochronological studies. Moreover, the physical and chemical properties of biomolecules in eggshells were well preserved. Early human settlements and various fossil deposits describe the presence of avian eggshells all over the world. During Pliocene and Pleistocene periods, ratites occupied wide areas of China, Southern Russia, India, Eastern and Southern Europe, Middle East as well as Africa. The present-day distribution of such ratites reveals the continental drift and they are considered to be of Gondwanan origin. Fossil avian eggshells have been found at more than 50 localities in India (Madhya Pradesh, Rajasthan, Maharashtra, and Gujarat). Besides eggshell pieces artifacts such as eggshell beads and bone fragments have also been reported from these sites, which were identified as *Struthio asiaticus* species.

Morphological and ultrastructure characterization of eggshells was done by Scanning Electron Microscopy (SEM), X-Ray Diffraction (XRD), Electron Back Scatter Diffraction (EBSD) as described in Chapter 2. SEM and XRD were conducted at IIC, IIT Roorkee, India, and EBSD was conducted at University of Alabama, USA. Data obtained from biominerals studies was of importance as they provide an understanding of natural evolutionary processes. SEM studies demonstrated the ultrastructure of fossil eggshells and formation of the calcified cuticular layer. The presence of calcified cuticle layer in the eggshell is the basis for ancient DNA studies as it contains preserved biomolecules. EBSD accentuates the crystallographic structure of the ostrich eggshells with sub-micrometer resolution. It is a non-destructive tool for

evaluating the extent of diagenesis in eggshell. EBSD analysis revealed the presence of dolomite in the eggshells. This research resulted in the complete recognition of the structure of ostrich eggshells as well as the nature and extent of diagenesis in these eggshells which is vital for genetic and paleoenvironmental studies. The primary aim of this research was to extract aDNA from ostrich eggshell and to successfully amplify and sequence it. The sequences obtained were then analyzed phylogenetically and were submitted in NCBI GenBank accession number KU251475 as mentioned in Chapter 3. aDNA extraction was carried out in a dedicated aDNA laboratory at CSIR-CCMB, Hyderabad. DNA hotspots were first observed using Confocal Laser Scanning Microscopy (CLSM). In this chapter, the designing and testing of primers for simplex and multiplex PCR was done that allow analysis of the minute amount of DNA and very short DNA fragments. Optimization of the DNA extraction procedure from eggshells through quantitative real-time PCR was done. Produced sequences were then analyzed in light of phylogeny, biogeography & molecular evolution of the corresponding species.

In chapter 4, Stable isotopic profiles of eggshells have established that help in the study of paleobiology and paleodietary. Carbon and oxygen stable isotope were analyzed for the diets and habitat of the ostriches. Carbonate eggshells were analyzed using acid digestion method. Released carbon dioxide was passed through Gas Chromatography and then analyzed by IMRS (Isotope Mass Ratio spectrometer). Carbon isotope revealed the diets of the ostrich to be a mixture of C₃ and C₄ plants with biases toward C₃ shedding the light on the paleoecology and paleodietary. Oxygen isotopes indicate the aridity and less humid conditions. In the next chapter, triple oxygen isotopes techniques have been detailed. Isotope analysis was conducted at stable isotope lab of Johns Hopkins University. Body water model for the animal has been developed to study the palaeoenvironment aspects. Eggshells possess the biochemical signature of the ostrich. The sample was digested with acid digestion and carbon dioxide was converted into water and then into oxygen to calculate the 17 mass isotope of oxygen. This isotope is in very low abundance and thus its calculation with maximum precision and minimum error is a tough task. State of art mass spectrometry was used to analyze this isotope. D¹⁷O values of samples lie below the maximum evaporation model suggesting that relative humidity and water economy index to low. It indicates that ostriches are from arid climates and consumed lots of evaporated leaf waters. The research revealed how these samples can provide insights into the biology, ecology and extinction of this species. Last chapter summarizes the main findings and the importance of the results and also leads path for future directions.

Highlights of research:

- ❖ Dolomitization in fossil eggshells from Upper Paleolithic sites revealed by EBSD.
- ❖ Calcite crystallization and microstructure of fossilized eggshell layers observed.
- ❖ Determination of nature and extent of diagenesis in fossils eggshells.
- ❖ Optimization of extraction protocol from ancient eggshells to maximize the recovery of ancient DNA; quantification of the extracted DNA using quantitative real-time PCR.
- ❖ Production of ancient DNA sequences using a targeted multiplex PCR approach followed by high throughput sequencing.
- ❖ Phylogenetic analysis of the obtained sequences submitted to NCBI GenBank (Access. No. KU251475).
- ❖ DNA-based species identification confirmed the first genetic evidence for presence of ostriches in India
- ❖ Stable isotope and clumped isotope analysis were done to study the paleodietary, habitat and body temperature
- ❖ Triple oxygen isotope studies were conducted to reconstruct paleoenvironment.

ACKNOWLEDGEMENT

First and foremost I would like to thank God. You have given me the power to believe in myself and pursue my dreams. I could never have done this without the faith I have in you, the Almighty.

I would like to express my sincere gratitude to my supervisors, Dr. Vikas Pruthi, and Dr. Sunil Bajpai, for their encouragement, guidance, support and positive feedback throughout the course of my Ph.D. I deeply appreciate their down to earth nature and humbleness. While working in my own way, I have been given freedom to work and explore. It helped me learn to a great extent, nurture myself as an independent researcher, and face the challenges of future. I would also like to thank our Head of department Dr. Partha Roy, all faculty members, and my SRC committee.

It's an honor to me to thank Dr. Thangaraj, CCMB Scientist, Dr. Parul Pruthi and Dr. Niraj Rai for their continuous guidance, encouragement, and kind support as well as their help in critically analyzing the data. Their unceasing enthusiasm has always inspired me in going ahead. I am equally grateful to Dr. Ch. Mohan Rao, Director, CCMB for providing unparalleled facilities in the CCMB for carrying out the research.

I would like to thank Dr. Benjamin Passey, Dr. Naomi Levin from Johns Hopkins University and Dr. Alberto Perez-Huerta, the University of Alabama for providing me world-class facility to work in their laboratory and special thanks to my USA labmates Haoyuan Ji, Shunning, Laiming, Huanting, Dana, Sophie, and Nikki. I enjoyed the provoking discussions and their help and support during my stay at Johns Hopkins University, USA.

This work could not have been possible without our collaborators, Dr. Giriraj Kumar, and Mr. O.P. Sharma. I extend my sincere gratitude to them for providing samples.

During my stay at Roorkee, I have been blessed with a cheerful group of people Akki, Pal, Saja and Anna. Their company always helped me to vent out all the worries and enjoy the life. A heartfelt thanks to all of them. Special thanks to my lifelong friends; Gunjan, Kittu, Aafrin, Nanu and Vinod for their help and support during these years. Friendly moments spent with all of them would always remain as memories forever. I will always cherish my Fulbright

experience and would like to thank my friends in the USA who were like family: Rajita, Saumya, Neha, Aditya, Princy, Anand, Ambhi and Akanksha.

I acknowledge the support and encouragement of my seniors, colleagues, and labmates; Nivi maam, Vivekanand sir, Abhishek sir, Suma, Priya, Richa, Harmeet ji, Navdeep ji, Alok, Sonam, Neha, Padma and Navneet. I express my heartfelt thanks to all of them, as some part of this work would not have been possible without their help. I would also like to thank my batch mates and all the staff members of the biotech department for their help and support at various stages of my stay.

I would like to thank Dr. S.S. Jain for his continuous help and in all sorts of lives during my stay in Roorkee.

Further, I gratefully acknowledge the financial supports from UGC, CSIR, and USIEF.

Finally, it's the incessant love, encouragement and blessings of my parents, my husband Abhishek, my in-laws, sisters, brothers and all family members that always empowered me to stand and proceed.

Sonal Jain
Ph. D. (Biotechnology)

PUBLICATIONS / AWARDS

PUBLICATIONS

1. **Jain S., Bajpai, S., Kumar, G., & Pruthi, V. (2016). Microstructure, crystallography and diagenetic alteration in fossil ostrich eggshells from Upper Palaeolithic sites of Indian peninsular region. *Micron*, 84, 72-78.**
2. **Jain S., Rai N., Kumar G., Pruthi P.A., Thangaraj K., Bajpai S., Pruthi V. “Ancient DNA sequences from the Late Pleistocene endorse biogeographical movement of ostriches”. *Nature Scientific Reports*, under review.**
3. **Jain S., Rai N., Kumar G., Pruthi P.A., Thangaraj K., Bajpai S., Pruthi V. “Analysis of Ancient DNA- Microscopic and Molecular techniques”** communicated and presented at International Conference New Frontiers in Industrial and Applied Biotechnology, GenPro 2015, Invertis University, Bareilly, Uttar Pradesh, India, 18th- 19th Sept 2015.
4. **Jain S., Rai N., Bajpai S., Thangaraj K., Pruthi V. "Recent trends in biotechnology-Studies on Ancient DNA from Indian fossil remains"** communicated and presented at International conference SGRRITS-2014, Dehradun, India, 14th -15th Feb, 2014.
5. **Jain S., Rai N., Bajpai S., Thangaraj K., Pruthi V “Role of Next Generation Sequencing in studying aDNA of fossil remains in India”,** Poster Presentation at NGBT Scigenome Conference IGIB, NewDelhi, 16th-18thNov, 2013.

AWARDS

1. Fulbright Nehru Doctoral Fellowship 2014-2015
2. Young Scientist Award at GenoPro 2015
3. Patel Grant 2015

CONTENTS

ABSTRACT.....	i
ACKNOWLEDGEMENT	v
PUBLICATIONS / AWARDS	vii
CONTENTS.....	ix
LIST OF FIGURES	xv
LIST OF TABLES.....	xxi
CHAPTER 1	1
LITERATURE REVIEW	1
1.1 Avian Eggshell.....	1
1.1.1 Structure and morphology of avian eggshell	1
1.1.2 Characterization of avian eggshell.....	2
1.1.2.1 Scanning electron microscopy	2
1.1.2.2 X-ray diffraction (XRD)	3
1.1.2.3 Electron back scatter diffraction (EBSD)	3
1.1.2.4 Confocal laser scanning microscopy (CLSM).....	4
1.2 The Indian Ostrich	5
1.2.1 Taxonomical classification of ostrich	5
1.2.2 Habitat.....	6
1.2.3 Archaeological and geological perspective.....	6
1.2.4 Dating of eggshells.....	9
1.2.5 Engraved eggshells and eggshell beads	9
1.2.6 Paleoenvironment and ultrastructure studies	10
1.2.7 Ostrich rock art.....	11
1.2.8 Human expansion and ostrich extinction	11
1.3 Ancient DNA	11

1.3.1	Ancient DNA	11
1.3.2	History of aDNA studies.....	12
1.3.3	Hurdles and errors in aDNA analysis	12
1.3.3.1	aDNA extraction	12
1.3.3.2	Post-mortem DNA decay.....	13
1.3.3.3	Authentication of aDNA results.....	15
1.3.4	Use of aDNA in evolutionary studies	15
1.3.5	Genetic markers and their use in modern and aDNA studies	16
1.3.6	DNA polymorphisms.....	16
1.3.6.1	Mitochondrial DNA (mtDNA) polymorphisms.....	16
1.3.7	Short tandem repeats (STRs)	18
1.4	Stable Isotope Studies.....	18
1.4.1	Biochemical signatures from avian eggshells.....	18
1.4.2	Stable isotopes in the field of palaeontology and archaeology.....	18
1.4.2.1	$\delta_{13}\text{C}$ and $\delta_{18}\text{O}$ Isotopes.....	19
1.4.2.2	Palaeodiets, palaeoecology and extinction processes	21
1.4.3	Triple oxygen isotope body water model and compositions of biogenic carbonates	21
1.4.3.1	Background.....	21
1.4.3.2	Body water model.....	22
CHAPTER 2		29
ULTRASTRUCTURE AND CRYSTALLOGRAPHIC STUDIES ON FOSSIL EGGSHELLS		
.....		29
2.1	Introduction.....	29
2.2	Sample Details	31
2.2.1	Materials	31
2.2.2	Methods.....	31

2.2.2.1	Scanning electron microscopy (SEM)	31
2.2.2.2	X-ray diffraction (XRD)	32
2.2.2.3	Electron backscatter diffraction (EBSD)	32
2.3	Result and Discussion	32
2.3.1	SEM data	32
2.4	Concluding Remarks	42
	CHAPTER 3	43
	CONFOCAL MICROSCOPY AND ANCIENT DNA ANALYSIS ON EGGSHELLS	43
3.1	Introduction	43
3.2	Materials	47
3.2.1	Common chemicals/plastic wares	47
3.2.2	Reagents and kits	47
3.2.3	Solutions, buffer, and media	48
3.2.4	Samples	48
3.3	Methodology	50
3.3.1	Confocal laser scanning microscopy studies	50
3.3.2	Ancient DNA analysis	50
3.3.2.1	Ancient DNA lab set-up and precautions	50
3.3.2.2	Ancient DNA extraction	50
3.3.2.3	Ancient DNA quantification using real-time PCR	51
3.3.2.4	Ancient DNA quantification using Bioanalyzer	51
3.3.2.5	Ancient DNA primer designing	51
3.3.2.6	Polymerase chain reaction (PCR)	52
3.3.2.7	DNA sequencing	53
3.3.2.8	Multiplex PCR and genotyping using sequenom	53
3.3.2.9	Cloning of PCR products in pMOS blunt end-cloning vector	54
3.3.3	Statistical analysis	55

3.3.3.1	Gene Tool 2.0.....	55
3.3.3.2	Primer 3.....	55
3.3.3.3	Amplify 3X.....	55
3.3.3.4	NCBI Primer BLAST.....	55
3.3.3.5	AutoAssembler™.....	55
3.3.3.6	Codon Code Aligner.....	56
3.3.3.7	Clustal W and X.....	56
3.4	Results.....	56
3.4.1	CLSM studies of eggshells.....	58
3.4.2	DNA extraction and species determination.....	60
3.4.3	Phylogenetic analysis.....	62
3.5	Discussion.....	64
CHAPTER 4.....		67
BIOCHEMICAL SIGNATURE OF FOSSIL EGGSHELL USING CARBONATE CLUMPED ISOTOPE ANALYSIS.....		67
4.1	Background.....	67
4.1.1	Stable isotope analysis.....	67
4.1.1.1	Carbon isotopes.....	67
4.1.1.2	Oxygen isotopes.....	67
4.1.2	Measuring stable isotopes.....	68
4.1.3	Isotope fractionation.....	70
4.1.4	Carbonate clumped isotope thermometry.....	73
4.2	Sample Details.....	73
4.3	Experimental.....	76
4.3.1	Measurements of stable isotopes.....	76
4.3.2	Data analysis and reduction.....	77
4.4	Results and Discussion.....	78

4.5	Conclusion	82
	CHAPTER 5	83
	TRIPLE OXYGEN ISOTOPE STUDIES IN BIOGENIC CARBONATES AND ITS APPLICATION IN ANIMAL PHYSIOLOGY	83
5.1	Background	83
5.1.1	Triple Oxygen Isotope Analysis	83
5.2	Sample Details	85
5.3	Experimental	87
5.3.1	Extraction of CO ₂ from carbonate	88
5.3.2	Reduction of CO ₂ to produce H ₂ O	89
5.3.3	Fluorination of water to produce oxygen	92
5.3.4	Isotopic analysis of oxygen and carbon dioxide	92
5.4	Results and Discussion	93
5.5	Concluding Remarks	98
	CHAPTER 6	101
	GENERAL DISCUSSION AND FUTURE DIRECTIONS	101
6.1	General Discussion	101
6.2	Future Directions	103
	BIBLIOGRAPHY	105

LIST OF FIGURES

Figure 1.1 Image of an ostrich eggshell radial cross-section. Schematic representation showing the cuticle layer, the palisade layer, and the mammillary layer of the eggshell (Jain et al., 2016)	1
Figure 1.2 Diagram depicting functional working of Scanning Electron Microscopy (Humphry et al., 2012).....	2
Figure 1.3 Schematics of X-Ray Diffractometer (Modified from Cullity, 1956).....	3
Figure 1.4 Schematics of EBSD diagram (Rollett, 2009).....	4
Figure 1.5 Schematic representation of confocal laser scanning microscopy (Rossetti et al., 2013)	4
Figure 1.6 Image of Ostrich and Ostrich complete egg.	5
Figure 1.7 Continental drifting and vicariant speciation of ratites. The breakup of supercontinent Gondwanaland during Early Cretaceous endorsing biogeographical movement of ratites.....	8
Figure 1.8 Engraved ostrich eggshell from Patne (Bednarik, 1993).....	9
Figure 1.9 Perforated eggshell beads from Bhimbetka, M.P (Bednarik, 1994).....	10
Figure 1.10 Rock shelter paintings from Bhopal (Badam, 2005)	11
Figure 1.11 Principle site of damage of one strand of the double helix (adopted from Hofreiter et al., 2001).....	13
Figure 1.12 Schematic presentation of deamination pattern of cytosine to thymine conversion (adopted from Llamas et al., 2012).....	14
Figure 1.13 Image depicting heavy and lighter isotope of oxygen.	19
Figure 1.14 ¹⁷ O-enabled body water model for animals based on ¹⁸ O model of Kohn (1996). The oxygen isotope output and input fluxes are in mass balance relationship. Inputs can be expressed in terms of fractionated meteoric water plus the term of atmospheric O ₂ . Outputs can be expressed in terms of fractionated body water. Fractionation factors (α) and fraction (f) are in light of previous work (Kohn, 1996; Barkan and Luz, 2005; Hofmann et al., 2012). Leaf water models are based on the ¹⁸ O/ ¹⁶ O model of Roden and Ehleringer (1999). Relative humidity and the oxygen isotope fractionation exponent λ relationship is given by Landais et al., 2006.....	23
Figure 1.15 “Minimum Evaporation” and “Max Evaporation” model (dashed lines) predicted by the ¹⁷ O-enabled body water model. Actual measurements of body water isotopes (from	

analysis of eggshells) for modern birds are shown in black circles. The minimum evaporation model limit is for animals with high WEI, from humid climates, and consuming little evaporated leaf waters. The maximum evaporation model limit is for animals with low WEI, from arid climates, and consuming lots of evaporated leaf waters. These limits bracket possible body water compositions for modern birds and the measured body water data show consistent observations with the model. 26

Figure 2.1 Anatomy of avian egg. Inset image showing inner shell membrane, outer shell membrane, cuticle and shell (Horst Frank, 2007). 30

Figure 2.2 SEM morphology of the cross-sectional plane of ostrich eggshell. A) Organic membrane B) Cone layer C) Palisade layer D) Cuticle layer 33

Figure 2.3 Internal surface of eggshell shows mammillary knobs. Image captured at A) 20 μm B) 10μm 34

Figure 2.4 Palisade layer of eggshell. Irregular appearance of the crystallized layer 35

Figure 2.5 Pores on the exterior surface of eggshell. Pores are observed on the exterior surface at 20 μm. 36

Figure 2.6 Outer shell membrane of eggshell. Cup-shaped structure observed at 10μm. 37

Figure 2.7 XRD patterns of the powdered eggshell samples from three different locations. (A) Bundi, India (B) Chandresal, India (C) Modern eggshell from Africa. 38

Figure 2.8 High-resolution EBSD data in modern ostrich eggshell, Africa. A) Diffraction intensity map at the top of the shell showing calcite prisms at 500 μm B) Corresponding color crystallographic map to (A) at 500 μm C) Corresponding pole figure to (B) in reference to {0001} D) Color-key for crystallographic planes in calcite. 40

Figure 2.9 High-resolution EBSD data in fossil eggshell from Bundi, India. A) Diffraction intensity map at the top of the shell showing calcite prisms at 300 μm B) Corresponding color crystallographic map to (A) at 300 μm C) Corresponding pole figure to (B) in reference to {0001} D) Crystallographic color coded map showing distribution of calcite and dolomite Red color denotes calcite and green color denotes dolomite. 41

Figure 2.10 High-resolution EBSD data in fossil eggshell from Chandresal, India A) Diffraction intensity map at the top of the shell showing calcite prisms at 400 μm B) Corresponding color crystallographic map to (A) at 400 μm C) Corresponding pole figure to (B) in reference to {0001}. D) Crystallographic color-coded map showing the distribution of calcite, dolomite, and aragonite. Red color denotes calcite, yellow color denotes dolomite and green color denotes aragonite. 42

Figure 3.1 Ostrich Eggshell. Pictorial view showing layers and membranes of eggshell (Hincke, 2012)	45
Figure 3.2 Ostrich eggshell sample collection locations from Indian subcontinent as shown on the map. (A) Bundi (B) Anjar (C) Chandresal-1 (D) Nagda (E) Runija (F) Khajurna (G) Ravishankarnagar (Source- cia.gov).....	46
Figure 3.3 Size selection and quantification of an ancient DNA sample extracted from eggshell	52
Figure 3.4 Confocal images showing radial outer surface of ratite eggshell (A) Stained with Hoechst 33342, displaying the DNA distributed throughout the matrix. The arrow indicates the presence of hotspots in fossilized eggshells. (B) Control sample, without fluorescence. Scale Bar- 500µm [Inset- Picture of eggshell. Marked area was observed under CLSM].....	57
Figure 3.5 Cross-section image of <i>Struthio</i> eggshell. Fluorescently labelled DNA can be observed on the periphery of mammillary cones. Scale Bar 50 µm [Inset- Picture of eggshell. Marked area was observed under CLSM].....	58
Figure 3.6 3-D imaging of inner layers of eggshell: DNA distributed throughout the matrix as observed through fluorescent hotspots. A) Horizontal view B) Vertical view [Inset- Picture of eggshell. Marked area was observed under CLSM]	59
Figure 3.7 Bioanalyzer image showing bands of fossilized DNA. The concentration of DNA in pg/ml is mentioned as calculated by bioanalyzer.....	60
Figure 3.8 Alignment of partial 16srRNA gene sequences of samples and ratites and evolutionary relationships of taxa. (A) and (B) Alignment of ratites sequences and sample GK/RN/011 and GK/RU/009. Dots signify identity to the <i>Struthio camelus</i> sequence. (C) The evolutionary history was deduced using the Neighbor-Joining method. The bootstrap consensus tree concluded from 1000 replicates is taken to denote the evolutionary history of the taxa analyzed. The evolutionary distances were calculated using the Maximum Composite Likelihood method and are in the units of the number of base substitutions per site. The analysis involved 7 nucleotide sequences. Codon positions included were 1st+2nd+3rd+Noncoding. All positions containing gaps and missing data were eliminated. There was a total of 87 positions in the final dataset. Evolutionary analyses were conducted in MEGA6.....	63
Figure 3.9 Estimates of evolutionary divergence between sequences. The number of base substitutions per site among sequences is presented. Maximum Composite Likelihood model was used for analysis. The analysis comprised of 7 nucleotide sequences. Codon positions used	

were 1st+2nd+3rd+Noncoding. All positions containing gaps and missing data were removed. There was a total of 87 positions in the final dataset. Evolutionary analyses were conducted in MEGA6..... 63

Figure 4.1 Heavier and lighter isotope of oxygen. Lighter isotope evaporates faster and heavier isotope evaporates easily (Kurt Hollocher, 2002)..... 69

Figure 4.2 Biological system will have a preference for a certain isotope based on bond ordering. Photosynthesis fixes more ¹²C while calcareous sediments prefer ¹³C..... 69

Figure 4.3 Isotope fractionation. Depending upon the process reaction product might be heavy or light..... 70

Figure 4.4 Carbonate clumped isotope thermometry is grounded on the principle of exchange reactions between carbonates ions. This image shows the atomic structure of calcite lattice (Eiler, 2011)..... 74

Figure 4.5 Autoline for clumped isotope analysis (Johns Hopkins University)..... 77

Figure 4.6 Stable oxygen and carbon isotope results of ostrich eggshells collected from Upper Paleolithic sites compared with Blinkhorn et al., 2015 illustrating the relationship between stable isotope values. 78

Figure 4.7 The relationship between calculated Δ_{47} values from ostrich eggshells and body temperature of ostriches. The X-axis shows the predicted body temperature of ostriches and Y-axis depicts the mean Δ_{47} values obtained from the extractions of carbon dioxide from eggshells 82

Figure 5.1 Autoline for triple oxygen isotope analysis at Johns Hopkins University 87

Figure 5.2 An overall analytical procedure used in this study (Passey et al. 2014) 88

Figure 5.3 Diagram of the system used to transform oxygen into carbon dioxide to oxygen in the water and to introduce carbon dioxide samples into the circulating loop. (v- valve, vac-vacuum; Passey et al, 2014)..... 90

Figure 5.4 Reaction progress in the circulating loop of reduction line. (A) Before the introduction of each sample decrease in pressure during the ‘pre-reduction’ step performed. (B) The decrease in pressure following the introduction of sample carbon dioxide (Passey et al., 2014)..... 91

Figure 5.5 ¹⁷O-enabled body water model for animals based on ¹⁸O model of Kohn, 1996. The oxygen isotope output and input fluxes are in mass balance relationship. Inputs can be expressed in terms of fractionated meteoric water plus the term of atmospheric O₂. Outputs can be expressed in terms of fractionated body water. Fractionation factors (α) and fraction (f) are

in light of previous work (Kohn, 1996; Barkan and Luz, 2005; Hofmann et al., 2012). Leaf water models are based on the $^{18}\text{O}/^{16}\text{O}$ model of Roden and Ehleringer (1999). The relationship between relative humidity and the oxygen isotope fractionation exponent λ is given by Landais et al., 2006.....93

Figure 5.6 “Minimum Evaporation” and “Max Evaporation” model (dashed lines) predicted by the ^{17}O -enabled body water model. Actual measurements of body water isotopes from analysis of eggshells are shown in black circles.....98

LIST OF TABLES

Table 1.1 Classification of <i>Struthio</i> genus	5
Table 1.2 Summary of eggshells collected by various archaeologists from different sites of India (Sahni et al., 1989, 1990; Badam et al., 2005).....	7
Table 1.3 Summary of commonly used stable isotopes. Modified from Fry, 2006 and Newsome, 2007.....	20
Table 2.1 Sample collection sites of fossil eggshells and their respective states.....	31
Table 3.1 Ostrich eggshell sample collection sites and their respective states	49
Table 3.2 Primer sequences used for PCR and sequencing of 16s and control regions of mitochondrial DNA.....	52
Table 3.3 List of eggshell specimens from India, with associated genes and predicted taxon...	61
Table 4.1 Fossil eggshell sample collection sites, their respective states and taxa.....	75
Table 4.2 Result of stable isotope studies from fossil ostrich eggshells collected from Upper Paleolithic sites of India (n= no. of times sample was run)	79
Table 4.3 Δ_{47} measurements from fossil ostrich eggshells	81
Table 5.1 Ostrich eggshell sample collection sites and their respective states	86
Table 5.2 Measured isotopic compositions of eggshells from India (carbonates) and calculated isotopic compositions of parent waters of the eggshells (carbonates). Values are given in units of per mil relative to the VSMOW-SLAP scale of Schoenemann et al. (2013), with $\lambda = 0.52897$	

CHAPTER 1

LITERATURE REVIEW

1.1 Avian Eggshell

1.1.1 Structure and morphology of avian eggshell

The avian eggshell has a characteristic structure consisting of several layers (mammillary layer, palisade layer, and cuticle layer) from the inner surface to outer surface (Fig 1.1). The matrix of the avian eggshell is porous, ordered and heterogeneous complex, which is coupled with extracellular structure, composed of mineralized and non-mineralized regions having calcium carbonate (calcite 97%) and 3.5% organic matrix (Carrino et al., 1996; Hincke et al., 2000; Feng et al., 2001). The intracrystalline organic matrix of avian eggshells restrains diffusion losses and prevents the isotopic exchange of its organic constituents (Miller et al., 1992; Johnson et al., 1997; Oskam et al., 2010). This structural hallmark provides an external skeletal support to the developing avian embryo and controls gases, water exchanges as well as guards it from microbial interventions and physical stresses (Nys et al., 2004; Wellman-Labadie et al., 2008a; 2008b; Oskam et al., 2010). This well-defined eggshell ultrastructure and microparticles of CaCO_3 imparts stability and excellent mechanical strength to the eggshell. This, in turn, provides antibacterial and antifouling properties to the avian eggshell and results in biomolecule preservation (Fink et al., 2006; Nys et al., 2004).

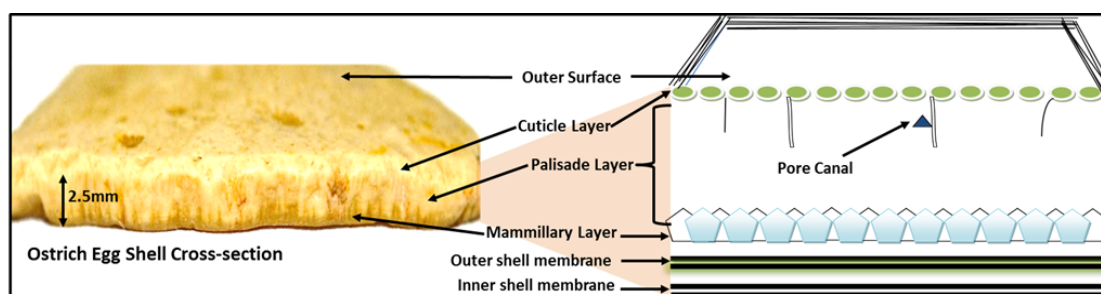


Figure 1.1 Image of an ostrich eggshell radial cross-section. Schematic representation showing the cuticle layer, the palisade layer, and the mammillary layer of the eggshell (Jain et al., 2016)

1.1.2 Characterization of avian eggshell

1.1.2.1 Scanning electron microscopy

Biomaterials studies are of importance as they provide an understanding of natural evolutionary processes. In this study, we have investigated the fossil ostrich eggshells using Scanning Electron Microscopy (SEM), X-Ray Diffraction (XRD) and Electron Backscatter Diffraction (EBSD). SEM studies demonstrated the ultrastructure of fossil eggshells and formation of the calcified cuticular layer. Schematic representation of SEM is depicted in Fig 1.2. The presence of calcified cuticle layer in the eggshell is the basis for ancient DNA studies as it contains preserved biomolecules.

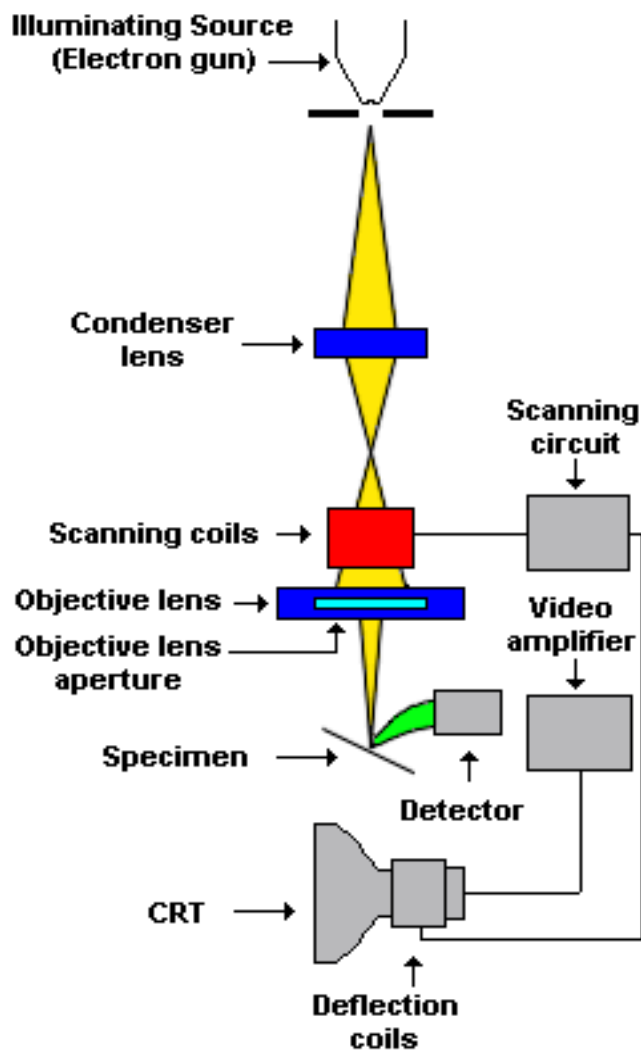


Figure 1.2 Diagram depicting functional working of Scanning Electron Microscopy (Humphry et al., 2012)

1.1.2.2 X-ray diffraction (XRD)

XRD is a technique to study the composition of the eggshell. Samples were broken into small pieces and also used in powdered form. Eggshells were composed mainly of calcium carbonate and composition was analyzed both qualitatively and quantitatively. XRD has certain limitations, which were overcome by EBSD. The working of a standard X-Ray Diffractometer is depicted in Fig 1.3.

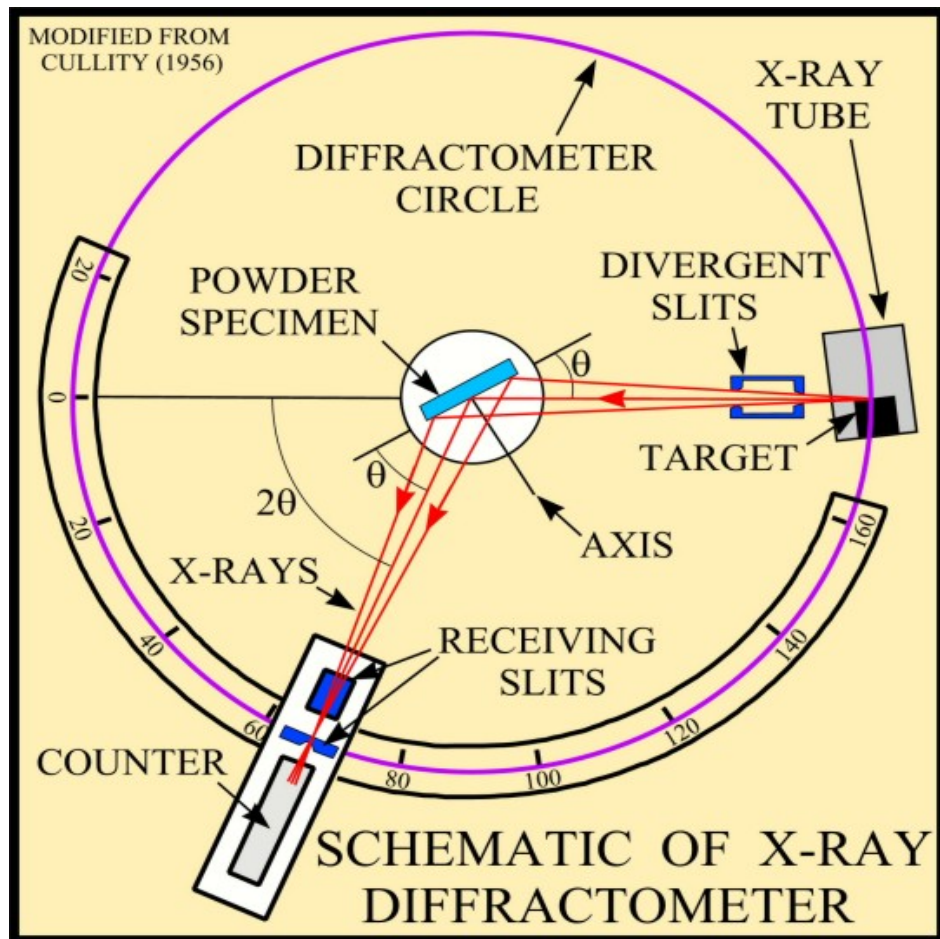


Figure 1.3 Schematics of X-Ray Diffractometer (Modified from Cullity, 1956)

1.1.2.3 Electron back scatter diffraction (EBSD)

EBSD accentuates the crystallographic structure of the ostrich eggshells with sub-micrometer resolution. It is a non-destructive tool for evaluating the extent of diagenesis in a biomineral (Fig 1.4). EBSD analysis revealed the presence of dolomite in the eggshells. This research resulted in the complete recognition of the structure of ostrich eggshells as well as the nature and extent of diagenesis in these eggshells which is vital for genetic and paleoenvironmental studies.

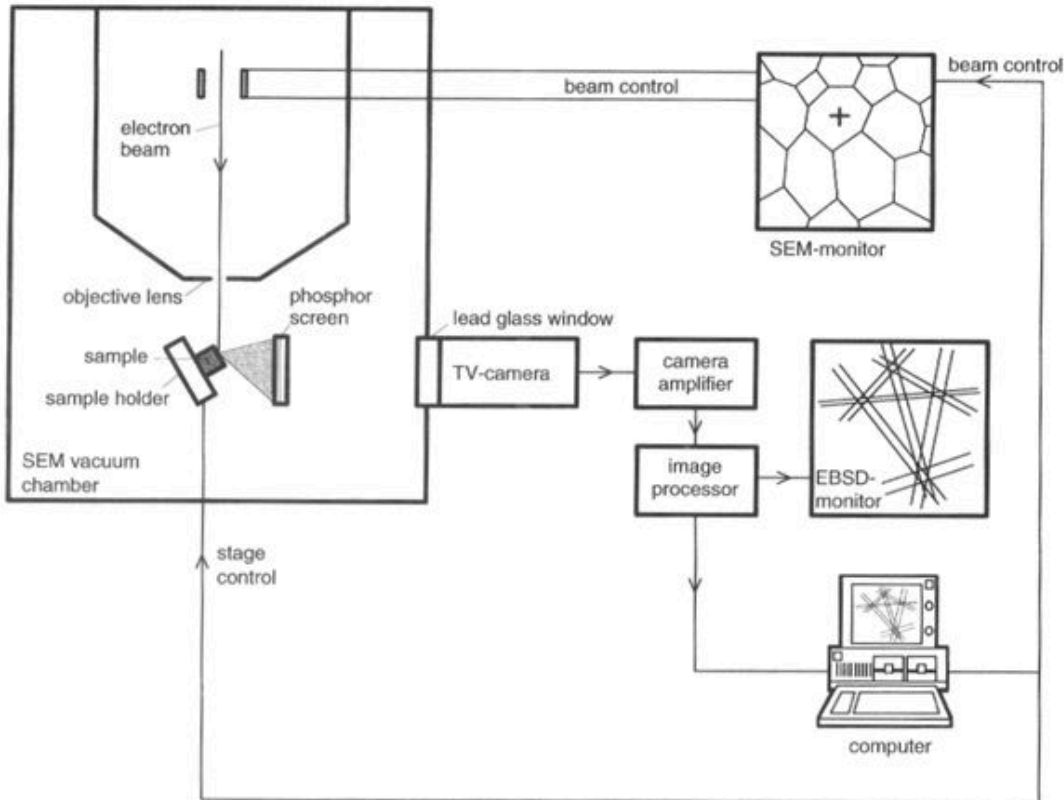


Figure 1.4 Schematics of EBSD diagram (Rollett, 2009)

1.1.2.4 Confocal laser scanning microscopy (CLSM)

Confocal laser scanning microscopy is a method to obtain high-resolution optical images with depth selectivity. Eggshell samples are stained with dye to obtain fluorescent images via optical sectioning.

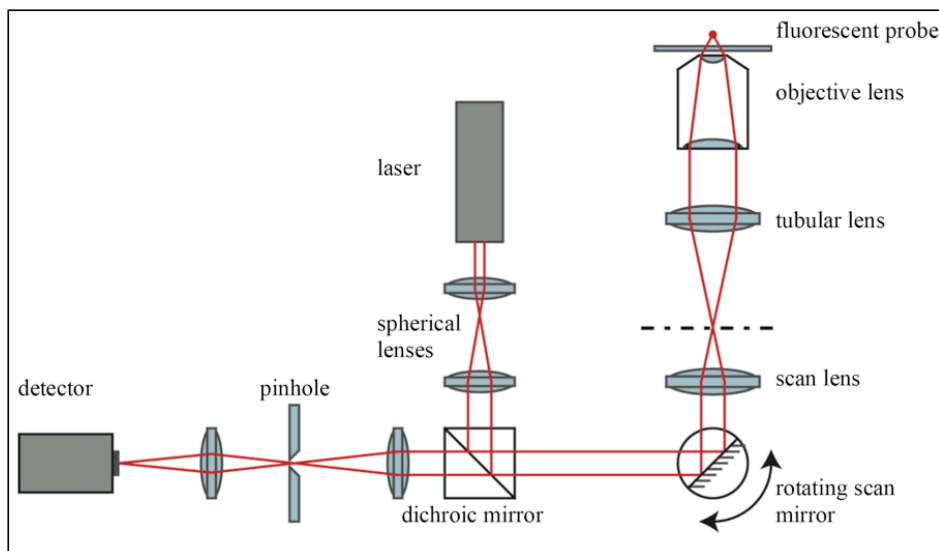


Figure 1.5 Schematic representation of confocal laser scanning microscopy (Rossetti et al., 2013)

DNA hotspots were observed in the layer of eggshell and it helped in the maximum DNA recovery from the eggshells (Oskam et al; 2010). Diagrammatic representation of confocal laser scanning microscopy is presented in Fig 1.5.

1.2 The Indian Ostrich

1.2.1 Taxonomical classification of ostrich

Ostriches belong to order Struthioniformes along with other flightless birds emus, rheas, kiwis, and tinamous. The taxonomical classification of the ostrich is shown in Table 1.1.

Table 1.1 Classification of Struthio genus

Class	Aves
Order	Struthioniformes
Family	Struthionidae
Genus	Struthio
Species	<i>S. asiaticus</i>

Struthio is a Greek word, which means ‘camel sparrow’ because it has a long neck (Harper, 2001). It is the largest living bird. Ostrich has a height of 3m and weighs around 150 kg. They usually live in a group of 5 or 6 and runs at a speed of 50-70 km/hr (Badam, 2005).



Figure 1.6 Image of Ostrich and Ostrich complete egg.

Ostrich eggs weigh around 1.5 kg and are spherical in shape (Fig 1.6). Eggshell fragments are around 2-2.5 mm and are yellowish white in color.

1.2.2 Habitat

Ostriches were widely dispersed in western parts of India during Late Pleistocene and were adapted to arid climate (Mishra, 2001). They preferred short grasses with semi-arid regions, open plains, and also desert with annual grasses. Ostriches resided in areas that were deprived of water but when water is accessible to them they consumed it often (Cooper et al., 2009).

1.2.3 Archaeological and geological perspective

The presence of ratites in India is evidenced by the eggshell fossils found in various parts, ranging in age from the Middle Miocene to Late Pleistocene as shown in Table 1.2 (Roberts et al., 2014; Blinkhorn et al., 2015).

The presence of these eggshell fossils in India and other South Asian countries raises the question of the evolution of these ratites all over the world. Richard Dawkins describe the evolution of ratites in his book “The Ancestor’s Tale”. One hundred and seventy million years ago ratite birds roamed over the whole Gondwanaland. As the sudden drifting of continents begins around 100 million years ago, rheas, emu, elephant bird, and ostriches got separated. Rhea and Emu moved to South America and Australia respectively while Elephant bird and ostriches were together in India and Madagascar. 60 million years ago India drifted towards north and Madagascar broke apart separating the two lineages. Cooper et al. suggested that ostriches arrived in Africa via the land route of Arabia through India about 20 million years ago and are still present in Africa (Fig 1.7). This theory is supported by the presence of ostrich fossils on this route (Cooper et al., 2001; Dawkins, 2004).

Table 1.2 Summary of eggshells collected by various archaeologists from different sites of India (Sahni et al., 1989, 1990; Badam et al., 2005)

DISCOVERY IN CHRONOLOGICAL ORDER	SITE	SIGNIFICANCE	REMARKS
1847; Falconer	Unspecified Siwalik Localities	1 st Ostrich fossils	Identified as <i>Struthio palaeindicus</i> and then changed to <i>Struthio asiaticus</i>
1880; Archibald Carleyle	Ken river, UP	1 st Eggshell reported	
1884, 1886; Lydekkar	Middle Siwaliks of Northwest India Dhok Pathan Stage	Phalanges, Tibia and Fibula	<i>Struthio asiaticus</i> by Milne-Edwards
1935; Aiegner	Dhok Pathan Stage of Hasnot in Pakistan.	Eggshells	Preserved in AMNH; Sauer in 1972 identified them as <i>Aepyornis</i> .
1976; Wakankar	Bhimbetka, District Raisin, Madhya Pradesh	Eggshell beads	Bead necklace found around the neck of human skeleton
1980; Sali	Patne, District Jalgaon, Maharashtra	Eggshells	
1988; Sunil Bajpai and S. Srinivasan	Chandresal, Kota, Rajasthan	Eggshells	
1988; Kumar et al	Paleolithic sites in Peninsula	Ostrich eggshells with engravings	
1989; Mohabey	District Kachchh	Eggshells	Dated 25-40,000 years old
Bundi, District Kota, Rajasthan	Bundi, District Kota, Rajasthan	Eggshells	

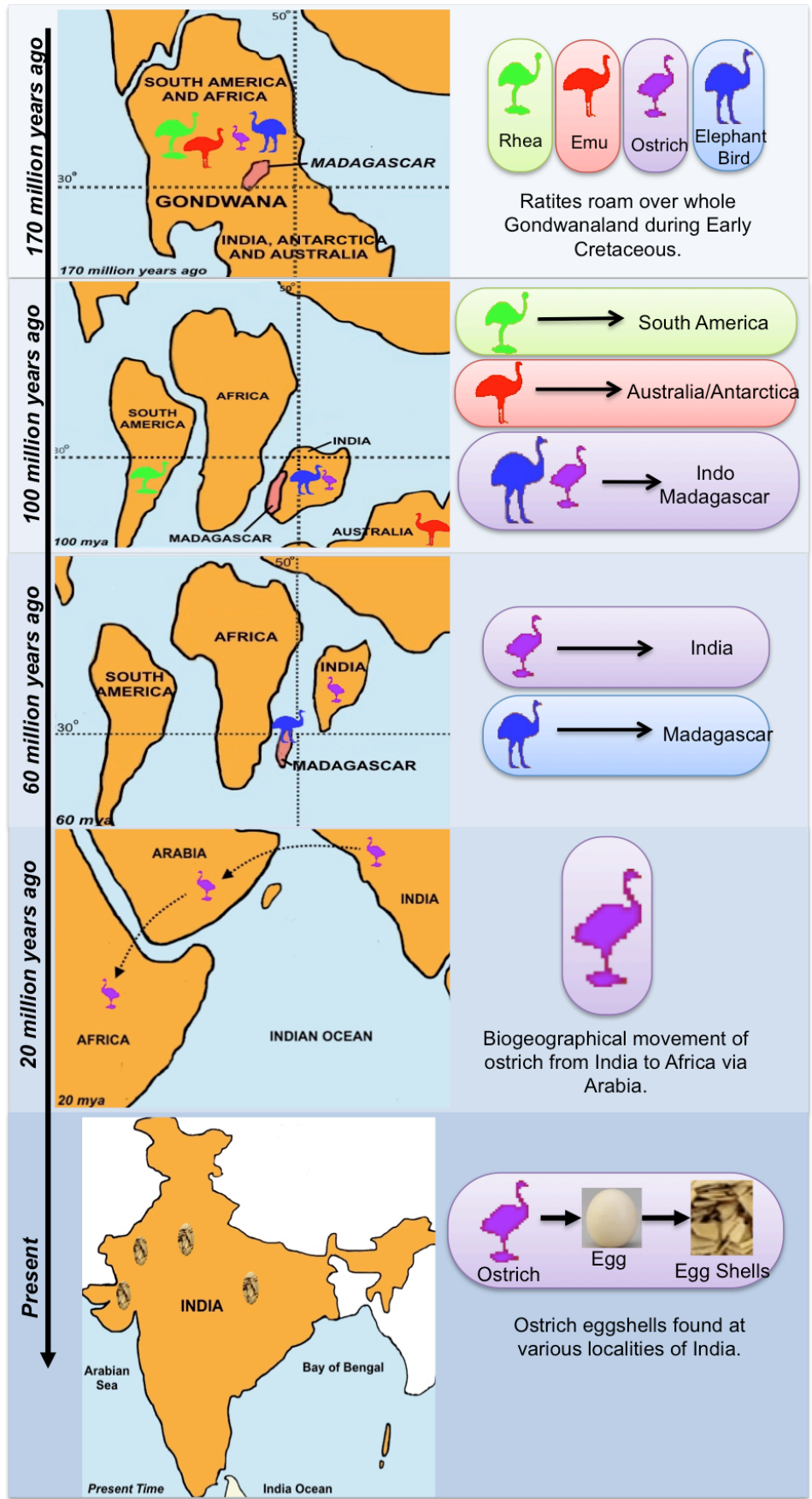


Figure 1.7 Continental drifting and vicariant speciation of ratites. The breakup of supercontinent Gondwanaland during Early Cretaceous endorsing biogeographical movement of ratites

1.2.4 Dating of eggshells

The eggshells from India have been dated at Upper Palaeolithic (25,000 to 40,000 years B.P), based on stone implements (Kumar et al., 1988; Sahni et al., 1989; 1990) and radiocarbon dating was done at Groningen University Lab, Germany (Kumar, 1983; Mohabey, 1989).

1.2.5 Engraved eggshells and eggshell beads

Eggshells with engravings were found at Patne (Fig 1.8) and eggshells engraved into finished or unfinished beads (Fig 1.9) were found at Bhimbetka (Kumar et al., 1983; Bednarik, 1993a; 1993b; 1994). The perforated beads belong to archaeological assemblages, which correspond to the same time period when human populations dispersed from Africa to South Asia (Mellars, 2006).

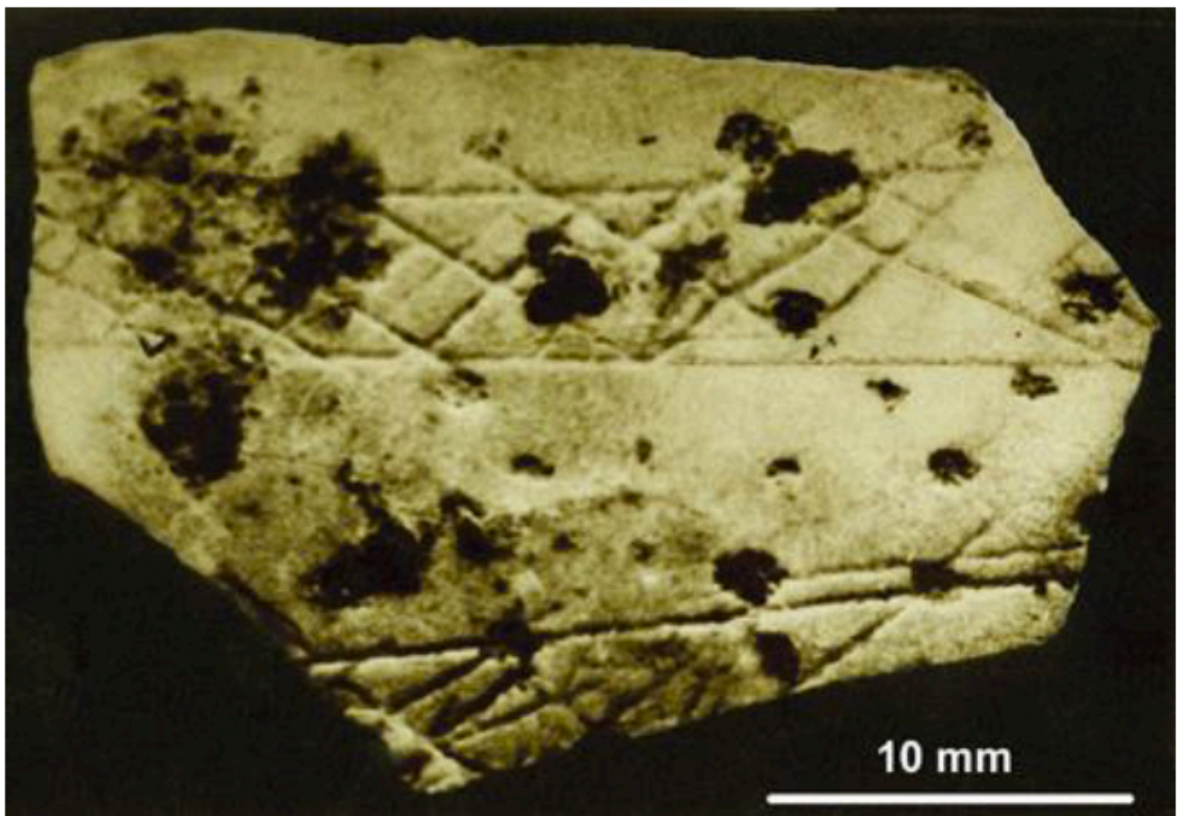


Figure 1.8 Engraved ostrich eggshell from Patne (Bednarik, 1993)

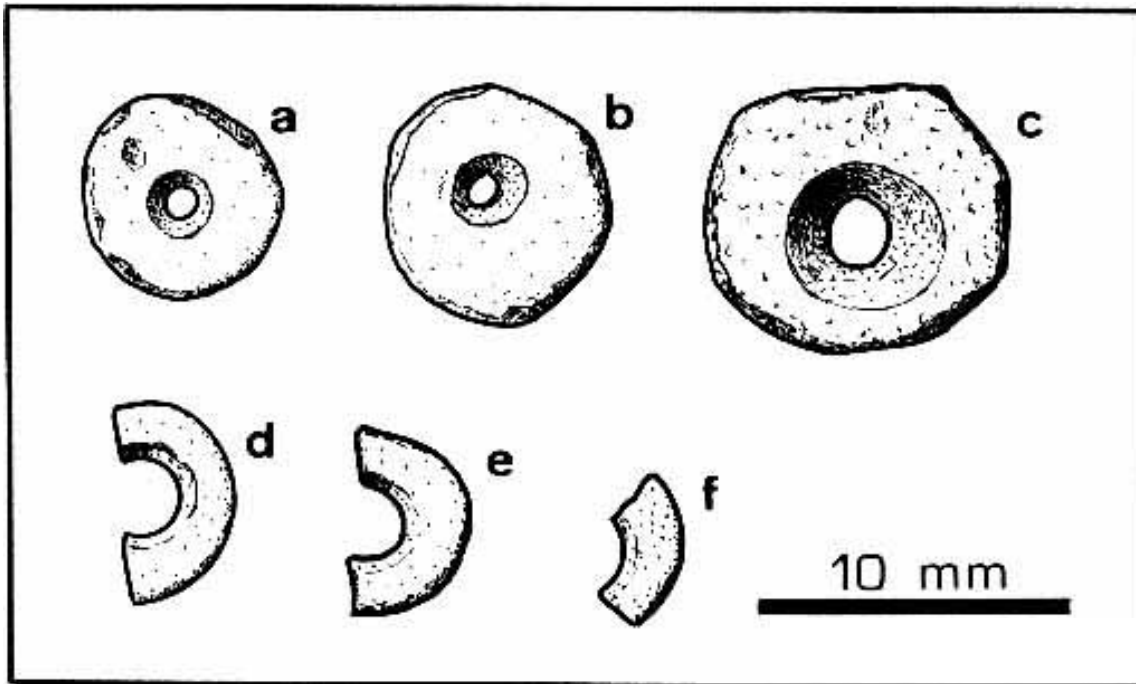


Figure 1.9 Perforated eggshell beads from Bhimbetka, M.P (Bednarik, 1994)

1.2.6 Paleoenvironment and ultrastructure studies

Paleoenvironmental studies on these eggshells provide valuable insights about the debate regarding the time period of dispersion of humans out of Africa, indicating that during the late Pleistocene the continental dispersal of ostrich into India contrasts with the hypothesis of movement of modern humans in India (Blinkhorn et al., 2015). The paleogeological and archaeological significance of these eggshells are well recognized but their origin continues to be poorly understood (Badam, 2005; Nys et al., 2004; Patnaik et al., 2009).

Taxonomically, eggshells can be identified on the basis of characters such as eggshell thickness, pore complex shape, density and diameter (Harris and Leakey, 2003; Pickford and Senut, 2000; Sauer and Sauer, 1978; Stidham, 2004). Comparative ultrastructural and thin section studies suggest that these eggshells are closely similar to those of modern East African subspecies *Struthio camelus* subsp. *molybdophanes*, although assignment to this subspecies based on external characteristics may not be correct (Johnson et al., 1997; Hincke et al., 2000; Miller et al., 2000; Patnaik et al., 2009).

1.2.7 Ostrich rock art

Rock shelter paintings in central India also describe ostrich figures (Fig 1.10) but there is controversy about its identification (Wakankar, 1984, Tiwari, 2000).

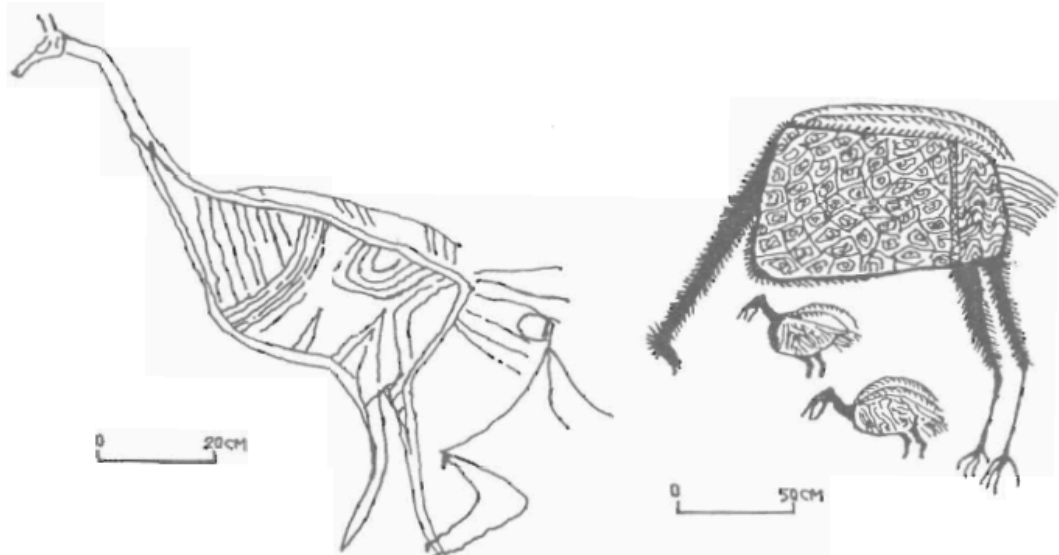


Figure 1.10 Rock shelter paintings from Bhopal (Badam, 2005)

1.2.8 Human expansion and ostrich extinction

Ostriches got extinct from India thousands of years ago and evidence of their existence is supported by fossil eggshells found at various localities (Badam, 2005). The arrival of *Homo sapiens* in India from Africa (August et al., 2011) and hunting of ostriches for their meat as well as the egg is well documented in books (Singh, 2008), which accounts for the main reason of extinction of this species from India.

1.3 Ancient DNA

1.3.1 Ancient DNA

“Ancient DNA (aDNA) is a field of molecular evolutionary biology that uses DNA sequence data recovered from poorly preserved organisms, usually deceased for hundreds to hundreds of thousands of years”. Ancient DNA can be isolated from a diverse range of specimens that includes; archeological and historical skeletal material, mummified tissues, fossilized flora and

fauna. aDNA recovered from well-preserved human remains postulates an exclusive opportunity to study the effect of historical events on ancient populations.

1.3.2 History of aDNA studies

The first study on aDNA was reported from recovery of DNA of Quagga species (Higuchi et al., 1984). Later on aDNA recovery was succeeded on several mummified humans, who were dated back thousands of years (Paabo, 1985). Due to the limitation of technology, the researchers used to clone them in bacteria and amplify DNA sequences (Paabo, 1985). The discovery of polymerase chain reaction (Mullis and Faloona, 1987) provided a revolution in aDNA research by amplifying a very small quantity of DNA from the archeological remains. The first application of PCR in aDNA research was the amplification of mitochondrial DNA from 300-year-old skeletal remains of human (Hagelberg et al., 1989). Working with ancient human DNA is a tough task as chances of contamination with modern DNA are very high. Moreover, the lack of ability to discriminate modern DNA sequences contamination from the ancient DNA sequence is also challenging. To confirm that the endogenous aDNA has been retrieved from ancient remains, authentication norms have been established (Cooper and Poinar, 2000).

1.3.3 Hurdles and errors in aDNA analysis

There are several limiting factors, which create the routine problem in aDNA analysis. Since there is no lower limit of how old a specimen should be, the major restriction in this field is the extraction of aDNA. Following limiting factors affect the quality and quantity of aDNA analysis

1.3.3.1 aDNA extraction

Most of the studies pertaining to aDNA extraction have been done on archeological relics from well-preserved caves and museum collections of fossil samples (Tripathy, 2014). Though much of the work has been done on human skeletal and other bone remains, still research on avian aDNA is infancy especially in tropical countries like India. The successful extraction of aDNA and its reliable analysis from the poorly preserved skeletal material is still a great challenge for the researcher. The specific quantification of DNA recovered from the archeological remains has great importance in downstream aDNA experiments (Hofreiter et al., 2001). aDNA quantity is a major hurdle in the interpretation of the consistency and reliability of the PCR-based nuclear and mitochondrial DNA sequence analysis (Navidiet al., 1992). Quantification

studies of aDNA have been carried out on different specimens by the researchers, which includes frozen and unfrozen sediments (Haile et al., 2007; Crivellaro, 2001) and have found that amount of aDNA decreased as the age of sediments increased.

1.3.3.2 *Post-mortem DNA decay*

DNA of an organism is damaged by endogenous nucleases, after the death of an organism. Conditions like rapid desiccation, the high concentration of salts or low temperature inactivates the nucleases before the entire DNA is reduced to mononucleotide. In this scenario, DNA is affected by slower but persistent DNA decaying activities (Fig 1.11).

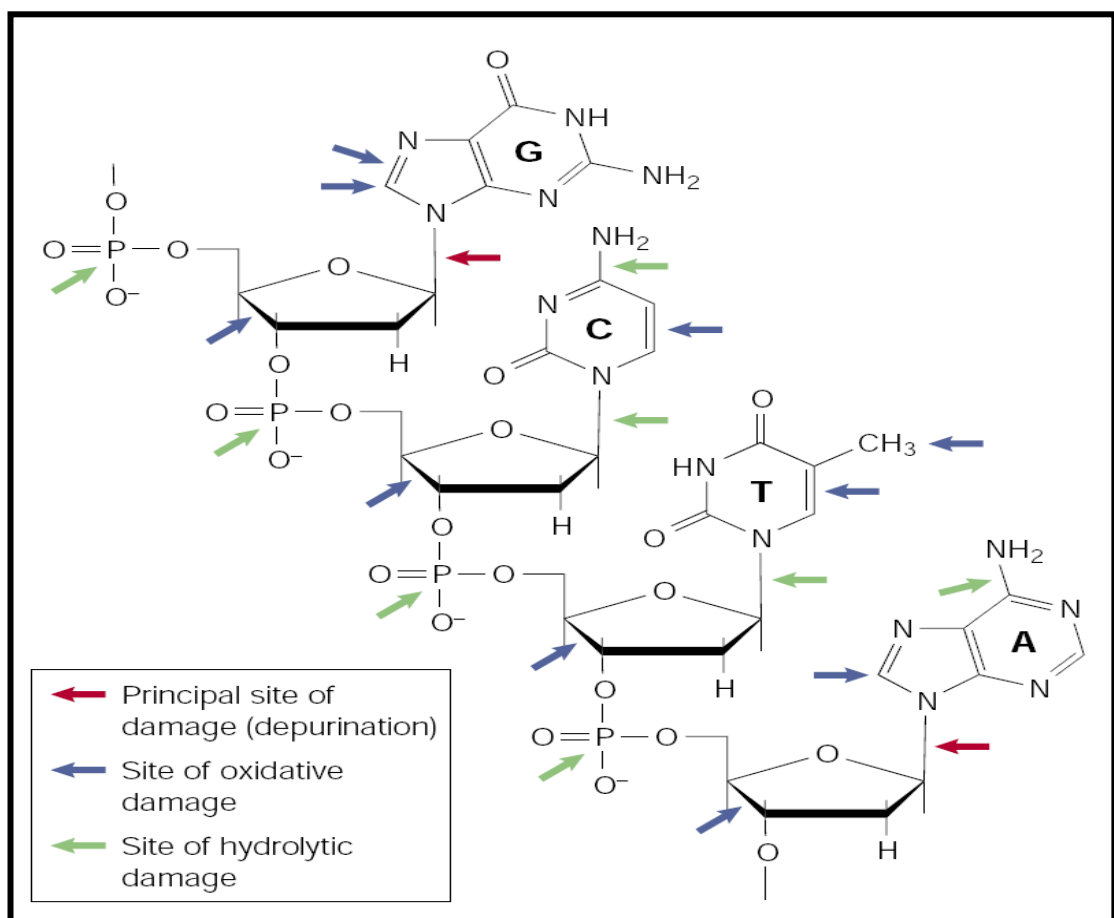


Figure 1.11 Principle site of damage of one strand of the double helix (adopted from Hofreiter et al., 2001).

Besides nuclease, there are other factors that could alter the sugar-phosphate backbone and nitrous base of DNA such as oxidation, direct and indirect effects of background radiation. Additionally, depurination, deamination and further hydrolytic reactions in the surrounding environment could lead to breakage in and destabilization of DNA molecules (Hofreiter et al.,

2001). A major limitation in aDNA deamination is due to the conversion of Cytosine to Thymine (Fig 1.12).

All these reactions routinely create the problem in aDNA extraction and its successful sequence retrieval by blocking the DNA polymerase (Hosset al., 1996). Furthermore, deamination product of cytosine to thymine is very common and during PCR incorrect bases can be inserted (Paabo, 1989). These studies show that no useful aDNA molecule could sustain after a long time due to the combined effect of all the aforementioned effects. However, Some environmental factors, such as humidity and lower temperatures, can prolong this limit by reducing the physiological activity of the dead organism and its surrounding microbes (Smith et al., 2001).

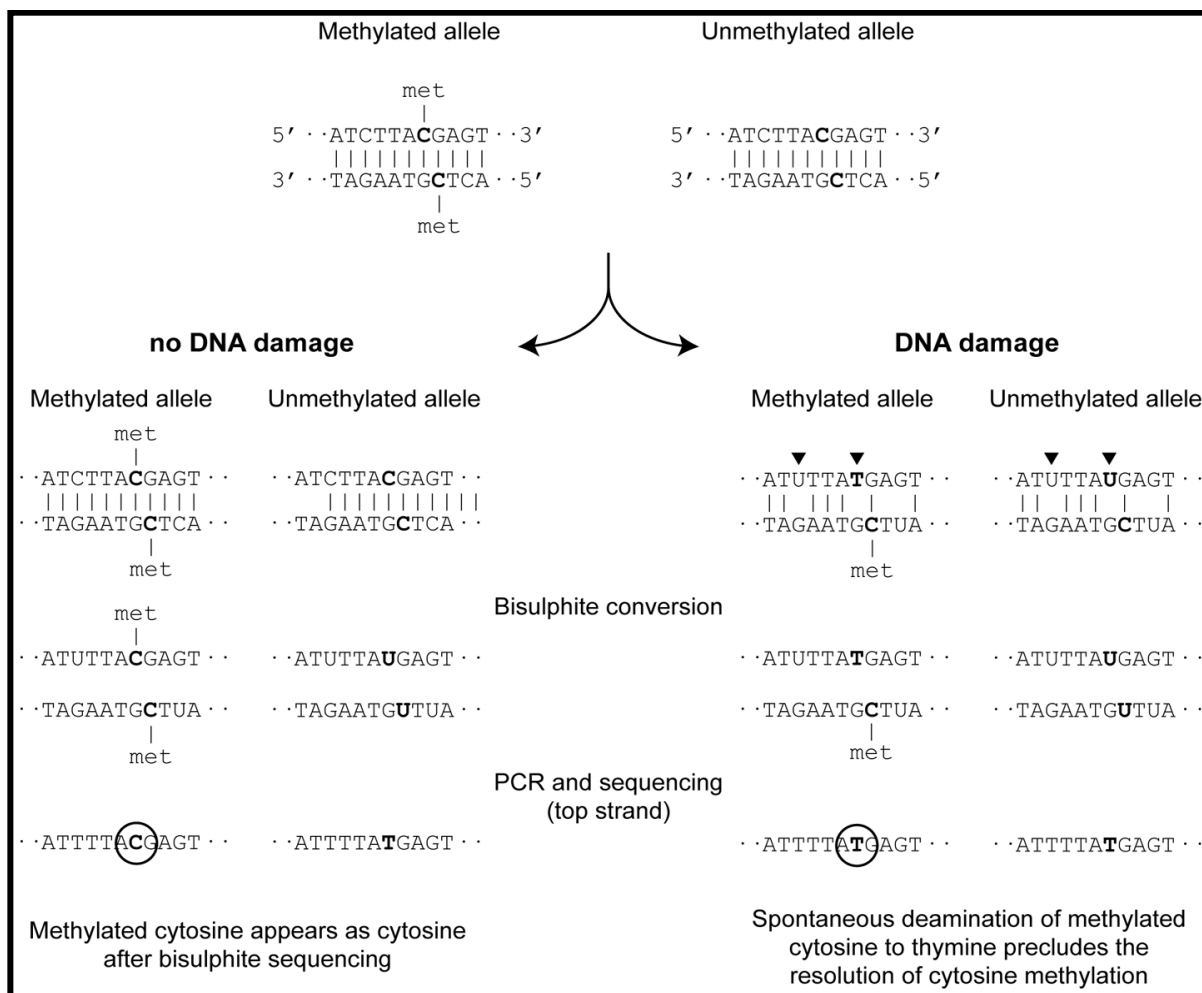


Figure 1.12 Schematic presentation of deamination pattern of cytosine to thymine conversion (adopted from Llamas et al., 2012)

1.3.3.3 Authentication of aDNA results

Considering the fact that very less amount of DNA exists in archeological and paleontological specimens and modern DNA is persistent in the environment, the great challenge for the researcher is to prevent the extraneous DNA while doing PCR. For example, PCR cocktails must be prepared in a laboratory, which is strictly disconnected from labs that are involved in contemporary DNA. Laboratory equipment should be treated with bleach and the entire lab should be irradiated with UV, positive pressure throughout the lab and use of protective clothes and face shields are some routine precautions that need to be followed (Handt et al., 1994). Regardless of all these measures, the risk of contamination by the specimens itself might be tainted with the contemporary DNA. The utmost problems are met with the analysis of human remains because human DNA is mainly predominant in the museums and laboratory environment, and cannot differentiate from aDNA of human remains.

1.3.4 Use of aDNA in evolutionary studies

Over the past 20 years, aDNA studies have investigated the wide range of topics by the investigation of extinct species and populations (Higuchi et al., 1984; Hadly et al., 1998; Orlando et al., 2002; Thangaraj et al., 2003, 2005, 2006; Raghavan et al., 2014, 2015; Prakash et al., 2015; Der Sarkissian C et al., 2015). The diachronic explanation of prehistoric samples, as representative of earlier human settlement and their migration, can be directly linked with contemporary samples of current ethnic groups (Vernesi et al., 2004). This is also a fact that large probability of contamination of prehistoric extracts with contemporary human DNA is the main hindrance for the study involving remains of humans. For example, the first study of aDNA reported from 4,000-year old mummy involves a case of contamination (Paabo, 1985) and also the false positive case from Australia of Mungo man; (Cooper et al., 2001). The latest publication depicting “Ancient human genome sequence of an extinct Palaeo-Eskimo” (Rasmussen et al., 2010) is a remarkable landmark for aDNA. Another ancient DNA study on our evolutionarily closest relative “Neanderthals”, that inhabited Western Asia and parts of Europe before 30,000 years, has open new insights and proved that they are directly linked with modern humans as compared to chimpanzees (Paabo, 2012). Complete mtDNA sequence of Neanderthal, uncovered in 1856 in western Germany, also demonstrated that they have diverged with the modern human around 500,000 years ago (Krings et al., 1999), and about 170,000 years ago the common forefather of all humans lived (Ingman et al., 2000).

1.3.5 Genetic markers and their use in modern and aDNA studies

As like genome of any organism, DNA of the human genome is not a stagnant entity. Instead, it is subject to a variety of changes and these changes give rise to what we call as genetic polymorphisms or sequence variation among individuals, groups or populations. Polymorphisms point to a genetic locus with two or more alleles that occur in appreciable (>1%) frequency in a given population. Several markers have been routinely used for genetic studies that comprise (Indels) insertions / deletions polymorphisms duplications, SNPs (single nucleotide polymorphisms), etc. This change can be simple chance procedures or might be stimulated by an external agent. Like in aDNA there are several factors, which can lead to misincorporation of a mutation.

1.3.6 DNA polymorphisms

DNA polymorphisms is a result of mutation varying from a change in single nucleotide base to numerous of thousands of bases as mutation is a major force that acts to diversify the haplotypes. Understanding mutational dynamics is important for studying the human origin and diseases (Tennekoon et al., 2012). During the production of cells, some mutations occur and if they exist as neutral without any phenotypic effects that are called as polymorphisms. These might lead to organism death or inhibit breeding of organism. If these mutations occur in the non-coding region have no harmful effects and will be just passed to next generation. Mutation can occur in DNA in various forms and with different degrees of incidence. Polymorphism at a specific site on chromosome might be an outcome of one mutation event. Haplotypes are the different kinds of polymorphisms, which are associated with the same chromosome with different rates of occurrence. However, the phenotypes and phylogeny can be predicted by genetic differences in people, which is the foremost idea behind SNP related work.

1.3.6.1 Mitochondrial DNA (mtDNA) polymorphisms

Human mtDNA variation has been widely used as a genetic marker to examine the contemporary *Homo sapiens* dispersals all over the world (Chandresekhar et al., 2009). mtDNA is a non-recombining haploid genome that inherits from mother to their children. The mutation causes changes between mtDNA sequences. With the course of time mutations occur in the molecules, which are less related. The entire DNA sequence of the human mitochondrial genome - 16,569 nucleotides - was established in 1981 (Anderson et al., 1981) and has been recently revised (Andrews et al., 1999). Human variom project has been done to share genetic

information on one common platform (Platrinós et al., 2012). Variation in the mtDNA sequence have been widely analyzed in human populations, in terms of evolutions, population dispersal, diseases, and wildlife (Torróni et al., 1996; Howell et al., 2000; Ingman et al., 2000; Muruganathan et al., 2010; DE Silva et al., 2011; Gaur et al., 2011; Kumar et al., 2011; Juras et al., 2014; Biswas et al., 2014; Wickaramasinghe et al., 2015).

The mitochondrion genome and mutations are inherited maternally and intact over hundreds of generations. There is no mixing of genes from the paternal genome. New mutations sometimes occur in a lineage and can be easily distinguished as they are very few. Mutations in mitochondrial DNA can be called as haplotypes as the mitochondrial genome is haploid and occur only from the mother. Comparisons of DNA variations, which are genetic, can reveal relationships between different population groups within the same species. In nuclear DNA mutations occur at a faster level than mtDNA control regions. SNP patterns are steadily heritable in a non-Mendelian fashion over many generations. However, the evident mutation rate centered on a number of detected mtSNPs amongst populations does not reveal the actual mutation rate. The elevated mutation rate of mtDNA prophesies that there might be a "back-mutation" or mutated many times throughout primate evolution (Handt et al., 1994).

Aboriginal Australian population studies on variation in mtDNA (Huoponen et al., 2001) revealed that Papua New Guinea populations and Aboriginal Australian populations might have once emerged from a prehistoric ancestral population. These populations then might have quickly deviated as well as geographically separated from each other. Overall, they concluded that mtDNA data confirm the genetic individuality of Aboriginal Australian populations (Kumar et al., 2009).

For modern-day population genetics the lineage of the non-recombining mitochondrial genome has become a foundation. Data suggested the origin of modern human to be either African or multi-regional (Eckhardt et al., 1993). Recent evidence support the African origin of the human population, based on the mtDNA studies (Ingman et al., 2000; Chaubey et al., 2014). MtDNAs represents component of a single phylogenetic tree and the human mitochondrial family tree which proposes that anatomically humans originated in Africa about 100,000 - 200,000 years ago (Cann et al., 1987; Vigilant et al., 1991).

1.3.7 Short tandem repeats (STRs)

DNA polymorphisms where short DNA sequences are randomly repeated are termed as STR. They are usually called “junk DNA” as they are introns and they do not code for proteins. STR varies among different people and a number of repeats in DNA sequence also varies in an individual, which forms the basis for various genetic and forensic studies (Singh et al., 2004, 2012). In a Y chromosome DNA, the STR pattern is unique and the descendants will have either similar or exactly same DNA STR pattern. Geographical differentiation can also result in variation in STR pattern (Jobling and Tyler-Smith, 1995; Jonnalagadda et al., 2011). Hence, their polymorphic characters make them exclusively suited for genetic and forensic studies (Gerstenberger et al., 1999).

1.4 Stable Isotope Studies

1.4.1 Biochemical signatures from avian eggshells

Samples like can tissue, bones, mollusk shell, feathers, hair etc. be used for the isolation of biochemical signatures (Koch, 2008). However, eggshells are more preferably used for this study as they postulate an additional constrained temporal context. Eggshells are formed in a single breeding season within a few days or hours as compared to hairs that grow uninterruptedly or bones which experience continuous remodeling. Thus, eggshells are more suitable for carbon dating or uranium-series disequilibrium or stable isotope analysis (Brooks et al., 1990; Higham, 1994; Johnson et al., 1997; Miller et al., 1999a; Magee et al., 2008). Thus, eggshells more notably represent environment and diet of the bird, at that particular instant as they offer less noise or variation compared to other samples (Miller et al., 2005; Clarke et al., 2006; Emslie and Patterson, 2007). Also, Avian eggshell structure is made up of crystalline matrix of carbonate components and refuses postmortem decay and diffusional loss (Miller et al., 1992; Johnson et al., 1997).

1.4.2 Stable isotopes in the field of palaeontology and archaeology

Atoms with the same number of protons but having additional neutrons are stable isotopes (Fry, 2006). Thus, having an additional neutron results in greater mass and the isotope is thus known

as heavy isotope (Fig 1.13). The ratio of the heavy isotope and the known standard tell us the abundance of that isotope as shown in Table 1.3. This ratio is calculated using Mass Spectrometry, a specialized technique IRMS - Isotope Ratio Mass Spectrometry is used. This ratio is notified by symbol δ and is expressed as parts per mil (‰). Carbon and oxygen isotopes are most commonly analyzed isotopes and differences in the stable isotope ratios form the basis of paleodietary and paleoenvironment studies (Koch, 2008).

Stable Isotopes (Oxygen as an Example)

Same element with two different atomic masses:



Changes in $^{18}\text{O}/^{16}\text{O}$ ratios are TOO small to directly measure.

$$\delta^{18}\text{O} = \left[\frac{{}^{18}\text{O}/{}^{16}\text{O}_{(\text{sample})} - {}^{18}\text{O}/{}^{16}\text{O}_{(\text{SMOW})}}{{}^{18}\text{O}/{}^{16}\text{O}_{(\text{SMOW})}} \right] \times 1000$$

Sample is compared to a standard; in the case of oxygen, the standard is seawater:

SMOW = Standard Mean Ocean Water

$\delta^{18}\text{O}$ in units of per thousand, called 'per mil' and denoted as ‰ .

$\delta^{18}\text{O} = 0$ Sample has same ratio as that in seawater.

$\delta^{18}\text{O} > 0$ Sample **enriched** in heavy isotope (^{18}O) relative to seawater.

$\delta^{18}\text{O} < 0$ Sample **depleted** in heavy isotope (^{18}O) relative to seawater.

Figure 1.13 Image depicting heavy and lighter isotope of oxygen.

1.4.2.1 $\delta^{13}\text{C}$ and $\delta^{18}\text{O}$ Isotopes

$\delta^{13}\text{C}$ values are the outcome of the fractionation of CO_2 into the plants representing three different photosynthetic pathways (Marshall et al., 2008). Thus, carbon isotopic signatures

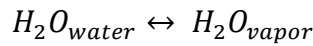
provide the information about the diet of the animal. C₃ plants follow Calvin cycle and are mainly trees and shrubs, which are found in the temperate climate and have a range of $\delta^{13}\text{C}$ -22 to -35 ‰ and an average of -27‰. C₄ plants follow Hatch-Slack pathway and are grasses, which are adapted to the shortage of water. They are found in tropical arid climate and have a range of -9 to -19‰ and an average of -13‰. The gap between C₃ and C₄ is bridged by succulents, which follow CAM (Crassulacean Acid Metabolism) pathways. Thus, the diet of an animal can be determined based on their $\delta^{13}\text{C}$ values.

Table 1.3 Summary of commonly used stable isotopes. Modified from Fry, 2006 and Newsome, 2007

Element	Isotopes	Abundance	High values	Low values	Standard	Application
Carbon	¹² C	0.98889	C ₄ , high trophic level, marine, xeric, high altitudes	C ₃ , low trophic level, terrestrial, low altitudes, mesic/hydric	Pee Dee Belemnite Limestone (PDB)	Diet C ₃ , C ₄ and CAM plants, habitat
	¹³ C	0.01111				
Nitrogen	¹⁴ N	0.99634	Marine, low latitudes, xeric, oxic	Low trophic level, anoxic,	Air	Trophic level, diet, habitat
	¹⁵ N	0.00366				
Oxygen	¹⁶ O	0.99755	Warmer temperature	Cooler temperatures	SMOW	Water source, habitat and climate
	¹⁷ O	0.00039				
	¹⁸ O	0.00206				

Carbon isotope signatures focus purely on animal diet. Combining carbon 13 isotope studies with oxygen 18 isotope studies throw light on animal interaction with its habitat both in present and past (Table 1.3). $\delta^{18}\text{O}$ values reflect the water source, therefore, they are used to study changes in habitat and climate (Koch, 2008). These values differ temporally and geographically. Warmer climates are represented by higher $\delta^{18}\text{O}$ values while cooler climates have lower $\delta^{18}\text{O}$ value. For a substrate, the stable isotopic composition is the isotope value of the diet offset by the fractionation factor (Fry, 2006). This value is unique for each sample. Substrates undergo a chemical process of fractionation that results in the enrichment or depletion of given isotope, which results in the formation of a new substance and is important in the analysis of isotope data (Johnson et al., 1998; Miller et al., 2005; Clarke et al., 2006).

$$\alpha = \frac{R_{\text{reactants}}}{R_{\text{products}}}$$



$$\alpha^{18}O_{water-vapor} = \frac{(^{18}O/^{16}O)_{water}}{(^{18}O/^{16}O)_{vapor}}$$

During the eggshell formation process shell gland secretes calcium and metabolic carbon dioxide in the oviduct with uterine fluid. These are converted into calcium carbonate by carbonic anhydrase and then absorbed by the matrix of the shell (Berg et al., 2004; Fernandez et al., 2004). As the egg rotates along the oviduct, proteins, fats, and carbohydrates- the organic components in the eggshells are added along with calcium carbonate and cellular debris. $\delta^{13}C$ or $\delta^{18}O$ carbonate fractions are not affected by direct intake of calcium carbonate in dietary by birds (von Schirnding et al., 1982). Thus, combining both carbon isotopes and oxygen stable isotopes provides a clear picture of the ecology and diet of birds.

1.4.2.2 Palaeodiets, palaeoecology and extinction processes

Fossil avian eggshells have been analyzed for the stable isotope to study paleodietary and human migration (Stern et al., 1994). Ostrich extinction and human migration is a hotly debated topic over past few years (Blinkhorn et al., 2015). Numerous eggshell deposits found at various archaeological sites confirm the presence of these extinct birds (Miller et al., 1999b, 2005). Eggshells are found as a deposit and might comprise of multiple eggs. Stable isotope analysis can precisely differentiate between eggs of two different individuals. Studies on these biochemical signatures would be helpful in the understanding of ecology, diet, and extinction processes and narrow the gap related to the studies on extinct ostrich eggshells from India.

1.4.3 Triple oxygen isotope body water model and compositions of biogenic carbonates

1.4.3.1 Background

Earlier researchers have recognized that the compositions of oxygen isotope of animals are strongly influenced by animal physiology, habitat, and climate (Johnson et al., 1997). Several models based on oxygen isotope mass balance have been built to help understand these relationships (Luz and Kolodny, 1985; Luz et al., 1990; Bryant and Froelich, 1995; Kohn, 1996; Pack et al., 2013). Meanwhile, biominerals like eggshell carbonate or bioapatite precipitated in isotopic equilibrium with body H_2O and hence record the oxygen isotope composition of body

water. Consequently, the O₂ isotope compositions of biominerals have been used as indicators of climate and habitat change. For instance, the ¹⁸O/¹⁶O compositions of tooth enamel apatite and bone phosphate, Ca₅(PO₄,CO₃)₃(OH,CO₃) are strongly influenced by meteoric water δ¹⁸O values, relative humidity and animal physiology, and are widely used as a proxy for rainfall and seasonality of present and past environments (Longinelli, 1984; Ayliffe, 1990; Luz et al., 1990; Kohn, 1996; Fricke et al., 1998; Dettman et al., 2003; Sirocko et al., 2005; Levin et al., 2006;Lahr et al 2008) A ¹⁷O-enabled body water model for animals is also needed to enhance the triple oxygen isotope study for biominerals. This model will have great potential applications as D¹⁷O is a promising tracer for the water source, humidity, animal physiology, and also for the D¹⁷O value of atmospheric oxygen that itself is related to global carbon cycling (Pack et al., 2013).

1.4.3.2 *Body water model*

Following the approach of the ¹⁸O-body water model presented by Kohn, 1996, a new oxygen isotope mass balance model is developed that includes all three isotopes of oxygen in the form of ¹⁸O/¹⁶O and ¹⁸O/¹⁷O ratios. The basic scenario for this model is the oxygen mass balance of outputs and inputs for an animal as shown in Fig 1.14.

Animals exchange oxygen with the ecosystem mostly in the form of oxygen, water, carbon dioxide and chemically bound oxygen in food. Fig 1.14 shows that oxygen inputs for body water are drinking water, atmospheric O₂, free H₂O in food, chemically bound O₂in food, and inhaled air water vapor. These oxygen components are related to two main oxygen reservoirs: atmospheric O₂ and surface water.

Oxygen outputs are described as liquid excreted water (urine and sweat), fecal water, CO₂, water vapor (nasal, breath, and transcutaneous water), and O in urea and uric acid. As the inputs and outputs oxygen isotope fluxes should be balanced to keep the animal body water at a steady state, it can be equated as:

$$\sum_i f_{in,i} \cdot {}^xR_i = \sum_j f_{out,j} \cdot {}^xR_j, \quad ({}^xR = {}^xO/{}_{16}O, \quad x = 17 \text{ or } 18)$$

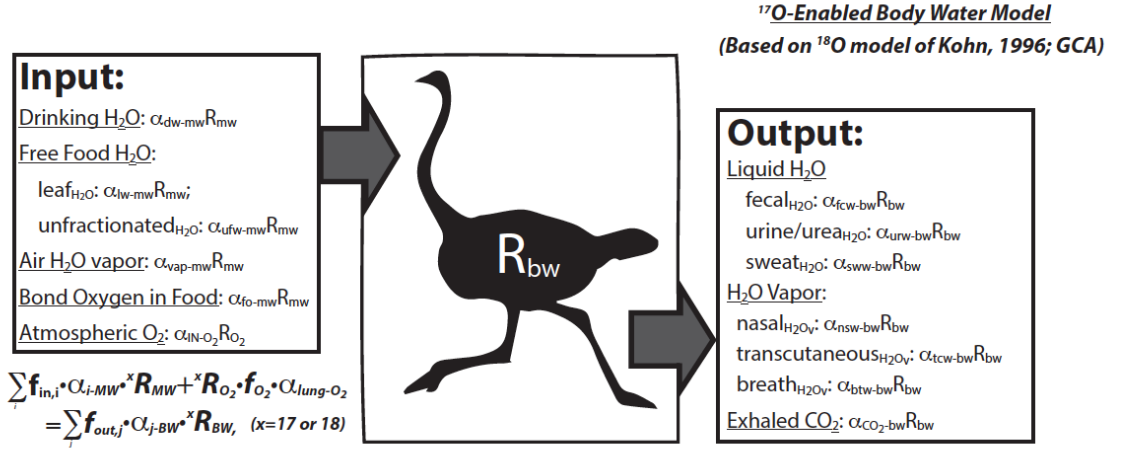
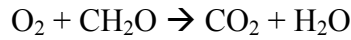


Figure 1.14 ¹⁷O-enabled body water model for animals based on ¹⁸O model of Kohn (1996). The oxygen isotope output and input fluxes are in mass balance relationship. Inputs can be expressed in terms of fractionated meteoric water plus the term of atmospheric O₂. Outputs can be expressed in terms of fractionated body water. Fractionation factors (α) and fraction (f) are in light of previous work (Kohn, 1996; Barkan and Luz, 2005; Hofmann et al., 2012). Leaf water models are based on the ¹⁸O/¹⁶O model of Roden and Ehleringer (1999). Relative humidity and the oxygen isotope fractionation exponent λ relationship is given by Landais et al., 2006.

where $f_{in,i}$ and $f_{out,j}$ are the fraction of moles for each input oxygen component (i) and output oxygen component (j). Animals incorporate atmospheric O₂ into metabolic water through respiration:



Therefore, the metabolic H₂O constitutes part of the body water and strongly affects body water D¹⁷O signals because of the large ¹⁷O anomalies from atmosphere O₂. The atmospheric O₂ inputs can be expressed as $R_{O_2} \cdot f_{O_2} \cdot \alpha_{lung-O_2}$, where f_{O_2} is the molar fraction of O from O₂ relative to all oxygen input fluxes and α_{lung-O_2} is the fractionation factor between O₂ absorbed by the lungs and atmospheric O₂. All the other oxygen input fluxes are related to ambient meteoric water by specific fractionation factors and can be expressed by $R_{MW} \cdot f_{in,i} \cdot \alpha_{i-MW}$, where R_{MW} is the oxygen isotope ratio of local meteoric water, $f_{in,i}$ is the fraction of input component i, α_{i-MW} is the fractionation factor between component i and the meteoric water. Similarly, all output oxygen components are related to animal body water. So the right side of the equation can be expressed in the form of $R_{BW} \cdot f_{out,j} \cdot \alpha_{j-BW}$, where R_{BW} is the oxygen isotope ratio of animal body water, α_{j-BW} is the fractionation factor between output component j and the body H₂O. Finally, isotopic mass balance equation can be expressed as:

$$\sum_i f_{in,i} \cdot \alpha_{i-MW} \cdot {}^xR_{MW} + {}^xR_{O_2} \cdot f_{O_2} \cdot \alpha_{lung-O_2} = \sum_j f_{out,j} \cdot \alpha_{j-BW} \cdot {}^xR_{BW}, \quad (x = 17 \text{ or } 18)$$

Specific and fractionation factors (α) and ranges of input or output fractions (f_i, f_j) for each component can be obtained from previous studies (O'Neil and Adami, 1969; Majoube, 1971; Friedman and O'Neil, 1977; Epstein and Zeiri, 1988; Kohn, 1996; Roden and Ehleringer, 1999; Barkan and Luz, 2005; Landais et al., 2006)

The triple oxygen isotope compositions in animal body H₂O are mostly measured by ambient humidity, the fractional contribution of metabolic water, animal water uses efficiency, and the fraction of evaporated water (like leaf water) consumed by animals. Variability in the relative contributions and isotopic compositions of these inputs can lead to a wide range in D¹⁷O of animal body water. The highest animal body water D¹⁷O values are expected for animals that live in humid climates, consume little-evaporated water (leaf water) from food, and have poor water use efficiency (= high water economy index, WEI, the amount of water needed for per unit energy metabolized, e.g., ml/KJ). Conversely, the lowest body water D¹⁷O values are expected for animals that live in arid climates, consume a large amount of evaporated water from food, and have high water use efficiency (low WEI). There seem to be no clear differences in WEI across broad taxonomic groups, such as birds, mammals, reptiles, and arthropods, and no clear correlations with body mass (Nagy and Peterson, 1988). For instance, typical values for desert-adapted animals are ≤ 0.15 mL/KJ and for humans are ≥ 0.3 mL/KJ.

The lower and upper limits of body water D¹⁷O were explored at Johns Hopkins laboratory by running a “maximum evaporation body water model” and a “minimum evaporation body water model”, respectively. In the “maximum evaporation model”, the relative humidity (Rh) is assumed 0.2, fraction of evaporated leaf water relative to whole food water is 0.4, and the WEI value is 0.1 mL/KJ. Similarly, the limits for the “minimum evaporation model” by holding Rh at 0.8, the WEI value at 0.5 mL/KJ, and fraction of leaf water at 0.01 (Fig. 1.16). This model is widely applicable to both modern and fossil animals for determining variations in climate and animal physiology.

To validate the model, modern samples were analyzed including captive bird eggshells (chicken, duck, ostrich and emu) from the northeastern U.S., China and Japan; wild bird eggshells (ostrich, starling, and dove) from Africa and the northeastern U.S.; and wild mammal tooth enamel from Africa. In order to analyze the isotopic compositions of parent H₂O for these

carbonates, knowledge of the isotopic fractionation factors between parent water and carbonate is required. Egg white water from fresh chicken and duck eggs was extracted using a vacuum distillation method. Assuming there is no substantial fractionation amongst egg white H₂O and body H₂O, the distilled water is taken as the parent water for eggshell carbonate. By analyzing both the parent water and carbonates, the fractionation factors between carbonate and water under a constant temperature were calculated (that is, bird body temperature, ~38-40 °C) by using the equation of

$${}^x\alpha_{\text{Carb-H}_2\text{O}} = \frac{1000 + \delta^x \text{O}_{\text{Carb}}}{1000 + \delta^x \text{O}_{\text{H}_2\text{O}}}, \quad (x = 17 \text{ or } 18)$$

The mean fractionation factors based on these experiments are ${}^{18}\alpha = 1.0380 \pm 0.0008$, and ${}^{17}\alpha = 1.0197 \pm 0.0004$, translating to a fractionation exponent of $l = 0.5245 \pm 0.0003$ (95% confidence interval). These calculated fractionation factors combine the carbonate-water fractionation, the so-called “acid” fractionation (as we analyze O₂ ultimately produced from CO₂ derived from carbonate by acid digestion), and any other fractionations from this analytical method. Therefore, the triple oxygen isotope composition of carbonate parent water (body water) can be calculated based on these fractionation factors and analyzed eggshell carbonate data.

The samples analyzed so far are from climates varying from arid (Ethiopia, Kenya, South Africa) to humid (Baltimore, New Jersey, Japan, eastern China), and include species that intake a large amount of evaporated leaf water (ostrich and wild birds) to domestic animals that consume very little leaf water. The observed body water $d^{18}\text{O}$ and $D^{17}\text{O}$ values have a large range, from -6‰ to +10‰ and +0.02‰ to -0.15‰ which reflects the effects from different environments and physiologies (Fig. 1.15). Similar trends were also observed in these data that are consistent with our model predictions. In Fig. 1.15, the highest $d^{18}\text{O}$ values are from animals consuming lots of evaporated water and living in arid environments (Africa); the lowest are from animals consuming little evaporated water and living in humid environments. In contrast, the highest $D^{17}\text{O}$ values (least anomalous) are from animals living in humid environments with high WEI and small intake of leaf water, while the lowest $D^{17}\text{O}$ values (most anomalous) are from animals living in arid environments with low WEI and large intake of leaf water.

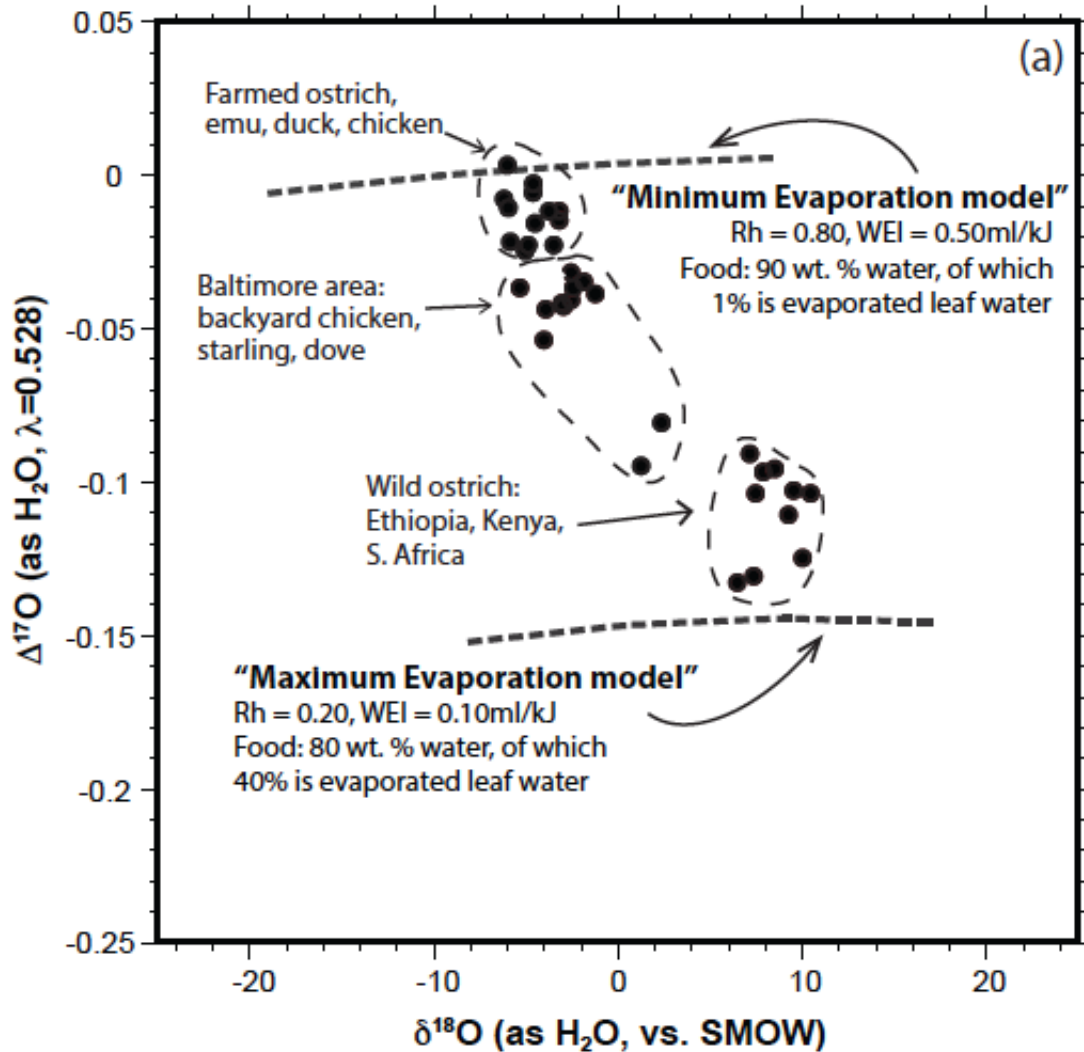


Figure 1.15 “Minimum Evaporation” and “Max Evaporation” model (dashed lines) predicted by the ^{17}O -enabled body water model. Actual measurements of body water isotopes (from analysis of eggshells) for modern birds are shown in black circles. The minimum evaporation model limit is for animals with high WEI, from humid climates, and consuming little evaporated leaf waters. The maximum evaporation model limit is for animals with low WEI, from arid climates, and consuming lots of evaporated leaf waters. These limits bracket possible body water compositions for modern birds and the measured body water data show consistent observations with the model.

To conclude, this model extends oxygen isotope studies in biogenic minerals from $^{18}\text{O}/^{16}\text{O}$ to include $^{17}\text{O}/^{16}\text{O}$ and could be widely used for studying animal physiology and climate. Furthermore, as the body water inherits information from atmospheric O_2 , this model can be applied to fossil biominerals to reconstruct paleo-atmospheric compositions. However, to refine and evaluate the body water model, more systematic data is needed to address the uncertainties brought up by the complex animal physiology and various climate parameters.

After in depth review of literature, various objectives of the studies were defined as under:

- ◎ To study the morphology and crystallography of eggshells for identification and diagenetic alteration
- ◎ To ascertain the origin of the extracted and amplified DNA
- ◎ To sequence DNA for studies of phylogeny, biogeography & molecular evolution and to obtain a reliable evidence for presence of ostriches in India
- ◎ To compare the sequence of ancient fossils with their closest extant descendants
- ◎ To study paleodietary, paleoecology and reconstructing paleoenvironment

CHAPTER 2

ULTRASTRUCTURE AND CRYSTALLOGRAPHIC STUDIES ON FOSSIL EGGSHELLS

2.1 Introduction

Ratite eggshells have been reported from more than forty Upper Paleolithic sites in peninsular India (Kumar et al., 1988). These fossil eggshells were dated from 25,000 to 40,000 years BP, either using radiocarbon dates or the presence of Upper Paleolithic tools (Kumar et al., 1988,1990). Fossil eggshell fragments represent biomineralized skeletal remains that provide important taxonomic, functional morphology, and evolutionary data (Trimby and Grellet-Tinner, 2011). Most of these fossilized eggshells are considered to be of Gondwanan origin which confirms the presence of ostriches in central and southern Asia, Africa, Middle East, and Europe in prehistoric times, whereas the more reduced geographical distribution of ratites nowadays is possibly related to an aftereffect of the continental drift (Cracraft, 1974; Sibley and Ahlquist, 1990a; Cooper et al., 2001).

Fossil eggshells rarely encompass embryonic remains either due to cracking of eggs during burial process or being damaged by microbial activity. Therefore, paleontologists rely on morphological aspects to study their origin and phylogenetic relationships prehistoric avian species. Also, the study of morphology, composition and microstructure is essential to understand the formation of avian eggshell (Richards et al., 2000). The process of formation of the eggshell in avian species is extremely rapid and it has been reported to have characteristic and conservative structure consisting of several layers (mammillary layer, palisade layer, and cuticle layer) from the inner surface to the outer surface (Feng et al., 2001) as shown in Fig 2.1. Indian fossil eggshells have the closest similarity with the widely distributed Neogene fossil taxon *Struthiolithus*, on the basis of the combination of eggshell surface, pore, pore canal morphology and cross-sectional features (Patnaik et al., 2009). Ratites monophyly is extensively recognized on the basis of morphological, skeletal and oological studies (Cracraft, 1974; Sibley and Ahlquist, 1990b; Lee et al., 1997; Cooper et al., 2001). However, these studies are not conclusive about the phylogenetic relationships and origin of fossilized eggshells from India. DNA-based species identification of these eggshells is necessary to understand the phylogeny of these ostriches. Prior to DNA analyses, the preservation of these

fossils has to be determined, even if they appear well preserved on the basis of external morphology.

The aim of this study is to determine the degree of preservation of Indian fossil eggshells of ostriches using a combination of scanning electron microscopy (SEM), and X-ray Diffraction (XRD), electron backscatter diffraction (EBSD), and X-Ray Diffraction (XRD). SEM studies done have shed light on the formation of the different layers of eggshells and how the cuticular layers preserve biomineral structures enriched in the organic matrix, mainly composed of proteoglycans and glycoproteins, from which genetic information can be extracted. XRD data provided the information of the eggshell mineralogy and the degree of mineral replacement associated to diagenesis. Besides this EBSD has emerged as a high-resolution, *in situ* technique for providing crystallographic information of biominerals (e.g., Pérez-Huerta et al., 2011 and references therein) and to detect diagenesis (e.g., Cusack et al., 2008), which has also been recently applied for studying eggshell structures (Trimby and Grellet- Tinner, 2011).

This investigation resulted in the complete crystallographic structure of ostrich eggshells as well as extent of preservation of biominerals in the eggshells, which is an essential requirement for genetic, paleoenvironmental and paleodietary studies.

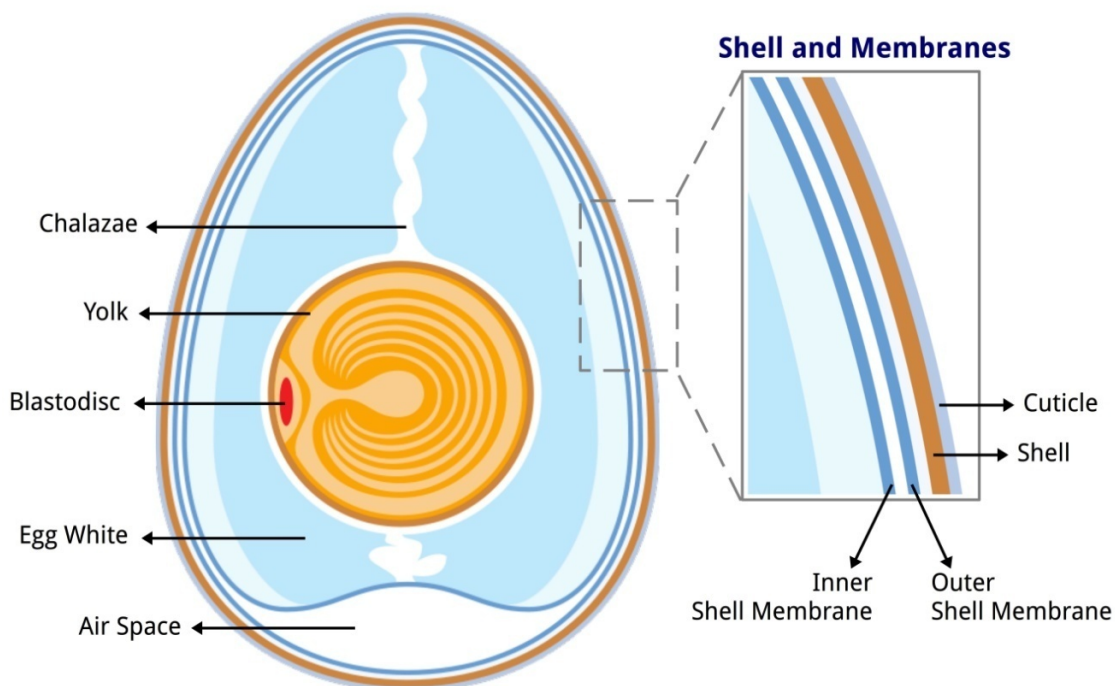


Figure 2.1 Anatomy of avian egg. Inset image showing inner shell membrane, outer shell membrane, cuticle and shell (Horst Frank, 2007)

2.2 Sample Details

2.2.1 Materials

Fossil eggshell fragments were recovered from five different localities of India and one modern African ostrich eggshell was also analyzed as control sample as shown in Table 2.1. The fossil eggshells collected from Indian sites were dated from 25,000 to 40,000 years BP, either using radiocarbon dates or the presence of Upper Paleolithic tools (Kumar et al., 1988, 1990).

Table 2.1 Sample collection sites of fossil eggshells and their respective states.

S.No.	Site	Area	State & GPS Co-ordinates	Catalogue No.
1	Chavni Baroda	Bundi	Rajasthan (25° 26' 24" N, 75° 38' 24" E)	SJ/CB/001
2	Anjar	Kachchh	Gujarat (23° 6' 48.32" N, 70° 1' 39.88" E)	SB/AN/003
3	Chandresal- 1	Kota	Rajasthan (25° 10' 48" N, 75° 49' 48" E)	GK/CH1/004
4	Chandresal -2	Kota	Rajasthan (25°13'34.1"N 75°55'34.7"E)	GK/CH2/006
5	Nagda	Chambal	Rajasthan (25°10'53.3"N 75°48'45.5"E)	GK/NA/008
6	Africa	-	Africa	CHA-2013

2.2.2 Methods

2.2.2.1 Scanning electron microscopy (SEM)

To prepare SEM samples fragments of ostrich eggshells were mounted on aluminum stubs so that the outer surface (attached to the mammillary layer) faces the detector. The eggshells were coated (8-10nm) with gold sputtering (Richards et al., 2000) using BALTEC SCD005 for 40-50 seconds and were then observed under a FEI Quanta 200 F.

2.2.2.2 X-ray diffraction (XRD)

XRD data were recorded with CuK α radiation over the 2 θ range from 5 to 100 with the scanning rate of 2 min⁻¹ θ (Feng et al., 2001). Plaque and powdered samples were analyzed to reveal the mineralogy of different layers. Origin software was used to analyze the plaque samples data and JADE were used to plot the powdered XRD data.

2.2.2.3 Electron backscatter diffraction (EBSD)

Two fossil eggshells, from Bundi and Chandresal, and one modern ostrich eggshell were chosen for the EBSD analysis. Eggshell fragments were embedded in epoxy resin to observe cross sections, from outer to inner surfaces, throughout the shell thickness. Samples were ground and subsequently polished with alumina of 1 μm and 0.3 μm and finally with colloidal silica (0.06 μm). Before analysis, samples were coated with a thin layer (2.5 nm) of carbon (Pérez-Huerta and Cusack, 2009) and the samples were surrounded by silver paint to avoid electron charging. The EBSD study was carried out with an Oxford Nordlys camera mounted on a Field Emission Scanning Electron Microscope (FE-SEM) JEOL 7000 located in the Central Analytical Facility (CAF) of The University of Alabama. EBSD data were collected with Oxford Aztec 2.0 software at high vacuum, 30 kV, large probe current, and a resolution of 1 μm step size for crystallographic maps and a work distance about 10 mm. Finally, data were analyzed using OIM 5.3 from EDAX-TSL. In this study, EBSD data obtained has been shown by crystallographic maps, phase maps, and pole figures, which represent the stereographic projection of crystallographic planes in reference to the {0001} calcite plane.

2.3 Result and Discussion

2.3.1 SEM data

In transverse section, the avian eggshell is clearly divisible into various layers: mammillary layer or cone layer, palisade layer, and cuticle layer (Fig 2.2). The innermost layer is the mammillary layer that showed a thickness of around 800 μm while the main thickness of the shell is that of the palisade layer (~1800 μm).

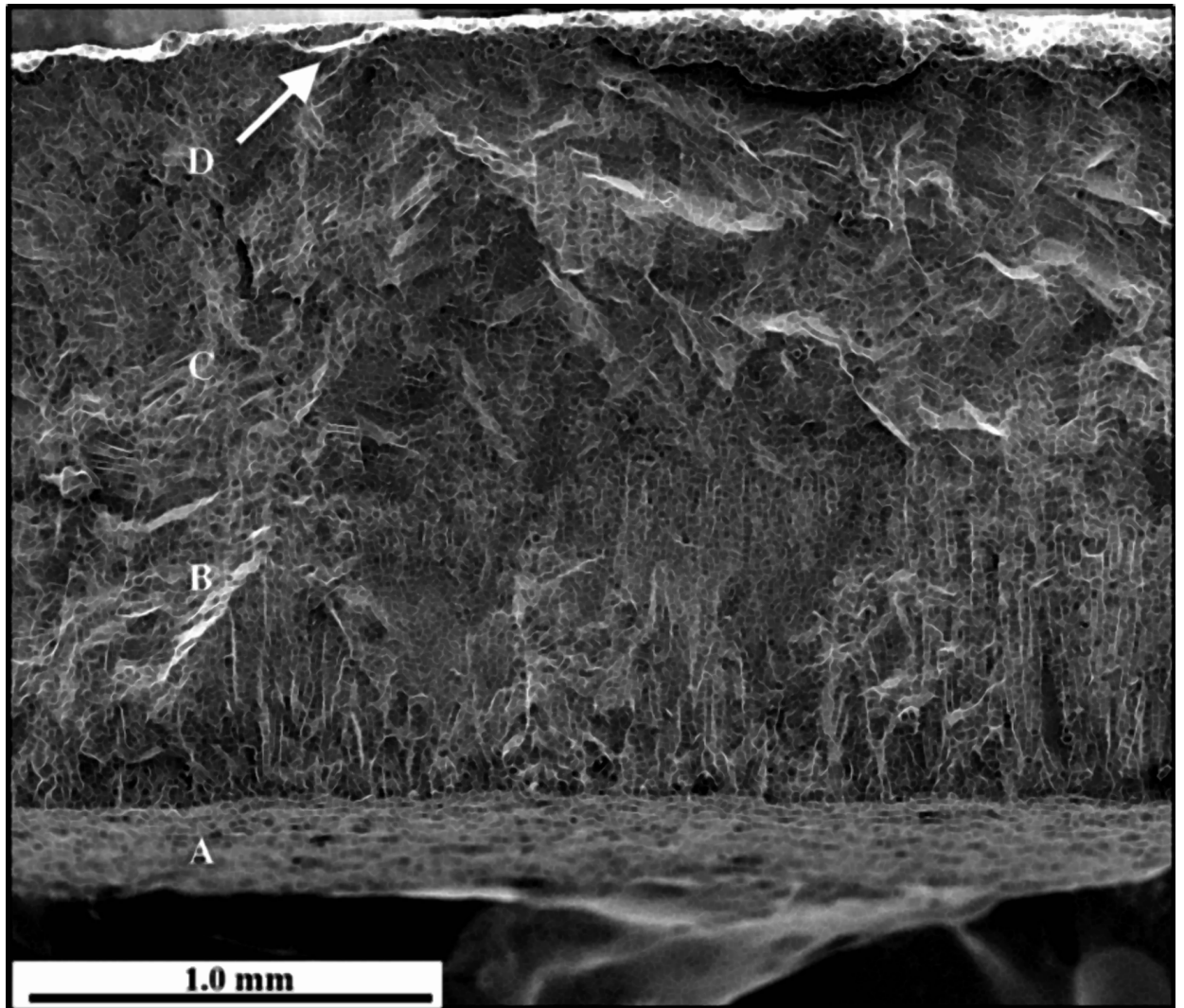


Figure 2.2 SEM morphology of the cross-sectional plane of ostrich eggshell. A) Organic membrane B) Cone layer C) Palisade layer D) Cuticle layer

The internal surface of the ratite eggshell showed well-developed mammillary knobs that were either circular or sub-circular in shape with irregular spacing that characterize inter-mammillary ventilation duct systems which separate the mammillae (Fig 2.3 A).

These duct systems pass through the inter-mammillary spaces and reaches the outer surface of the shell as observed in Fig 2.3 B.

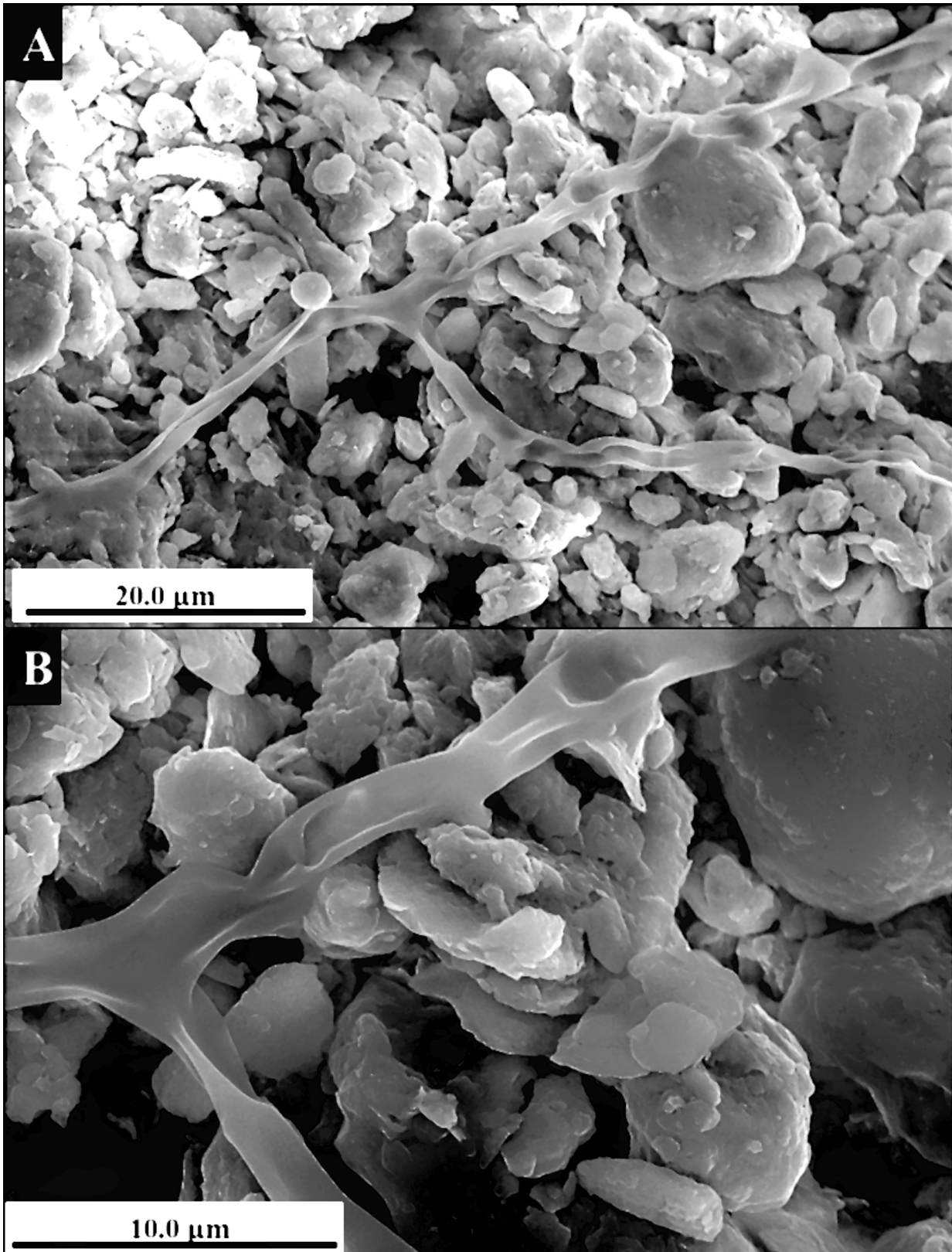


Figure 2.3 Internal surface of eggshell shows mammillary knobs. Image captured at A) 20 μm B) 10μm

The delineated crystallites consist of an asymmetrical appearance in the regions closer to the mammillary layers were analyzed using SEM (Fig. 2.4). The crystals run in a crisscross manner and this dissimilarity could be associated with differences in the demarcated crystallite morphology of the palisade layer.

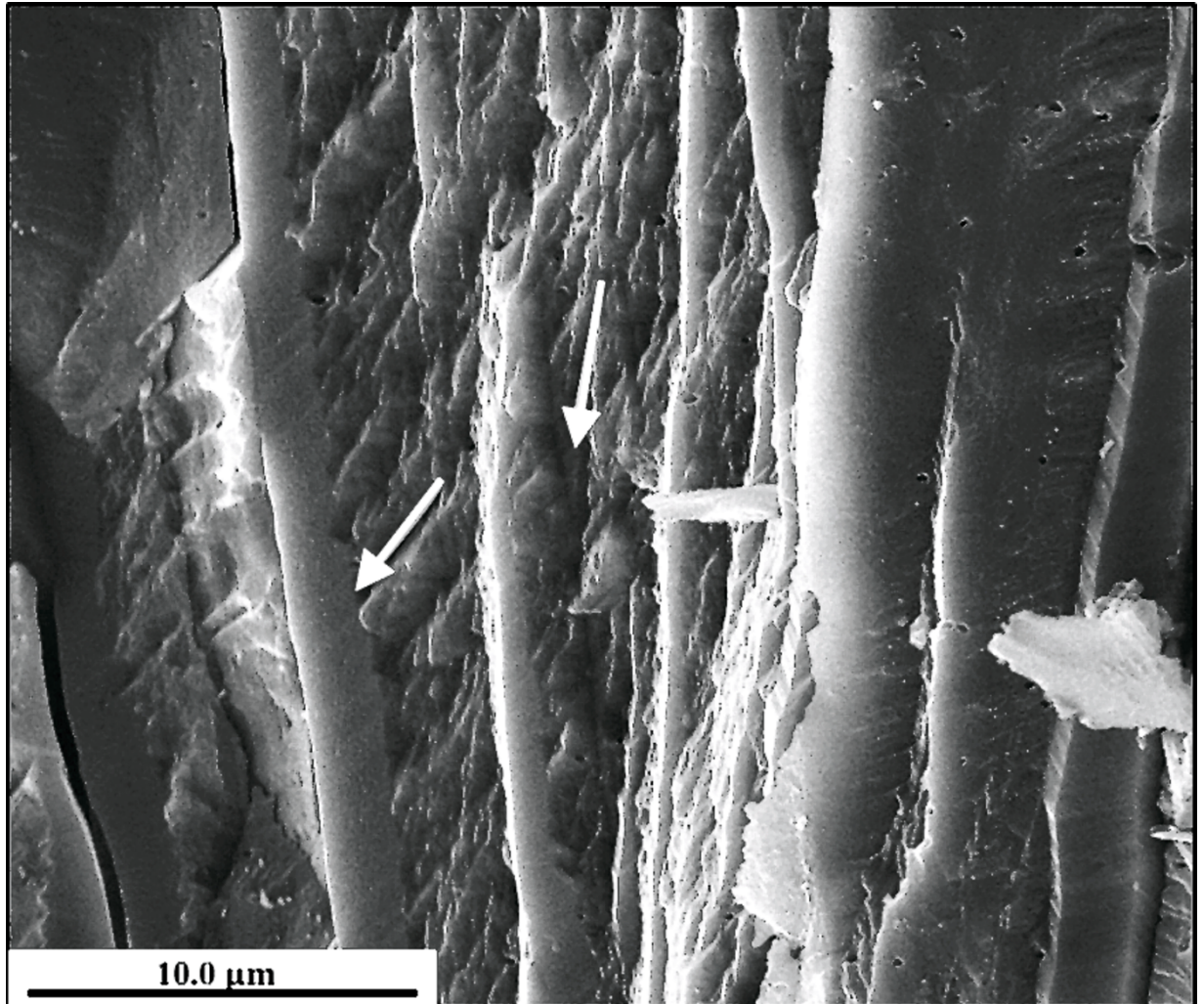


Figure 2.4 Palisade layer of eggshell. Irregular appearance of the crystallized layer

SEM analysis of the external surface of the eggshell showed the presence of pores in the shallow circular pits (Fig. 2.5). These pores vary in number from specimen to specimen. There is no clear pattern of distribution of the small pores that are observed on the eggshell surface.

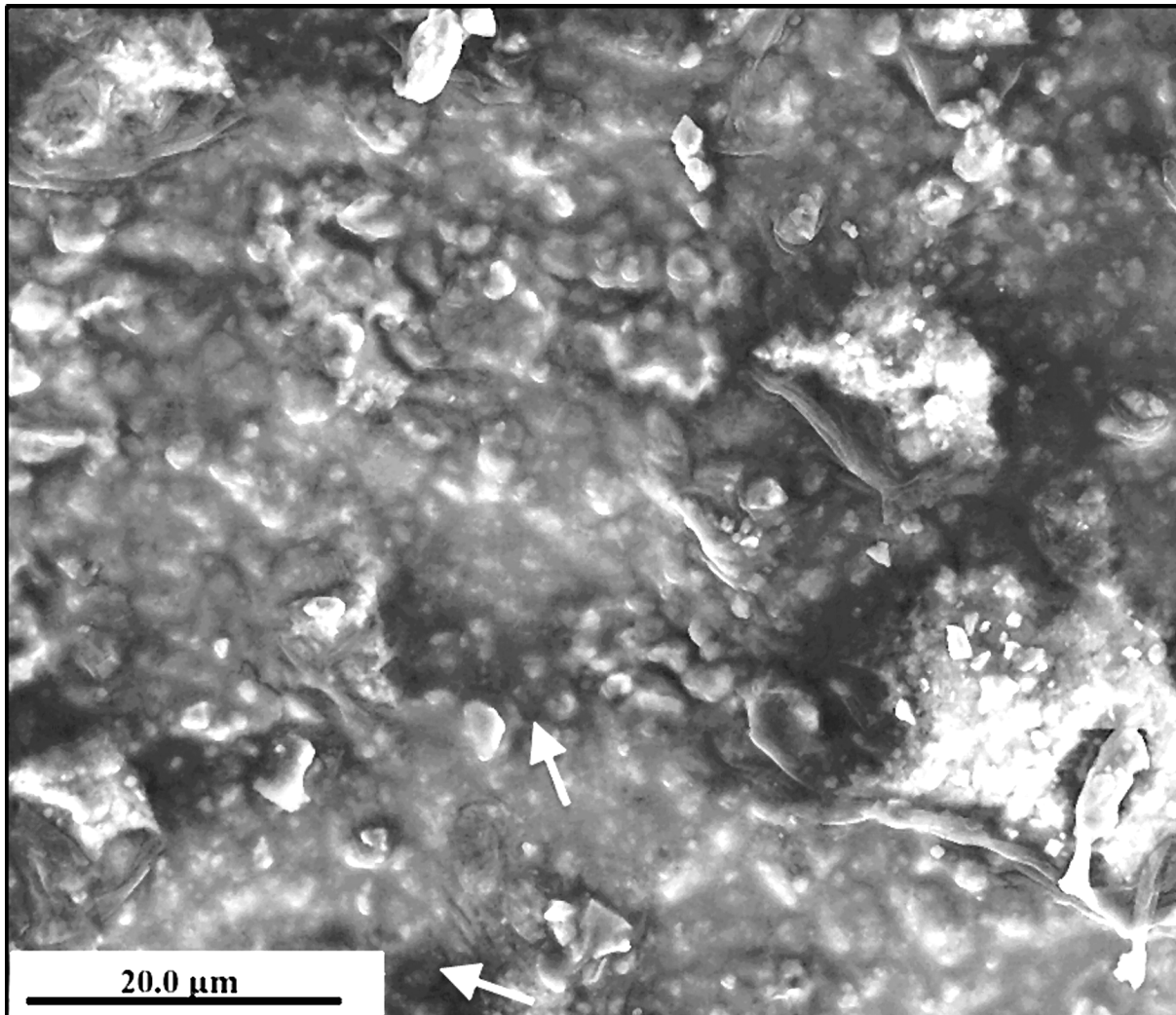


Figure 2.5 Pores on the exterior surface of eggshell. Pores are observed on the exterior surface at 20 μm .

The outer shell membrane (OSM) consists of a number of layers of fibrous material that seems to run at right angles to the layer above and below. Numerous cup-shaped structures were observed on the upper fibrous layer that faces the mammillary layer (Fig 2.6). This cup-shaped structure seems to be made from the same material as that of outer shell membrane. There is a close connection between cup-shaped structures present on the outer shell membrane and mammillary layer of the calcified portion of the eggshells. The preliminary calcium carbonate growth of the calcified shell was of dendritic nature with nucleation sites present on

the surface of the cup's content. The primary calcification is comprised within the cups and was further targeted outwards to form the shell and cuticle layer. The above observations indicated that primarily the calcification is contained within the cups and it is then directed outwards to form the shell, and may contain an evolutionary, calcified cuticular layer, which contains preserved biomolecules for ancient DNA studies.

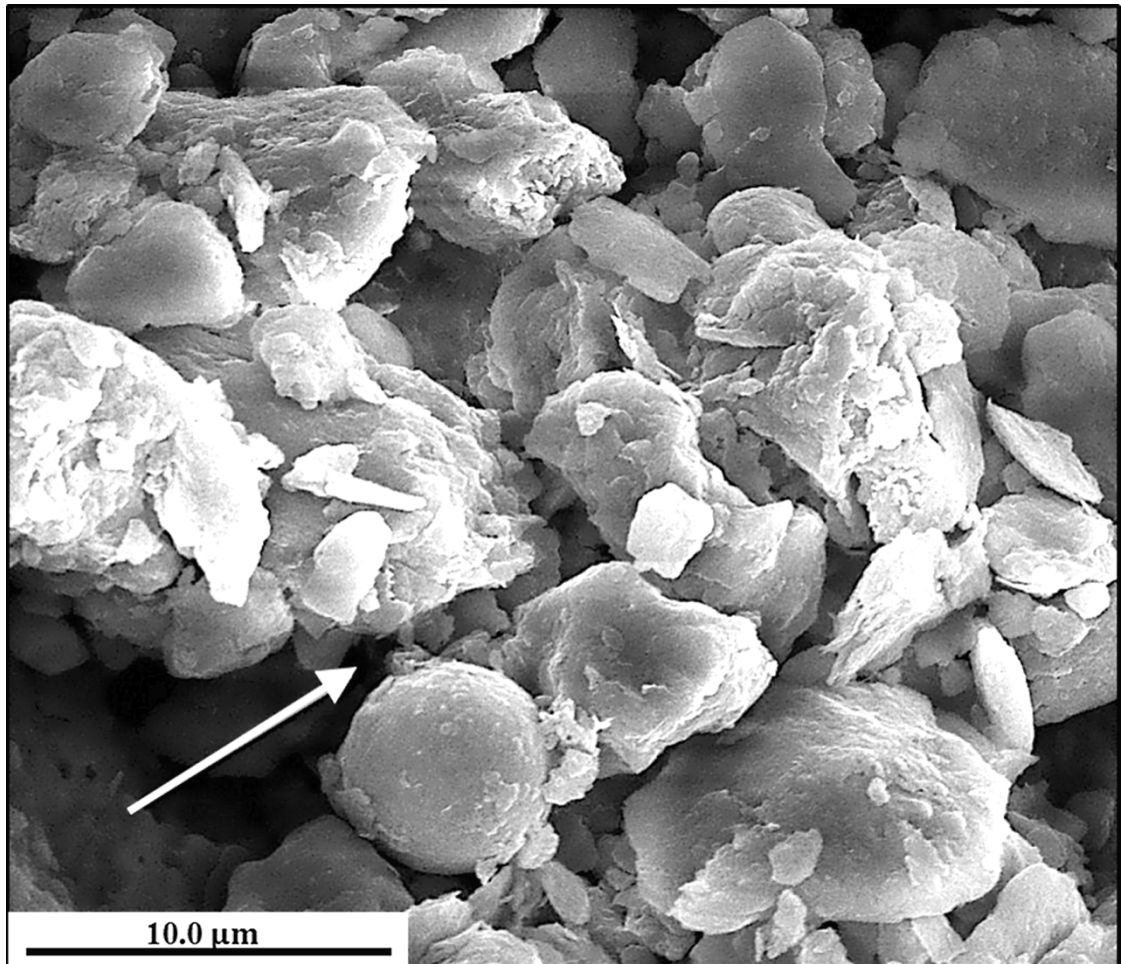


Figure 2.6 Outer shell membrane of eggshell. Cup-shaped structure observed at 10μm.

XRD data

XRD pattern of powdered and plaque samples were examined to explore the mineralogy and preferred orientation of eggshell layers. The graphs of X-Ray Diffraction for the powdered samples were plotted in JADE software as shown in Fig 2.7. Two samples and one standard were analyzed to study the extent of diagenesis in the fossil eggshell samples compared to the modern eggshell. The major component observed in both the samples was calcite and there was

no indication of any alteration to the secondary elements, considering them to be suitable for genetic studies.

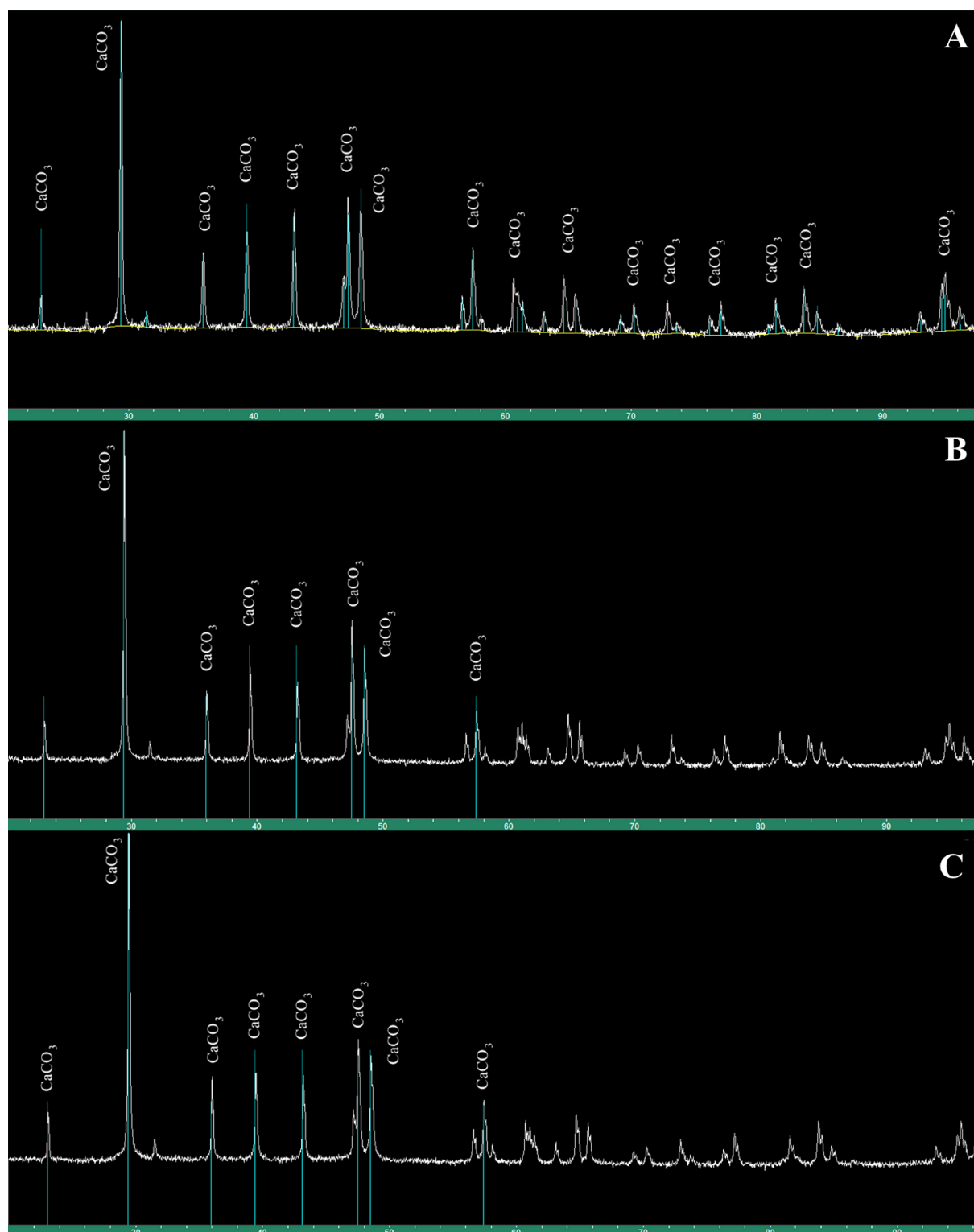


Figure 2.7 XRD patterns of the powdered eggshell samples from three different locations. (A) Bundi, India (B) Chandresal, India (C) Modern eggshell from Africa

EBSD data

EBSD analysis of the control modern ostrich eggshell showed the presence of well defined large calcite crystals, as seen in the diffraction map, with c-axis parallel to the elongation of the crystals and perpendicular to the outer eggshell surface (Fig 2.8). These observations were identical to those previously reported from an ostrich eggshell in a comparison of the structure and chemistry of modern avian eggshells (Dalbeck and Cusack, 2006). The subsequent analysis of fossil eggshells, from Bundi and Chandresal, produce similar results although there was more variability in crystal sizes (Figs 2.9 and 2.10). However, in several instances, the generated Kikuchi patterns were not perfectly matched with crystal lattice parameters of calcite, indicating the presence of a different carbonate mineral phase. Dolomite was the perfect match for these diffraction patterns and thus, EBSD phase maps were generated to determine the distribution of dolomite in relation to calcite in fossil eggshells. Overall results for both fossil eggshells show that the distribution of dolomite was not uniform across the eggshell thickness and there is more dolomite towards the outer surface, even generating continuous crystallographic domains in the sample collected from Chandresal (Fig 2.10). Also, higher concentrations of dolomite were localized in certain calcite crystals independently of the location within the eggshell, and that the dolomite was concentrated in nano to micro-domains. Despite the presence of dolomite, the overall preferred crystallographic orientation of calcite crystals was maintained. The distribution and amount of dolomite suggest an incipient transformation of calcite to dolomite in these fossil eggshells. The detection of dolomite on these samples represents an example of the advantage of in situ high-resolution EBSD analyses over other crystallographic techniques (i.e., XRD) in detecting diagenesis.

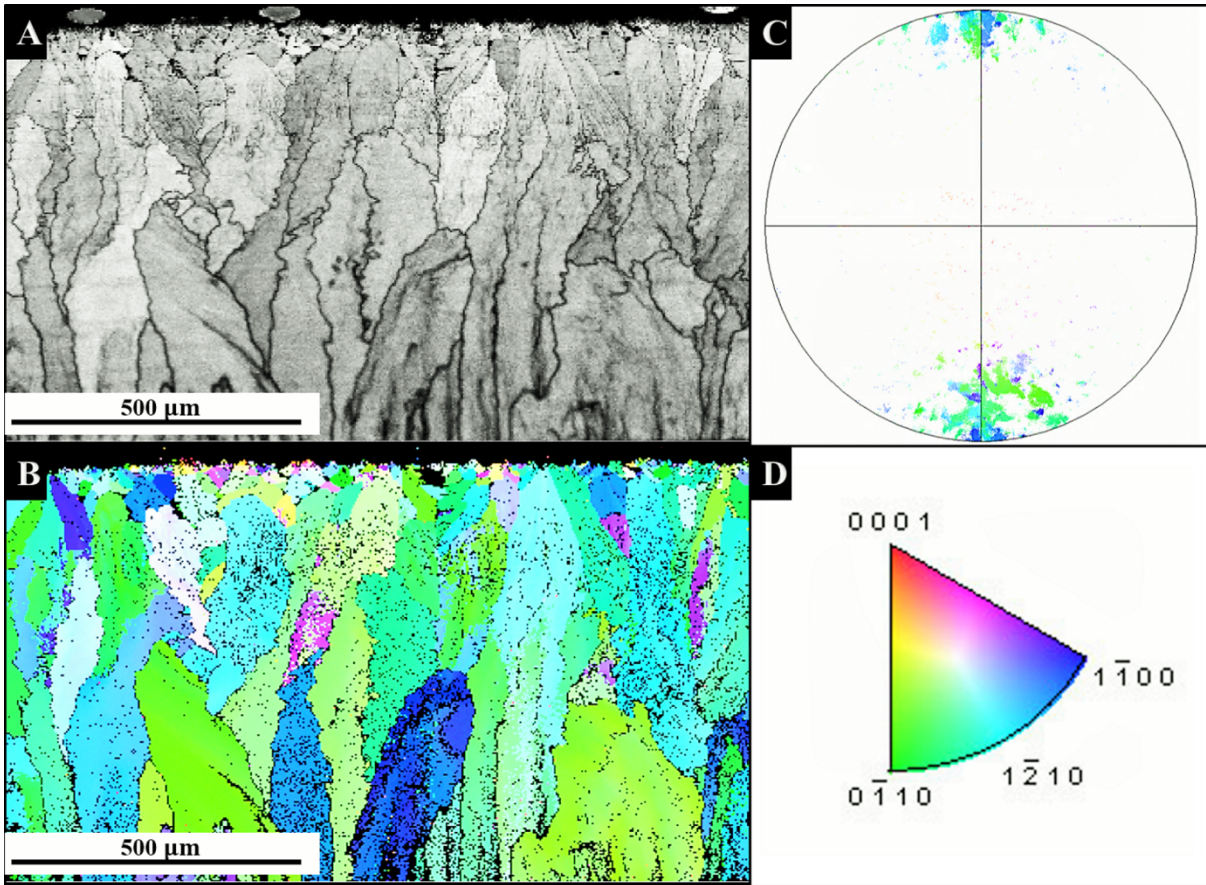


Figure 2.8 High-resolution EBSD data in modern ostrich eggshell, Africa. A) Diffraction intensity map at the top of the shell showing calcite prisms at 500 μm B) Corresponding color crystallographic map to (A) at 500 μm C) Corresponding pole figure to (B) in reference to {0001} D) Color-key for crystallographic planes in calcite.

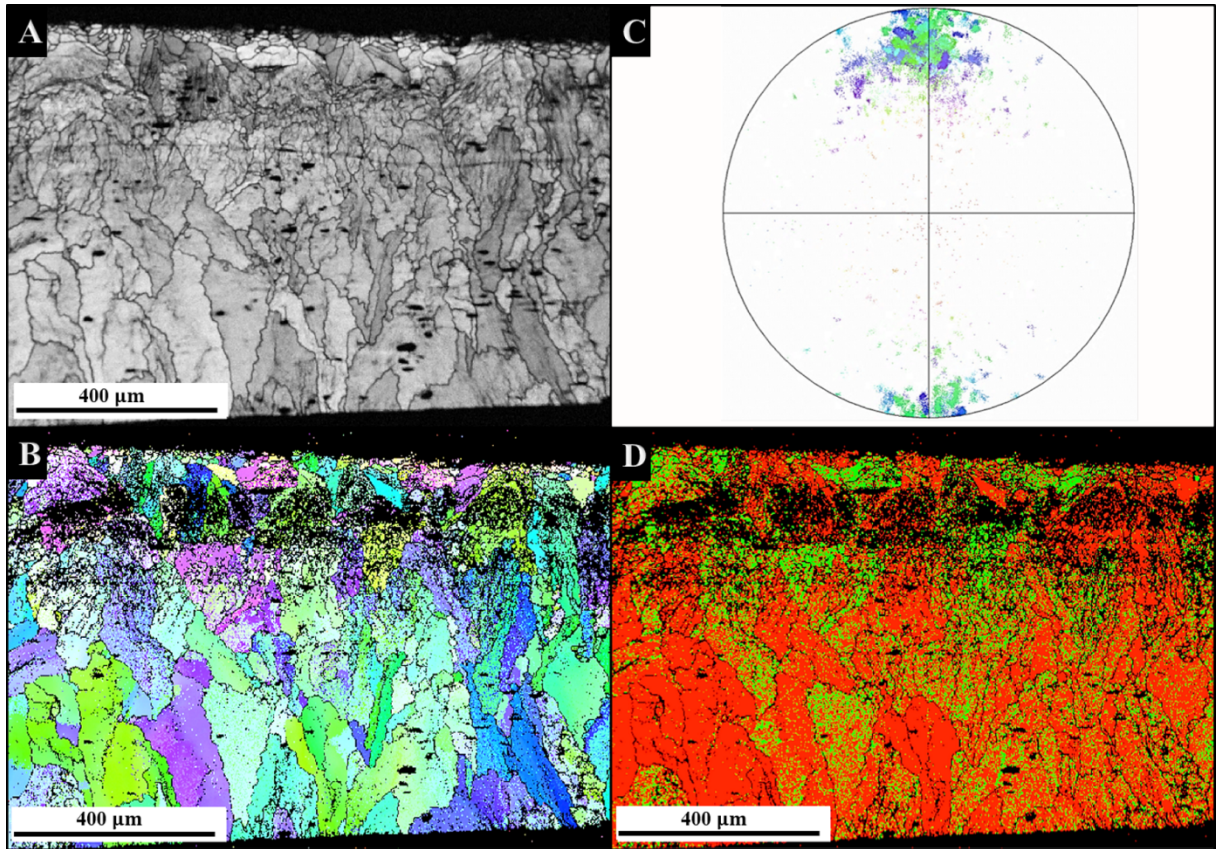


Figure 2.9 High-resolution EBSD data in fossil eggshell from Bundi, India. **A)** Diffraction intensity map at the top of the shell showing calcite prisms at $300\ \mu\text{m}$ **B)** Corresponding color crystallographic map to (A) at $300\ \mu\text{m}$ **C)** Corresponding pole figure to (B) in reference to $\{0001\}$ **D)** Crystallographic color coded map showing distribution of calcite and dolomite Red color denotes calcite and green color denotes dolomite.

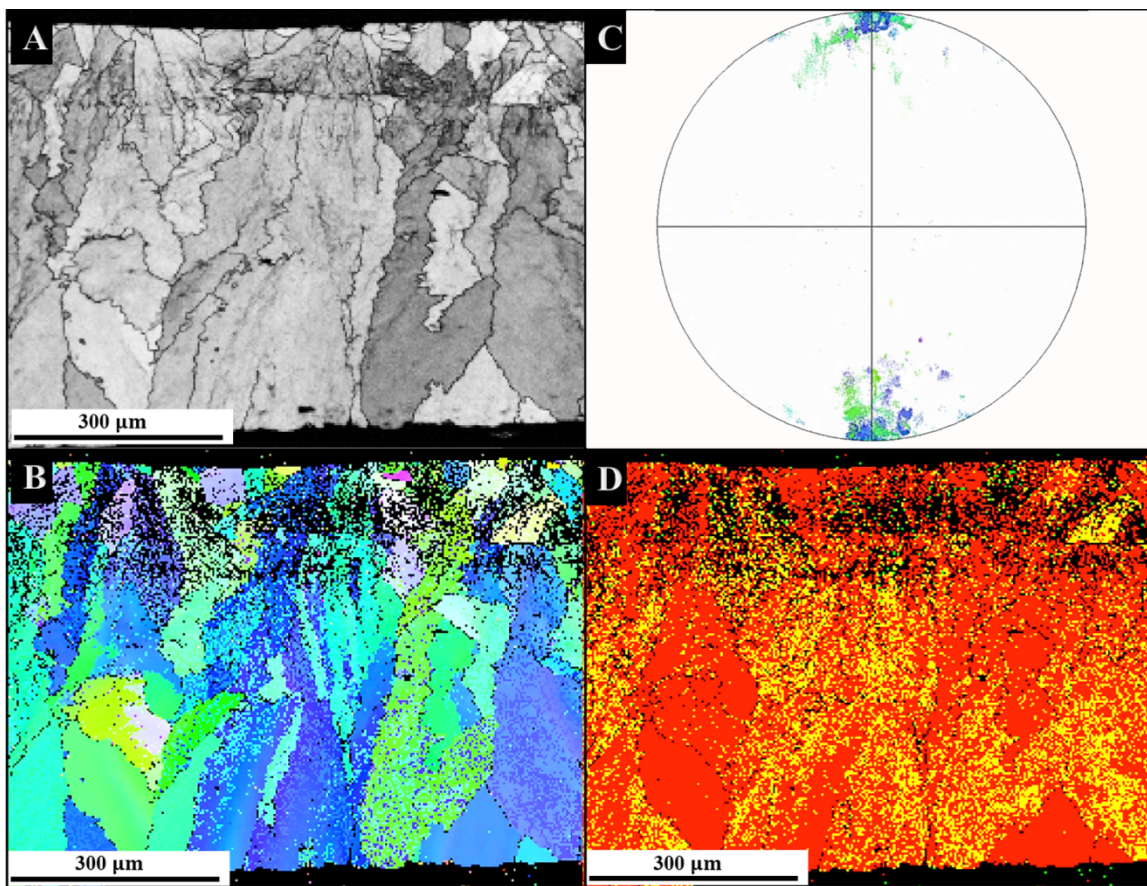


Figure 2.10 High-resolution EBSD data in fossil eggshell from Chandresal, India A) Diffraction intensity map at the top of the shell showing calcite prisms at 400 μm B) Corresponding color crystallographic map to (A) at 400 μm C) Corresponding pole figure to (B) in reference to $\{0001\}$. D) Crystallographic color-coded map showing the distribution of calcite, dolomite, and aragonite. Red color denotes calcite, yellow color denotes dolomite and green color denotes aragonite.

2.4 Concluding Remarks

The analysis of the eggshell fragments recovered from the Upper Paleolithic sites showed the detailed structure of various layers and calcite crystallization of ostrich eggshells. Despite the good preservation indicated by SEM and XRD data, EBSD revealed the presence of dolomite in samples from two localities. Although the dolomitization of these eggshells appeared to be incipient, it might have compromised the recovery of biomineral material for DNA analysis. Overall, our study determines the nature and extent of diagenesis in these eggshells and the importance of using multiple microscopy and chemical techniques to illustrate diagenesis in fossils from archeological sites.

CHAPTER 3

CONFOCAL MICROSCOPY AND ANCIENT DNA ANALYSIS ON EGGSHELLS

3.1 Introduction

Ratites are found in various parts of the world but are reported to be extinct from India. Early research showed the presence of ratites in India as evidenced by the eggshell fossils found at various sites, ranging in age since the Middle Miocene to Late Pleistocene (Roberts et al., 2014; Blinkhorn et al., 2015). The presence of these eggshell fossils in India and other South Asian countries raises the question of evolution and extinction of these ratites all over the world. Richard Dawkins describe the evolution of ratites in his book “The Ancestor’s Tale” (Dawkins, 2004). One hundred and seventy million years ago ratite birds roamed over the whole Gondwanaland. As the sudden drifting of continents begins around 100 million years ago, rheas, emu, elephant bird, and ostriches got separated. Rhea and emu moved to South America and Australia respectively while elephant bird and ostriches were together in India and Madagascar. 60 million years ago India drifted towards north and Madagascar broke apart separating the two lineages. Cooper et al. suggested that ostriches arrived in Africa via the land route of Arabia through India about 20 million years ago and are still present in Africa. This theory was supported by the presence of ostrich fossils on this route (Cooper et al., 2001; Dawkins, 2004). The eggshells from India have been dated at Upper Palaeolithic (25,000 to 40,000 years B.P), based on stone implements (Kumar et al., 1988; Sahni et al., 1989, 1990) and radiocarbon dating at Groningen University Lab, Germany (Kumar, 1983; Mohabey, 1989). Some of these eggshells are engraved into finished or unfinished beads (Kumar et al., 1983; Bednarik, 1993a; 1993b; 1994). The perforated beads belong to archaeological assemblages, which correspond to the same time period when contemporary humans dispersed from Africa to South Asia (Mellars, 2006).

Paleoenvironmental studies on these eggshells provide valuable insights about the debate regarding the time period of dispersion of contemporary human population out of Africa, indicating that during the late Pleistocene the continental dispersal of ostrich into India contrasts with the hypothesis of movement of modern humans in India (Blinkhorn et al., 2015). The paleogeological and archaeological significance of these eggshells are well recognized but

their origin continues to be poorly understood (Badam, 2005; Nys et al., 2004; Patnaik et al., 2009).

Taxonomically, eggshells can be identified on the basis of characters such as eggshell thickness, pore complex shape, density and diameter (Sauer and Sauer, 1978; Pickford and Senut, 2000; Harris and Leakey, 2003; Stidham, 2004). Comparative ultrastructural and thin section studies suggest that these eggshells are closely similar to those of modern East African subspecies *Struthio camelus* subsp. *molybdophanes*, although assignment to this subspecies based on external characteristics may not be correct (Johnson et al., 1997; Hincke et al., 2000; Miller et al., 2000; Patnaik et al., 2009). Evidence gathered from rock shelter paintings in central India also describes ostrich figures but there was controversy raised about its identification (Wakankar, 1984; Tiwari, 2000), which could only be ascertained by molecular evidence.

In spite of over two decades of aDNA studies, fossil eggshells have only recently been recognized as a source of aDNA with excellent preservation of biomolecules (Oskam et al., 2010). The avian eggshell has a characteristic structure consisting of several layers (mammillary layer, palisade layer, and cuticle layer) from the inner surface to outer surface (Figure 3.1). The matrix of the avian eggshell is porous, ordered and heterogeneous complex, which is coupled with extracellular structure, composed of mineralized and non-mineralized regions having calcium carbonate (calcite 97%) and 3.5% organic matrix (Carrino et al., 1996; Hincke et al., 2000; Feng et al., 2001). The intracrystalline organic matrix of avian eggshells restrains diffusion losses and prevents the isotopic exchange of its organic constituents (Miller et al., 1992; Johnson et al., 1997; Oskam et al., 2010). This structural hallmark provides an external skeletal support to the developing avian embryo and controls gases, water exchanges as well as guards it from microbial interventions and physical stresses (Nys et al., 2004; Wellman-Labadie et al., 2008a, 2008b; Oskam et al., 2010). This well-defined eggshell ultrastructure and microparticles of CaCO₃ imparts stability and excellent mechanical strength to the eggshell, which in turn provides antibacterial and antifouling properties to the avian eggshell and results in biomolecule preservation (Nys et al., 2004; Fink et al., 2006).

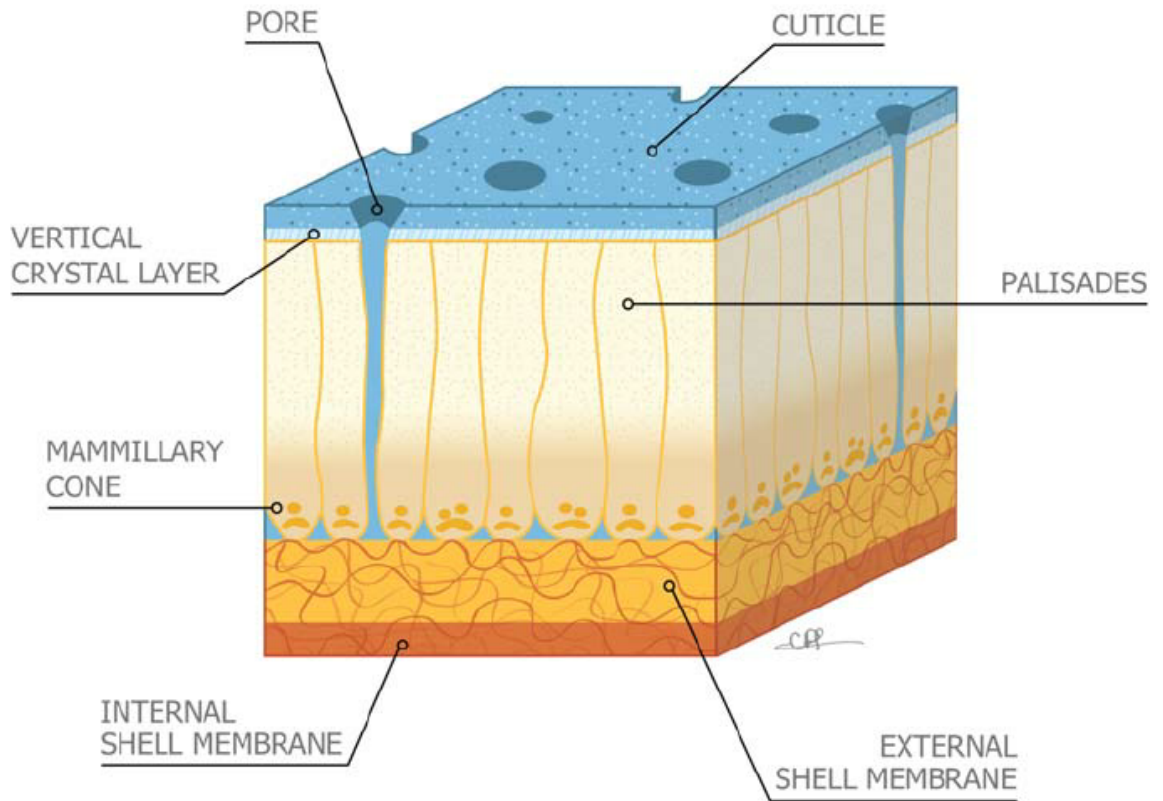


Figure 3.1 Ostrich Eggshell. Pictorial view showing layers and membranes of eggshell (Hincke, 2012)

In this investigation, we analysed the extent of aDNA present in fossilized avian eggshells; collected from various Upper Paleolithic sites in India (Fig 3.2). DNA hotspots were found using DNA binding fluorescent dye Hoechst 33342 and imaged through CLSM. aDNA was then successfully extracted and quantized using Bioanalyzer and then amplified using species-specific primers. Obtained DNA sequences were submitted in NCBI with GenBank accession number KU251475.



Base 802813AI (CO0213) 10-01

Figure 3.2 Ostrich eggshell sample collection locations from Indian subcontinent as shown on the map. (A) Bundi (B) Anjar (C) Chandresal-1 (D) Nagda (E) Runija (F) Khajurna (G) Ravishankarnagar (Source: cia.gov)

3.2 Materials

3.2.1 Common chemicals/plastic wares

Chemicals such as chloroform, isopropanol, methanol, formamide, glacial acetic acid, glycerol, molecular biology grade water, ethylene diaminetetraacetic acid (EDTA), ethidium bromide, b-mercaptoethanol, Sodium Dodecyl Sulfate (SDS) and agarose etc. were procured from Sigma-Aldrich (St. Louis, USA), Merck (Darmstadt, Germany). AmpliTaq gold, platinum Taq, PCR high fidelity master mix and DNA molecular size markers were obtained from Applied BioSystems (Foster City, CA, USA). Plastic ware such as PCR tubes, PCR plates, and centrifuge tube, micropipette tips, petri plates etc. was obtained from Axygen Scientific (San Francisco, CA, USA), Eppendorf (Hamburg, Germany), Tarson or Laxbro.

3.2.2 Reagents and kits

Reagents and kits used in this study are listed below:

- PCR Purification kit (Qiagen, Venlo, Netherlands).
- QIAamp DNA investigator kit (Qiagen, Venlo, Netherlands).
- pMOS Blue, Blunt ended cloning kit (Amersham, South East England, UK).
- Mass Array SNP genotyping kit (Sequenom, San Diego, USA).
- BigDye Terminator (v3.1) Cycle sequencing kit (Applied BioSystems, Foster city, USA).
- PCR hot start master mix (Thermofisher, Waltham, Massachusetts, USA).
- AmpF/STRidentifiler and minifilerPCR amplification kit (Applied BioSystem, Foster city, USA).

3.2.3 Solutions, buffer, and media

- 10X TAE 0.9 M Tris base, 10 mM EDTA, pH adjusted to 8.0 with glacial acetic acid.
- 10XTBE 0.9 M Tris base, 10 mM EDTA, pH adjusted to 8.0 with boric acid.
- LB 1% bactotryptone, 1 % NaCl, 0.5 % yeast extract, pH 7.0.
- LB agar LB containing 1.5 % bactoagar.
- Ampicillin 100 mg/ml stock in sterile distilled water
- IPTG 100-mg/ml stock of isopropyl thio- β -D-galactoside in sterile distilled water.
- X-gal 20 mg/ml of X-gal in dimethyl formamide.
- PBS 130 mM NaCl, 2.5 mM KCl, 5.3 mM Na₂HPO₄, 1.7 mM KH₂PO₄ pH adjusted to 7.4 with HCl.
- TE 10 mM Tris-HCl (pH-7.5-8.0), 1 mM EDTA

3.2.4 Samples

Fossilized eggshell samples used in this study came from the personal collections of Dr. Sunil Bajpai and Dr. Giriraj Kumar from the Pleistocene surface deposits of Gujarat, western India, and few eggshell fragments were recovered from excavation sites at Bundi (Rajasthan state, western India) as shown in Fig 3.2. Fossil avian eggshell fragments were analyzed, collected from eight different sites in India as shown in Table 3.1. These samples collected were referred to the genus *Struthio* on the basis of morphological characters, like thickness and pore pattern on eggshells (Kumar et al., 1998; Sahni et al., 1989).

Table 3.1 Ostrich eggshell sample collection sites and their respective states

S.No.	Site	Area	State & GPS Co-ordinates	Catalogue No.	Dates	Method	Reference
1	Chavni Baroda	Bundi	Rajasthan (25° 26' 24" N, 75° 38' 24" E)	SJ/CB/001 SJ/CB/002	-	-	-
2	Anjar	Kachchh	Gujarat (23° 6' 48.32" N, 70° 1' 39.88" E)	SB/AN/003	>25000	C ¹⁴	Sahni et al. (1989)
3	Chandresal-1	Kota	Rajasthan (25° 10' 48" N, 75° 49' 48" E)	GK/CH1/004 GK/CH1/005	38900 ±750	C ¹⁴	Mishra (1995)
4	Chandresal-2	Kota	Rajasthan (25°13'34.1"N75°55'34.7"E)	GK/CH2/006 GK/CH2/007	36500 ±600	C ¹⁴	Agarwal et al. (1991)
5	Nagda	Chambal	Rajasthan (25°10'53.3"N75°48'45.5"E)	GK/NA/008	>31000	C ¹⁴	Mishra (1995)
6	Runija	Ujjain	Madhya Pradesh (23°09'39.4"N75°16'02.6"E)	GK/RU/009	>25000	C ¹⁴	Mishra (1995)
7	Khajurna	Bijora	Madhya Pradesh (26°44'33.6"N78°47'45.6"E)	GK/KH/010	>25000	C ¹⁴	Mishra (1995)
8	Ravishankar Nagar	Bhopal	Madhya Pradesh (23°15'34.8"N77°24'24.9"E)	GK/RN/011	>25000	C ¹⁴	Mishra (1995)

3.3 Methodology

3.3.1 Confocal laser scanning microscopy studies

The confocal microscope was used to determine the location of DNA preserved in ratites eggshells. The samples were incubated in square chambered plates with DNA-binding fluorescent dye, Hoechst 33342 (1mg/ml) (Sigma, USA) at room temperature for 15 minutes and imaged under Leica TCSSP5AOPS Confocal system. Images were captured (405 nm) using 10X, 40X (1.25 oil immersion) objectives while 3-D sections snapshots were taken using Galvo-Z stage for Z sectioning. Cross-sectional images of eggshells obtained were analysed using LASAF LITE software. Unstained eggshells samples were used as the control.

3.3.2 Ancient DNA analysis

3.3.2.1 Ancient DNA lab set-up and precautions

Ancient DNA study is challenging research task, as there is always a chance of exogenous DNA contamination. The major concern throughout the entire work was to avoid contamination by exogenous DNA. Steps involved are eggshell cleaning; drilling, DNA extraction, and PCR preparation were carried out in two separate laminar airflow rooms. The ancient DNA rooms were designed with the positive pressure created by high filtered air (HEPA 0.5 micron filters), an exclusive water supply and ultraviolet (UV) irradiation to exclude contamination. Pipettes and other instruments used for DNA extraction were cleaned using commercial bleach and 70% alcohol, followed by UV irradiation for at least 45 minutes. DNA extraction and PCR was done in two different chambers. Disposable full body suits and gloves were used throughout the processing of the samples. Aerosol barrier tips (Fisher Scientific, Hampton, USA) and ultrapure DEPC treated water (Invitrogen, Carlsbad, USA) were used for all the experiments that were carried out in the ancient DNA laboratory.

3.3.2.2 Ancient DNA extraction

Eggshell samples were wiped out with 5% hypochlorite solution followed by surface cleaning using 70% alcohol. A small piece of eggshell was cut from the source eggshell using DremelMultiPro tools and powdered to 700-800mg. Eggshell powders were further subjected to the DNA isolation using Oskam and Bunce, 2012 protocol with slight modification). Powdered eggshell was incubated in a digestion buffer (700 mL per sample) containing final

volumes of 0.47 M EDTA (pH 8.0), 20 mM Tris (pH 8.0), 1% Triton X-100, 10 mM, Dithiothreitol (DTT), 1 mg/mL proteinase K for up to 24 h, followed by a final heating at 92⁰C. This heating step aids in solubilisation of calcite, which helps in releasing the DNA from the crystalline matrix. The heating step was modified as to prevent the complete denaturation of DNA. The solution was then concentrated with 30,000 KDaMWCO columns (Millipore) and purified using commercial silica spin columns (Qiagen).

3.3.2.3 Ancient DNA quantification using real-time PCR

Prior to amplification, quantitative PCR (qPCR) was used to determine the quantification of DNA, using DNA quantification kit (Applied Biosystems, Foster City, USA). Two microlitres of DNA was used in a final reaction volume of 10.0 µl as instructed by the manufacturer. ABI Prism 7500 Sequence Detection System (7500 SDS) and SDS software (V 1.0) were used for real-time PCR, data collection, and analysis (Applied Biosystems, Foster City, USA). All possible precautions were taken to avoid contamination with exogenous DNA.

3.3.2.4 Ancient DNA quantification using Bioanalyzer

Agilent 2100 Bioanalyzer (Agilent technologies) was used for the quantification of ancient DNA. One microliter of genomic DNA, extracted from the eggshell sample, was loaded into size selection and quantifier chip. The reagents and protocol were used as per the guidelines of Agilent 2100 DNA chip. Due to very high degradation of eggshell samples quantity of DNA observed was low (Fig 3.3). The quantification and size selection of ancient DNA helped in designing the PCR primers.

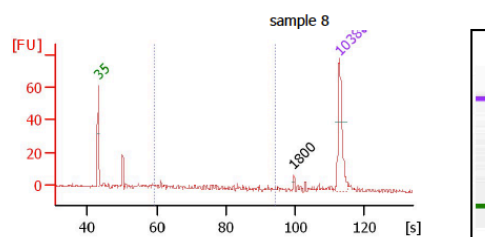
3.3.2.5 Ancient DNA primer designing

Since the mtDNA exist in high copy number and is transmitted maternally, recovery of mtDNA from the eggshell samples will be significantly higher than the nuclear DNA. PCR primers that can amplify overlapping mtDNA HVR and 16sRNA fragments were designed (Table 3.2) using Gene tools, Primer express and Primer 3 software. Amplify 3X tool was used to predict the primer dimer annealing probability and to check the GC content of the designed primers.

Electropherogram Summary Continued ...

Peak table for sample 7 :

Peak	Size [bp]	Conc. [pg/μl]	Molarity [pmol/l]	Observations
1	35	125.00	5,411.3	Lower Marker
2	132	216.09	2,474.0	
3	144	39.09	410.8	
4	173	24.62	216.1	
5	191	26.32	209.1	
6	225	15.97	107.5	
7	233	21.79	141.4	
8	244	37.45	233.0	
9	405	2.95	11.0	
10	1,709	3.40	3.0	
11	1,891	4.48	3.6	
12	2,293	4.87	3.2	
13	2,781	5.96	3.2	
14	3,477	4.97	2.2	
15	4,409	5.90	2.0	
16	6,388	6.79	1.6	
17	7,217	12.81	2.7	
18	8,135	8.26	1.5	
19	10,380	75.00	10.9	Upper Marker
20	14,921	0.00	0.0	
21	16,758	0.00	0.0	



Overall Results for sample 8 :

Number of peaks found:	1
Noise:	0.8
Corr. Area 1:	20.7

Region table for sample 8 :

From [s]	To [s]	Corr. Area	% Total	Average Size [bp]	Size distribution in CV [%]	Conc. [pg/μl]	Molarity [pmol/l]	Color
59.43	94.45	20.7	30	389	41.7	23.60	114.8	Blue

Figure 3.3 Size selection and quantification of an ancient DNA sample extracted from eggshell

Table 3.2 Primer sequences used for PCR and sequencing of 16s and control regions of mitochondrial DNA

Primer name	Sequences	Gene
2F	5'GTACCGCAAGGGAAAGATGA3'	16sRNA
2R	5'GGATGGCAAGCTTAAATTCG3'	
4F	5'GGGGTACCCTCTAATGGA3'	16sRNA
4R	5'AGCTGGTTGCCTGTGAAAAG3'	
7F	5'CGACTCAGGAGCGCCTATTA3'	16sRNA
7R	5'TGGCTGAAGGCTATGTTTTTG3'	
1CF	5'TCGCGATTAAGAGGGACAAT3'	Control Region
1CR	5'TCCATTCACGTTCCCCTTA3'	

3.3.2.6 Polymerase chain reaction (PCR)

Primers were custom-synthesized by Sigma-Aldrich Chemicals Pvt. Ltd, Bangalore, India & IDT, USA. All routine PCR reactions were set in a 25 μl PCR tube containing 100 - 200 pg of DNA, 1XPCR buffer, 150 μM dNTPs, 1.5-2.5 mM MgCl₂, 4 pico- moles of each primer, 100 mg/ml of BSA and 1 U of AmpliTaq Gold (Applied Biosystems). PCR was done in Veriti (Applied Biosystems, Foster city, USA) or GeneAmp (Applied Biosystems, Foster city, USA).

3.3.2.7 DNA sequencing

The amplified PCR product was sequenced using Sanger's di-deoxy chain terminator cycle sequencing method. PCR products were purified by treating with Exonuclease I and Shrimp Alkaline Phosphatase (ExoSAP-IT®; USB Corporation, Cleveland, Ohio, USA) and incubated at 37°C for 15 min. followed by 80°C for 15 min. Purified PCR products (1.0 ml) were subjected to sequencing reaction, by adding of 0.65-2.0 pico- moles of the primer and 3.2 µl BigDye™ (Applied Biosystems, Foster City, CA, USA; containing fluorescently labeled ddNTPs and unlabeled dNTP). The sequencing PCR conditions include; 30 cycles of 94°C for 10 sec, 55°C for 5 sec and 60°C for 4 min. The PCR product was precipitated using 3 M sodium acetate (pH 5.2) and ethanol and centrifuged at 4,000 rpm at 4°C for 15 min. The pellet obtained was washed with 70% alcohol, air dried and suspended in 10 µl of HiDi™ formamide (Applied Biosystems, Foster city, USA). The pellet was loaded onto ABI 3730 Automated DNA analyzer, after denaturation at 94°C for 10 min. The samples were then run using POP-7™ polymer and analyzed using 'Sequencing Analysis' software (Applied Biosystems, Foster city, USA).

3.3.2.8 Multiplex PCR and genotyping using sequenom

Degraded ancient DNA samples were genotyped using Sequenom iPLEX assay and the MassARRAY system (SEQUENOM, San Diego, CA). Sequenom-based method requires very less amount of DNA (in picograms) and has the ability to work with highly degraded small-size amplicons (~ 40 bp). Therefore, this technique is most appropriate for genotyping and to study the base modifications of ancient DNA samples. The SequenomMassARRAY system is based on matrix-assisted laser desorption/ionization time of flight mass spectrometry (MALDI-TOF MS). For the iPLEX assay, primers for the PCR and iPLEX reactions were designed and custom synthesized (SEQUENOM, San Diego, CA, USA).

Various concentrations of aDNA (100pg – 1ng) was amplified in 5.0 µl multiplexed PCR reaction, following manufacturer's instructions. Multiplex PCR was performed in GeneAmp 9700 thermal cycler (Applied Biosystems) using 10XPCR buffer, primer mix, dNTPs and HotStarTaq (Qiagen, Hilden, Germany). After PCR, the products were treated with shrimp alkaline phosphatase (SAP, Amersham, Freiburg, Germany) to dephosphorylate the left over dNTPs. The reaction conditions were for 37°C for 20 minutes to remove remaining dNTPs, followed by 85°C for 30 minutes to inactivate SAP and finally incubated at 4°C. After SAP treatment, multiplexed iPLEX reaction was performed. The iPLEX reaction components

were: 10XiPLEX buffer, iPLEX termination mix, and primer mix and iPLEX enzyme. The iPLEX reaction mixtures were then cleaned by adding 6 mg cationic resin SpectroCLEAN (Sequenom) using dimple plate and 16 µl of water. After that plate was sealed and kept in a rotating shaker for 20 min to desalt the iPlex solution. Completed iPLEX reaction products were marked in nanoliter volumes on a matrix-arrayed silicon chip with 384 elements (SequenomSpectroCHIP) using the MassARRAY Nanodispenser.

3.3.2.9 Cloning of PCR products in pMOS blunt end-cloning vector

Haplogroup defining mutations of ancient mtDNA were further cloned in pMOS blunt end cloning kit and sequenced. Cloning was carried out as per the manufacturer's instructions. Briefly, the pK reaction was carried out at 22°C for 40 min in the presence of 100-mM DTT and pK enzyme using the appropriate amount of the PCR product. The pK enzyme was heat inactivated at 75°C for 10 min. The treated product was ligated into pMOS vector in the presence of T4 DNA ligase at 22°C for overnight.

The ligation mix was transformed into ultra-competent DH5α cells by heat shock method. Frozen ultra competent cells (100µl) were thawed and incubated in ice for 20 - 30 min with 2.5 - 10 µl of the above ligation mix. The cells were subjected to heat shock for 90 seconds at 42°C. Quick chilling on ice followed it. Cells were incubated for 1 hr at 37°C in Luria-Bertani (LB) liquid medium (LB, 10 g Bactotryptone, 5 g Bacto yeast, 5 g NaCl per 1000 ml; pH 7.4) with gentle shaking. Transformed cells were plated on LB agar medium containing ampicillin (100µg/ml) and incubated at 37°C for 14 - 16 hours.

The multiple cloning sites (MCS) of pMOS Blunt End cloning vector are situated in the coding region of the lacZ gene. Colonies with recombinant plasmids remain white in the X-gal presence (5-bromo-4-chloro-3-indolyl- beta-D-galactopyranoside), because of disruption of lacZ genes. Colonies, which are self-ligated, will change into blue colour. Hence, X-gal (20 µg/ml) and IPTG (20 µg/ml; inducer of lac operon) were added during plating, for blue-white selection. White colonies were picked and were grown in LB media. Plasmid DNA was extracted using Qiagen plasmid purification kit (Qiagen, Germany). They were sequenced using universal M13 forward and reverse primers.

3.3.3 Statistical analysis

3.3.3.1 Gene Tool 2.0

Gene Tool 2.0 is a software package to design the primers and a tool for carrying out e- PCR to validate the primer affinity. This tool can also perform many analysis including sequence alignment, Vector construction, exon prediction and primer designing etc.

3.3.3.2 Primer 3

Primer3 is an online tool for designing primers for PCR and RT-PCR experiments. Primer3 is a widely used tool for PCR Primer designing. Both its online and downloadable versions are available; the online version (<http://frodo.wi.mit.edu/primer3/>) was used for designing primers.

3.3.3.3 Amplify 3X

Amplify 3X is a freeware mac program for simulating and testing PCRs. This Software was mostly used to validate the primers designed using other tools for the possibility if they make primer-dimer.

3.3.3.4 NCBI Primer BLAST

Primer BLAST is most commonly used tool of NCBI. It designs primers using Primer3 and used for checking the specificity of these primers across the selected database (full genome and selected regions). It also improves the difficulty in designing target-specific primers.

3.3.3.5 AutoAssemblerTM

AutoAssemblerTM is a software package from Perkin Elmer (Applied Biosystems, Foster City, USA) designed for assembly of DNA sequences. It works of Macintosh OS9. It provides tools for editing sequences and has the ability to display electropherograms synchronized with assembled sequences. Consensus sequences can be built and exported for the use in other programs. The graphical user interface is easy to use and allows the importation of text files as well as analysis files from Applied Biosystems automated sequencers (Models 310, 373, and 377). If Applied Biosystems analysis files are used, the accompanying electropherograms may also be displayed and edited. The assembly algorithm used by AutoAssembler generates very accurate assemblages and is ideal for incremental assembly projects.

3.3.3.6 *Codon Code Aligner*

CodonCode Aligner is an application (Codon Code Corporation) for DNA sequence assembly and alignment, and editing on both platforms Mac OS X and Windows. It can perform multiple sequence assembly, allows manual and automated sequence editing, can detect mutations etc. Moreover, it can export mutations detected to text files.

3.3.3.7 *Clustal W and X*

They perform a pairwise alignment and its output can be used for phylogenetic tree construction. This software package was mostly used for the alignment of mitochondrial DNA and autosomal DNA sequences. We also use this alignment tool to rule out the chance of bacterial contamination in ancient DNA analysis.

3.4 Results

Eleven fossil samples from India, collected from eight archaeological sites (Table 3.1) and from the personal collections of palaeontologists, were investigated to identify the extent of DNA preservation in these fossil avian eggshells and for DNA-based species identification. To maximize the DNA recovery from fossil eggshells, it is important to determine the physical location of DNA and to microscopically identify its presence in the inner, outer or calcified layers of the eggshell.

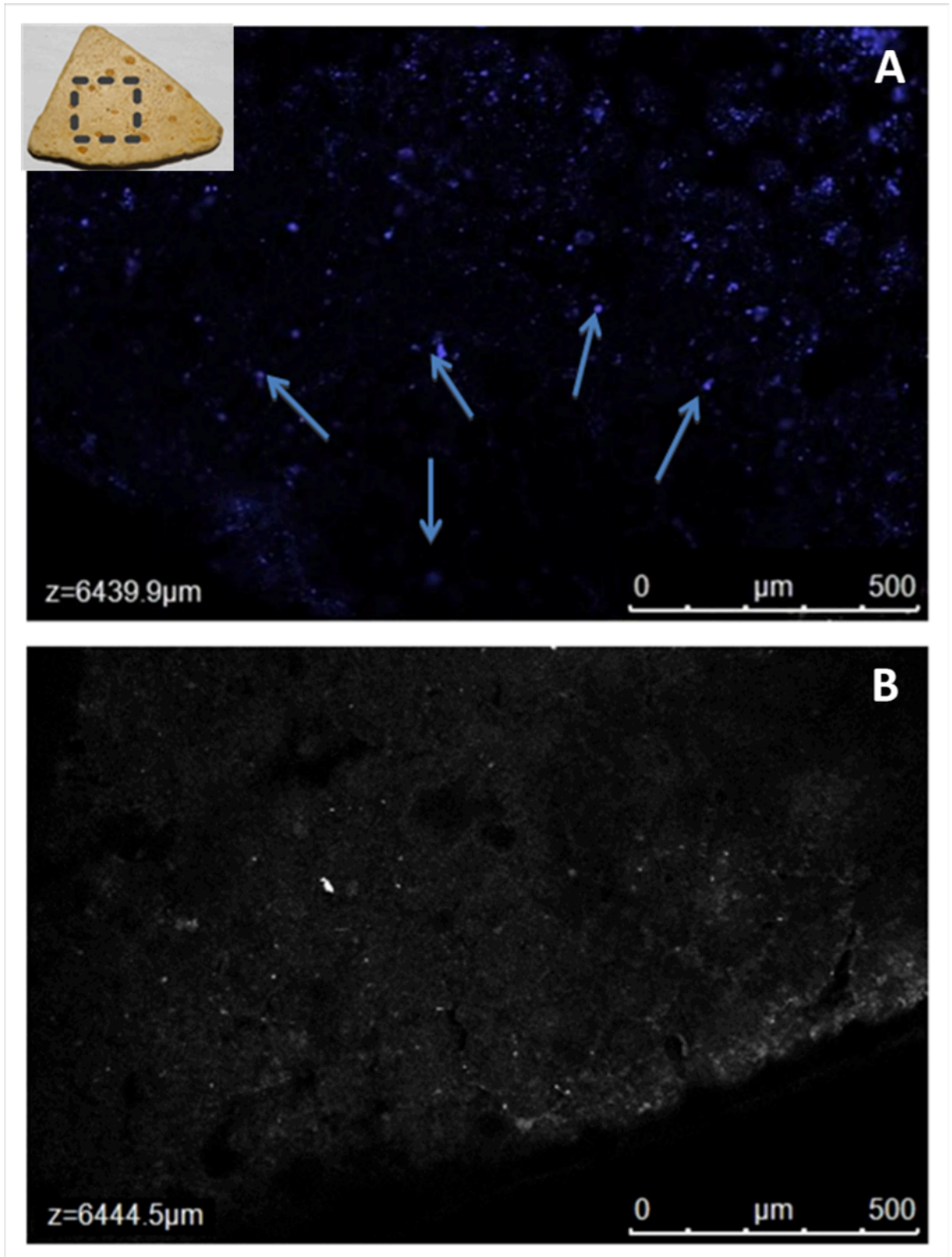


Figure 3.4 Confocal images showing radial outer surface of ratite eggshell (A) Stained with Hoechst 33342, displaying the DNA distributed throughout the matrix. The arrow indicates the presence of hotspots in fossilized eggshells. (B) Control sample, without fluorescence. Scale Bar- 500 μm [Inset- Picture of eggshell. Marked area was observed under CLSM]

3.4.1 CLSM studies of eggshells

DNA in fossil avian eggshells is thought to be present on the inner surfaces since the membranes desiccate against the matrix, as has been observed in the modern avian eggshells (Oskam et al., 2010). Confocal imaging of the avian eggshells studied here demonstrated the distribution of DNA throughout the eggshell matrix, as evident from the DNA hotspots observed after staining with Hoechst 33342, a fluorescent dye used to stain DNA (Fig 3.4). The control image of unstained eggshells did not show any hotspots, confirming that the fluorescence observed in sample images were due to the binding of dye with DNA. Inner surface images of the eggshell fragments showed the presence of DNA hotspots concentrated on the periphery of mammillary cones, as outlined in Fig 3.5. Images revealed that although DNA is disseminated throughout the eggshell matrix found to be more concentrated on the mammillary cones periphery. 3-D images captured using Z stage at different angles clearly validates the presence of DNA hotspots distributed uniformly throughout the matrix (Fig 3.6).



Figure 3.5 Cross-section image of *Struthio* eggshell. Fluorescently labelled DNA can be observed on the periphery of mammillary cones. Scale Bar 50 μm [Inset- Picture of eggshell. Marked area was observed under CLSM]

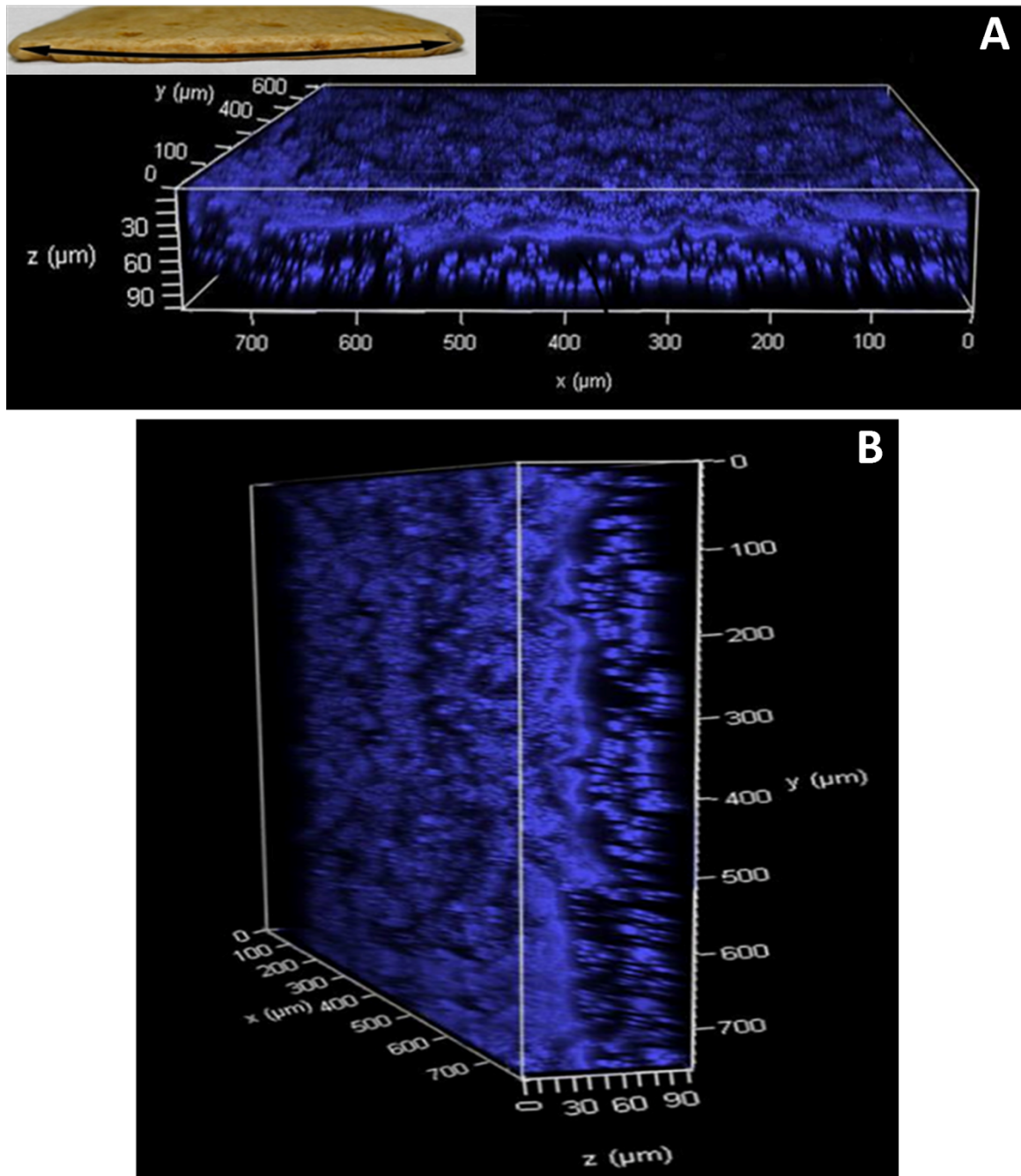


Figure 3.6 3-D imaging of inner layers of eggshell: DNA distributed throughout the matrix as observed through fluorescent hotspots. A) Horizontal view B) Vertical view [Inset- Picture of eggshell. Marked area was observed under CLSM]

3.4.2 DNA extraction and species determination

Five samples, from five different sites, yielded DNA with specimen id: GK/RN/011, GK/RU/009, GK/CH1/004, GK/KH/010 and GK/CH2/007 (Table 3.3). Since the copy number of DNA is traditionally low in ancient samples and aDNA is fragmented in nature, we optimized the amplification protocol targeting the mitochondrial hypervariable region (HVR) and 16SrRNA gene by using PCR primers designed to amplify short fragments, using multiple aliquots of the DNA extracts as the template for the PCR reactions. The extractions and PCR set up were done at CCMB, Hyderabad in facilities dedicated to the analysis of low copy number template. The DNA extracts were visualized on the Bioanalyzer 2100 (Agilent). Bioanalyzer revealed a concentration of <100pg/ml in the five specimens GK/RN/011 (123.6 pg/ml), GK/KH/010 (566.32 pg/ml) GK/CH1/004 (749.06 pg/ml), GK/RU/009 (316.94 pg/ml) and GK/CH2/007 (223.84 pg/ml). Quantification of the DNA extracted from the fossil eggshell samples showed a strong band around 43 bp in GK/RN/011 and 65bp in GK/KH/010 (Fig 3.7). Bioanalyzer images of other samples showed multiple bands and smears, which could be due to, degraded nature of aDNA. The extracted and amplified DNA was further cloned using pMOS blunt ended PCR cloning kit and multiple clones were sequenced.

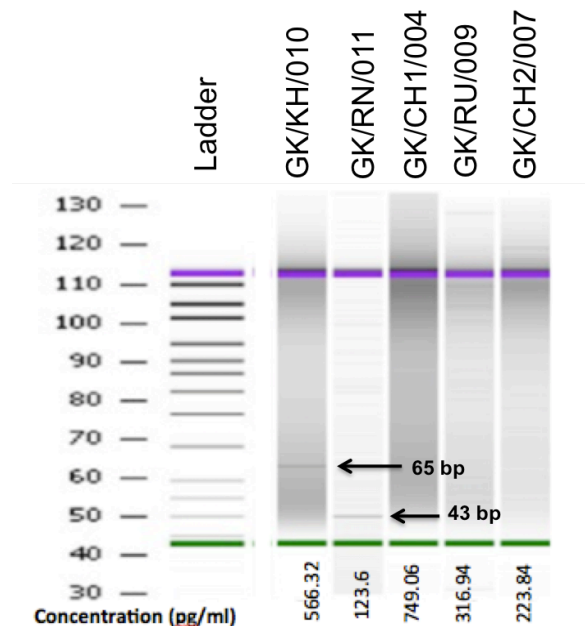


Figure 3.7 Bioanalyzer image showing bands of fossilized DNA. The concentration of DNA in pg/ml is mentioned as calculated by bioanalyzer.

Table 3.3 List of eggshell specimens from India, with associated genes and predicted taxon.

Site	Specimen ID	Dates	Predicted taxa	Gene	Amplicon site	Fragment length (bp)	E-value (NCBI)	Identity	Taxon	Common name
Ravishankar Nagar	GK/RN/011	>25000	<i>S. camelus</i>	16s RNA	1255-1298	43	2e-07	92%	<i>S. camelus</i>	Ostrich
Chandresal-1	GK/CH1/004	38,900 ± 750 BP	<i>S. camelus</i>	16s RNA	4859-4882	23	2e-07	96%	<i>A. mantellus</i>	Kiwi
Khajurna	GK/KH/010	>25000	<i>S. camelus</i>	CR	15586-15606	20	0.019	89%	<i>S. camelus</i>	Ostrich
Chandresal-2	GK/CH2/007	36,550 ± 600 BP	<i>S. camelus</i>	CR	15707-15724	17	1e-05	87%	<i>S. camelus</i>	Ostrich

Dates according to Kumar et al, 1988; 1990

Taxon based on the closest GenBank BLAST match

Predicted taxa on the basis of eggshell morphology and location

CR Control Region

A fragment length of 43 bp and 23 bp, corresponding to GK/RN/011 and GK/RU/009 respectively, was obtained from 25,000 years old samples collected from Ravishankarnagar (GK/RN/011) and Runija (GK/RU/009), respectively, which showed an identity of 92% and 100% with *Struthio camelus* species. Alignments of partial 16SrRNA gene sequence of ratites (obtained from NCBI) and samples GK/RN/011 and GK/RU/009 were done (Fig 3.8). Other samples GK/CH1/004, GK/KH/010 and GK/CH2/007 collected from Chandresal 1, Khajurna and Chandresal 2 also attained a fragment length of 23 bp, 20 bp and 17 bp, respectively. Obtained sequences were submitted in NCBI (Access. No. KU251475) and compared with published partial mitochondrial sequences on NCBI. BLAST (NCBI) and multiple sequence alignment show similarity with *Struthio* species.

3.4.3 Phylogenetic analysis

To explore the phylogenetic relationship with our DNA sequences, a comparative study with published avian mtDNA sequences was done and the phylogenetic tree was constructed (Fig 3.8) using MEGA 6.06. The phylogenetic analysis was centered on maximum parsimony, neighbour joining, and maximum likelihood methods. These three methods are based on different assumptions and, thus, can be used complementarily to confirm the obtained phylogeny. The neighbour joining method was further extended and the bootstrap consensus tree was inferred from 1000 replicates. The sample sequence shows phylogenetical similarity to the ratites family, forming a sister group with *S. camelus* (Fig 3.8). The phylogenetic tree showed the ostrich clade as basal to studied palaeognaths, which is consistent with the vicariant speciation model and other molecular phylogeny studies on ratites. The estimates of evolutionary divergence amongst sequences were conducted in MEGA6 (Fig 3.9) using the Maximum Composite Likelihood model.

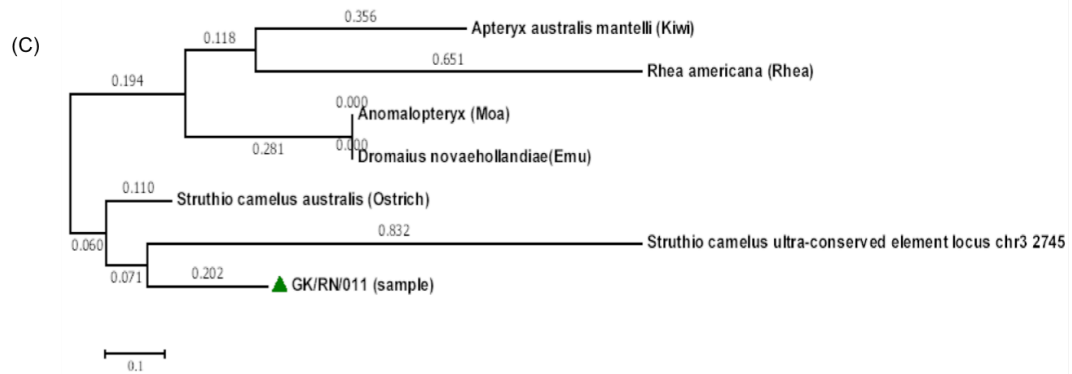
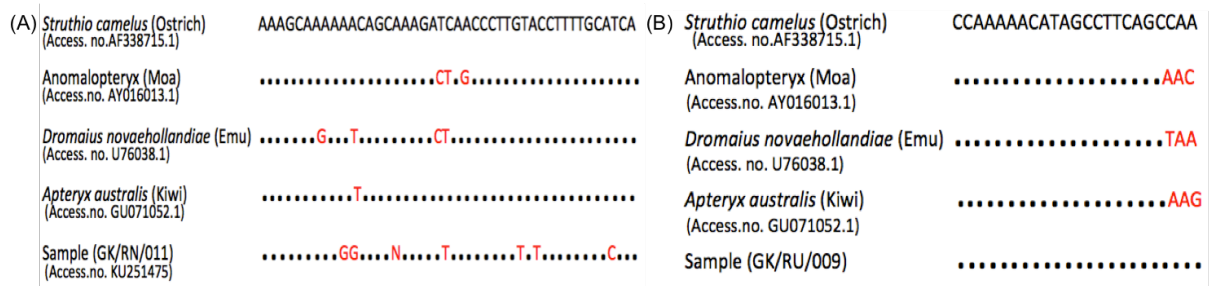


Figure 3.8 Alignment of partial 16srRNA gene sequences of samples and ratites and evolutionary relationships of taxa. (A) and (B) Alignment of ratites sequences and sample GK/RN/011 and GK/RU/009. Dots signify identity to the *Struthio camelus* sequence. (C) The evolutionary history was deduced using the Neighbor-Joining method. The bootstrap consensus tree concluded from 1000 replicates is taken to denote the evolutionary history of the taxa analyzed. The evolutionary distances were calculated using the Maximum Composite Likelihood method and are in the units of the number of base substitutions per site. The analysis involved 7 nucleotide sequences. Codon positions included were 1st+2nd+3rd+Noncoding. All positions containing gaps and missing data were eliminated. There was a total of 87 positions in the final dataset. Evolutionary analyses were conducted in MEGA6.

	1	2	3	4	5	6	7
1. <i>Struthio camelus australis</i> (Ostrich)							
2. <i>Struthio camelus</i> ultra-conserved element locus chr3 2745 genomic seence	0.991						
3. <i>Apteryx australis mantelli</i> (Kiwi)	0.974	1.404					
4. GK/RN/011 (sample)	0.404	1.033	1.005				
5. <i>Anomalopteryx</i> (Moa)	0.555	1.667	0.840	0.668			
6. <i>Dromaius novaehollandiae</i> (Emu)	0.555	1.667	0.840	0.668	0.000		
7. <i>Rhea americana</i> (Rhea)	1.176	1.776	1.007	1.486	0.964	0.964	

Figure 3.9 Estimates of evolutionary divergence between sequences. The number of base substitutions per site among sequences is presented. Maximum Composite Likelihood model was used for analysis. The analysis comprised of 7 nucleotide sequences. Codon positions used were 1st+2nd+3rd+Noncoding. All positions containing gaps and missing data were removed. There was a total of 87 positions in the final dataset. Evolutionary analyses were conducted in MEGA6.

3.5 Discussion

The breakup of supercontinent Gondwanaland during the Early Cretaceous resulted in the vicariant speciation of ratites, the flightless birds, to various countries that we know today as South America, Australia, New Zealand, India, and Madagascar. This continental drift theory indicates that ostriches migrated to India from other countries and is supported by the geographical distribution of fossil records of ratites. The fossil eggshells used in this study date to 25-40ka and morphologically characterized as belonging to *Struthio camelus*. Ostriches were believed to be extinct from India during the Late Pleistocene epoch and our investigation reports for the first genetic evidence of their presence on the subcontinent. Fossil eggshells have been reported as being more conducive to biomolecular preservation compared to fossil bones due to their intracrystalline structure, which minimizes microbial contamination. This study is significant as it is the first report, to our knowledge, of long-term DNA preservation in fossil eggshells collected from the tropical environment having extreme, heterogeneous climatic conditions as those encountered in India. aDNA survival in fossils is usually determined by the thermal age theory. This theory requires specific parameters including temperature, pressure and climatic conditions of fossil locations. These parameters cannot be applied to our samples that are from open sites and cannot be inferred back into the past.

To evaluate the presence of DNA, Hoechst 33342 stained fossil eggshells samples were visualized under CLSM. DNA hotspots observed on the periphery of the mammillary layer were consistent with shape and size of epithelial fossil cells instead of random shapeless patches, eliminating the possibility of these hotspots to be of microbial origin. Modifications in the aDNA isolation procedure of Oskam and Bunce were done at the heating step to prevent complete denaturation of aDNA. Species-specific primers based on *S. camelus* were designed to target short fragments. Amplified fragments were further cloned and sequenced. The multiple alignments of sequences confirm the relationship of our samples with other avian species and its identity with *Stuthio camelus*. Molecular phylogenetic tree further revealed the placement of our samples with the ostrich and this clade as being basal to other studied paleognaths, which complements the vicariant speciation theory and other ratites phylogenetic studies.

Morphological studies conducted earlier on these eggshells indicated their close proximity to *Struthio* species. The presented genetic study performed using species-specific primers confirms that the eggshell fragments belong to the *Struthio* species and that these

ratites were present in India thousands of years ago. Paleoenvironmental studies indicate the favorable environment for survival and expansion of these species in the Indian subcontinent during Late Pleistocene. Currently, ostriches are extinct in India and their sudden extinction coincides with the time period of expansion of humans from Africa towards South Asia. There is evidence in the archaeological context of ostrich eggshell beads and crisscross motif patterns on these eggshells have striking similarities to the material culture of Africa (Bednarik, 1993a). These records suggest a relation between the prehistoric humans in southern Asia and their likely forefathers in eastern and southern Africa.

The archaeological records of eggshells fragments, beads and rock shelter paintings discovered at Indian sites corroborates with our genetic study, which is the first molecular evidence indicating the presence of ostriches in India. These evidence further endorse the theory of the biogeographical movement of ostrich in India when Indo-Madagascar split. Furthermore, this genetic characterization of collected fossil eggshells would be of great importance in studying the aspects related to paleoecology and paleodiets that can stipulate insights into the biology, ecology and extinction of this species.

CHAPTER 4

BIOCHEMICAL SIGNATURE OF FOSSIL EGGSHELL USING CARBONATE CLUMPED ISOTOPE ANALYSIS

4.1 Background

4.1.1 Stable isotope analysis

Fossil ostrich eggshells can be used to measure the stable isotopes of Carbon (C) and Oxygen (O) and providing information about the paleodietary and paleoenvironment. The stable isotopes of C and O can be used as parameters to define the comparative changes in C₃ and C₄ vegetation abundances, rainfall and temperature since 40,000 years. These eggshells are extensively found at various archaeological sites in India and are dated using radiocarbon (Mishra, 2001).

4.1.1.1 Carbon isotopes

The characteristic carbon isotopic composition of a plant tissue is the result of the difference in utilization of C₃ (Calvin) and C₄ (Hatch- Slack) photosynthetic pathways fractionate while making of plant carbohydrate (Farquhar et al., 1989; Fogel and Cifuentes, 1993; B.J. Johnson et al., 1997). The carbon isotopic composition of animal matter (e.g. bone, muscle, and eggshell) shows a direct relation to the isotopic composition of the diet consumed by the animal. In the case of herbivores animals, the isotopic composition of the plants ingested is transported to its tissues in a way that the $\delta^{13}\text{C}$ measures of C₃ feeders are notably more negative than the $\delta^{13}\text{C}$ measures of C₄ feeders (B.J. Johnson et al., 1997). Therefore, any alteration in carbon isotopic composition of the herbivore tissue is an indicative of plants available in the ecosystem for the feeding of the animal (Ostrom and Fry, 1993; Koch et al., 1994; B.J. Johnson et al., 1997).

4.1.1.2 Oxygen isotopes

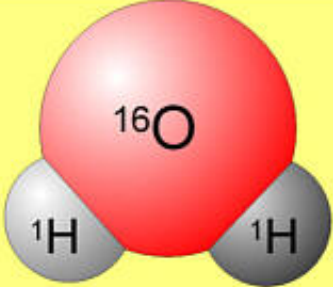
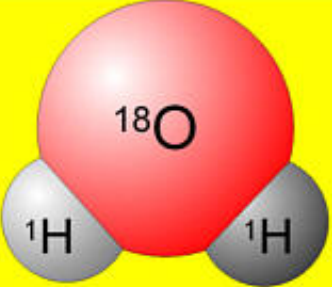
The oxygen isotopic composition of the inorganic phase of animal matter is correlated to the isotopic composition of the organism metabolic H₂O. This is primarily derived from the isotopic composition of water consumed by the animal. The isotopic composition of the animal's body water for obligate drinkers (animals that require access to standing water for existence) is mainly calculated by the isotopic composition of the drinking H₂O where as the

isotopic composition of the animal's body water for non-obligate drinkers such as ostriches (animals which can sustain without free standing water for survival), is mainly calculated by the isotopic composition of leaf water of the plants (Ayliffe and Chivas, 1990; B.J. Johnson et al., 1997). The alteration of rain and soil water via the methods of water uptake and evaporative transpiration is the cause of oxygen isotopic composition in plant-leaf waters (Dongmann et al., 1974; Ferhi and Letolle, 1977; Flanagan et al., 1991). There is an inverse correlation between oxygen isotopes in plant-leaf H₂O (Forstel, 1978; Ferhi and Letolle, 1977) and its direct correlation to temperature (Burk and Stuiver, 1981). Thus, the $\delta^{18}\text{O}$ of ostrich eggshells carbonate would have been isotopically depleted through periods of low evaporative effects (Low temperature and high relative humidity) and isotopically enriched through periods of high evaporative effects, which accounts for high temperature and low relative humidity (Johnson, 1995).

4.1.2 Measuring stable isotopes

Different isotopes of the same element are taken up differently depending on physical and biological conditions. The different masses of the isotopes result in different behavior in various chemical and physical processes. For example, the lighter isotope of water ($^1\text{H}_2^{16}\text{O}$) would evaporate faster than heavier isotope ($^2\text{H}_2^{18}\text{O}$) and heavier will be left behind while the process of evaporation (Fig 4.1).

Elements occur in the earth system in multiple isotopes, both stable and unstable. Proportions of stable isotopes in the earth system are constant over the entire system but vary within different parts of the system. The ratios of stable isotopes were set when the Earth was formed, with slight astronomical changes. Lighter isotopes are more reactive than heavier isotopes and are more likely to be lost by diffusion or evaporation. At higher temperatures, lighter isotopes are preferentially lost than heavier isotopes. Biological systems will differentiate between isotopes and have a preference for certain isotope based on bond order (Fig 4.2).

		<p>Superscripts show atomic masses of hydrogen and oxygen</p>
<p>$1+1+16 = \underline{18}$ Molecular weight of ^{16}O water</p>	<p>$1+1+18 = \underline{20}$ Molecular weight of ^{18}O water</p>	
<p>Makes up 99.8% of water, evaporates more easily, precipitates less easily.</p>	<p>0.2% of water, 11% heavier, evaporates less easily, precipitates more easily.</p>	

© Kurt Hollocher, 2002

Figure 4.1 Heavier and lighter isotope of oxygen. Lighter isotope evaporates faster and heavier isotope evaporates easily (Kurt Hollocher, 2002)

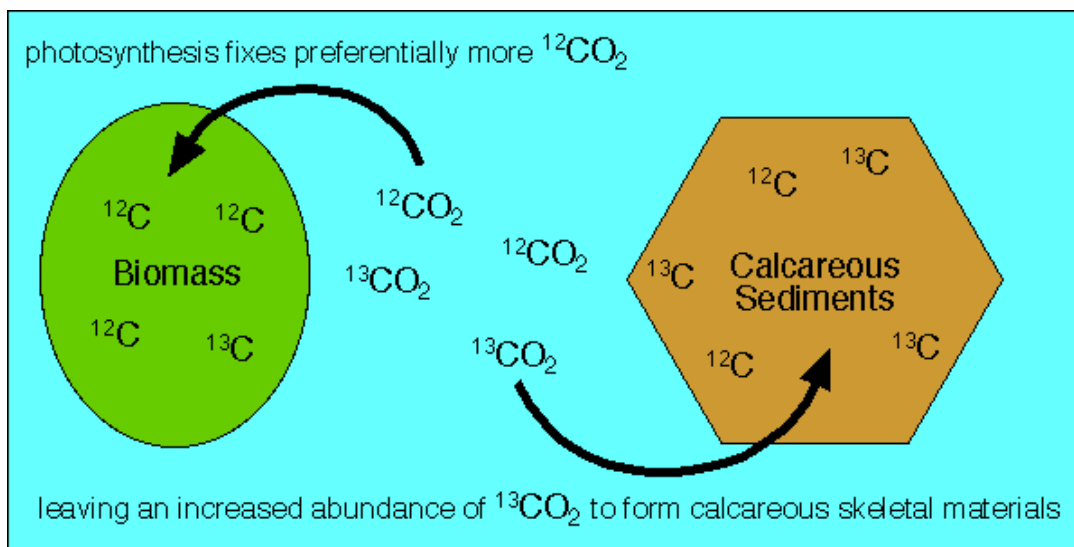


Figure 4.2 Biological system will have a preference for a certain isotope based on bond ordering. Photosynthesis fixes more ^{12}C while calcareous sediments prefer ^{13}C .

Isotope abundances are expressed as:

$$\delta^H X = ((R_{\text{sample}}/R_{\text{standard}}) - 1) \times 1000$$

where R = heavy/light isotope ratio for X element and units are described as parts per thousand (or per mil, ‰).

Differences between two isotopes of one element are very small – to measure them independently with enough accuracy is challenging for most isotope systems. Comparison of a sample ratio to a standard ratio and their difference can be determined more accurately. Various standards used for stable isotope measurements are:

- VSMOW- Vienna Standard Mean Ocean Water
- PDB- Pee Dee Belemnite
- CDT- Canyon Diablo Troilite
- AIR

4.1.3 Isotope fractionation

Isotopes of an element undergo the similar chemical and physical reactions. Mass differences may affect the rate or amount of these reactions, or lead to segregating of isotopes differentially between phases. This isotopic sorting during various processes is called Fractionation (Fig 4.3).

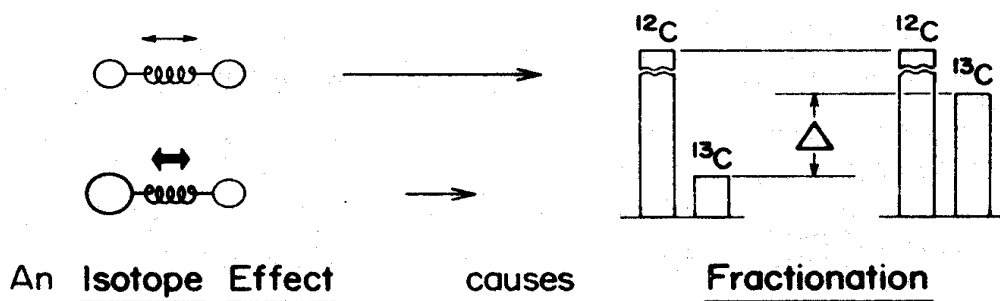
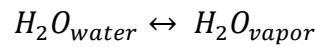


Figure 4.3 Isotope fractionation. Depending upon the process reaction product might be heavy or light.

Fractionation Factor is represented as α . Fractionation factor is the ratio between reactant and product.



$$\alpha^{18}O_{water-vapor} = \frac{(^{18}O/^{16}O)_{water}}{(^{18}O/^{16}O)_{vapor}}$$

Isotopes are measured as a ratio of the isotope vs. a standard material (per mil ‰).

$$\delta^{18}O = \left(\frac{R_{sample} - R_{standard}}{R_{standard}} \right) \times 10^3$$

Where R is heavy/light isotope ratio.

If $\delta > 0$, this value shows that the sample is enriched in the heavy isotope as compared to a standard.

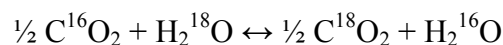
If $\delta < 0$, this value shows that the sample is depleted in the heavy isotope in comparison to a standard.

The relationship between α and δ is:

$$\alpha_b^a = \frac{\delta_a + 10^3}{\delta_b + 10^3}$$

$$10^3 \ln \alpha_b^a \approx \delta_a - \delta_b = \Delta_b^a$$

Isotope fractionation occurring in chemical processes is a result of exchange reactions:



At equilibrium, for the foregoing reaction, K- equilibrium constant is given as:

$$K = \frac{(C^{18}O_2)^{\frac{1}{2}}(H^{16}O_2)}{(C^{16}O_2)^{\frac{1}{2}}(H^{18}O_2)}$$

In this equation molar concentrations are used instead of activities as the activity coefficients will be same and would cancel out. If carbon dioxide and water did not differentiate between ^{16}O and ^{18}O , then K would be equal to one ($K = 1.00$). Though, at 25°C , $K = 1.0412$, which denotes that carbon dioxide slightly chooses ^{18}O and water prefers ^{16}O . This predilection is large enough for causing isotopic fractionation. As ^{18}O forms a tougher covalent bond with Carbon than ^{16}O . The following equations give vibrational energy of a molecule:

$$E_{\text{vibrational}} = \frac{1}{2} h \nu$$

$$\nu = \frac{1}{2\pi} \sqrt{\frac{k}{m}}$$

where E = vibrational energy, h = plack's constant, ν = velocity of molecule, m = mass, k = constant

Thus, the frequency of vibration is related to the mass of the atoms as well as the energy of a molecule. The isotope with greater mass forms a lower energy bond and vibrates less forms a stronger bond in the compound.

During physical processes like diffusion, evaporation, freezing, etc. fractionation occurs because of mass differences. It is the consequence of the difference in speed of isotopic molecules.

$$E_{\text{kinetic}} = \frac{1}{2} m v^2$$

As the kinetic energy for isotopes is the same:

$$\frac{v_L}{v_H} = \sqrt{\frac{m_H}{m_L}}$$

Where V_L is the velocity of lighter isotope and V_H is the velocity of heavier isotope.

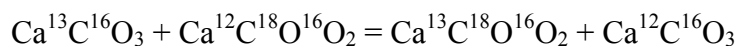
In the case of $^{12}\text{C}^{16}\text{O}$ and $^{13}\text{C}^{16}\text{O}$ we have:

$$\frac{v_L}{v_H} = \sqrt{\frac{28.99827}{27.994915}} = 1.0177$$

Irrespective of the temperature, the $^{12}\text{C}^{16}\text{O}$ molecule velocity is 1.0177 times of $^{13}\text{C}^{16}\text{O}$. Thus resulting in faster diffusion and evaporation of lighter molecule.

4.1.4 Carbonate clumped isotope thermometry

The principal of carbonate clumped isotope thermometry is based on physical chemistry. It studies a homogenous isotope exchange reaction of the form:



This is a reaction comprising of clumping of ^{13}C and ^{18}O in bonds together making $^{13}\text{C}^{18}\text{O}^{16}\text{O}_2$ as shown in Fig 4.4. This isotope thermometry has important applications to reconstruct paleoclimate. Dennis et al., 2011 has standardized Δ_{47} measurements in CO_2 gases produced by acid digestion of carbonate. As the vibrational dynamics of carbon dioxide is well recognized, thus for this reaction the temperature-dependent equilibrium constant can be calculated with certainty (Wang et al., 2004).

4.2 Sample Details

Fossilized eggshell samples used in this study were recovered either from excavation sites at Bundi (Rajasthan state, western India) or from the Pleistocene surface deposits of Gujarat, western India (Table 4.1). We analysed fossil avian eggshell fragments, collected from seven different sites in India which were referred to the genus *Struthio* on the basis of morphological characters, especially thickness and pore pattern on eggshells. The mineralogy of eggshells was confirmed by powder X-Ray Diffraction. The major component of eggshell was calcite and it was used for clumped isotope analysis.

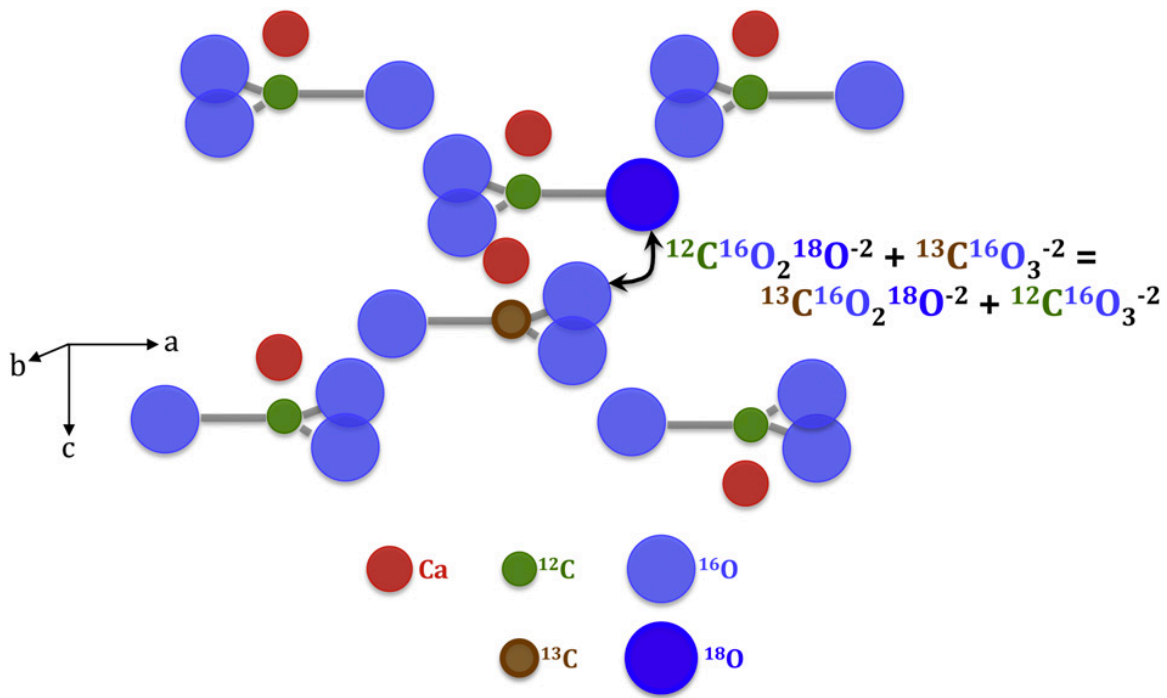


Figure 4.4 Carbonate clumped isotope thermometry is grounded on the principle of exchange reactions between carbonates ions. This image shows the atomic structure of calcite lattice (Eiler, 2011)

Table 4.1 Fossil eggshell sample collection sites, their respective states and taxa

Site	State & GPS Co-ordinates	Sample ID	Taxa
Chavni Baroda	Rajasthan (25° 26' 24" N, 75° 38' 24" E)	OSI-001	Struthinoid
Chavni Baroda	Rajasthan (25° 26' 24" N, 75° 38' 24" E)	OSI-002	Struthinoid
Chavni Baroda	Rajasthan (25° 26' 24" N, 75° 38' 24" E)	OSI-003	Struthinoid
Anjar	Gujarat (23° 6' 48.32" N, 70° 1' 39.88" E)	OSI-004	Struthinoid
Chandresal- 1	Rajasthan (25° 10' 48" N, 75° 49' 48" E)	OSI-005	Struthinoid
Chandresal- 1	Rajasthan (25° 10' 48" N, 75° 49' 48" E)	OSI-006	Struthinoid
Chandresal- 1	Rajasthan (25° 10' 48" N, 75° 49' 48" E)	OSI-007	Struthinoid
Chandresal- 2	Rajasthan (25°13'34.1"N75°55'34.7"E)	OSI-008	Struthinoid
Chandresal- 2	Rajasthan (25°13'34.1"N75°55'34.7"E)	OSI-009	Struthinoid
Chandresal -2	Rajasthan (25°13'34.1"N75°55'34.7"E)	OSI-010	Struthinoid
Nagda	Rajasthan (25°10'53.3"N75°48'45.5"E)	OSI-011	Struthinoid
Runija	Madhya Pradesh (23°09'39.4"N75°16'02.6"E)	OSI-012	Struthinoid
Khajurna	Madhya Pradesh (26°44'33.6"N78°47'45.6"E)	OSI-013	Struthinoid
Africa	-	CHA-2013	Struthinoid

4.3 Experimental

4.3.1 Measurements of stable isotopes

Isotopic measurements were carried out at Stable Isotope lab at Johns Hopkins University. An automated acid reaction and gas purification line was used coupled with a mass spectrometer (Thermo Scientific MAT 253, Fig 4.5). This line was designed to generate high-purity CO₂ gas from carbonate samples and standards, and reference ‘equilibrium CO₂ gases’ (Passey et al 2010). Firstly, ~ 10mg of carbonate was reacted in vacuum for 10 min in an acid bath containing phosphoric acid held at 90⁰C. The CO₂ gas was accumulated in a liquid nitrogen trap (LN) trap after moving via a -78⁰C H₂O trap. In the next step, the sample CO₂ was moved from the collection trap (kept at -78⁰C) to a second liquid nitrogen trap consuming a purified He carrier gas. Throughout this movement the sample and carrier gas was passed through a second -78⁰C trap, a getter containing silver wool and then into a 1.2 m gas chromatography (GC) column containing PorapakTM held at -20⁰C. Finally, the sample was transferred from the post-GC Liquid Nitrogen collection trap (at -78⁰C) to a smaller Liquid Nitrogen trap. This was done in the vacuum after the helium carrier gas was propelled away. The frozen sample CO₂ was then permitted to expand at room temperature for 3 min in the last trap before any other expansion into the bellows of the spectrometer dual inlet system. The other bellows encompassed of a reference gas.

For the precise measurement of carbonate clumped isotope a reference frame was required. This frame rectifies for changes in the ionization conditions inside of a gas source mass spectrometer and also for the ‘nonlinearities’ (Huntington et al., 2009; Dennis et al., 2011). Following this all the laboratories computing clumped isotopes can describe their data on a common platform as done by Dennis et al., 2011.

Every sample, standard, or reference gas was examined at a bellows pressure conforming to a signal of 12 V on the Faraday cup having mass 44 CO₂. The sequence comprised of six repetitions of nine cycles, each with 26 s of integration time for a total combined integration of 1404 s per gas. The isotope ratios were computed from these measurements is reported here. The measurements for a single sample were made during one analytical session. As all analyzed samples were corrected using the identical reference frame the possible reported error for all these samples were preciously small.



Figure 4.5 Autoline for clumped isotope analysis (Johns Hopkins University)

4.3.2 Data analysis and reduction

Data reduction was done post analysis as stated by Dennis et al., 2011; Henkes et al., 2013. In this, an empirical transfer function (ETF) was constructed using equilibrate CO₂ gases. ETF maps the measured sample Δ_{47} values onto a reference frame anchored to theoretical estimations of Δ_{47} of CO₂ gas at two different equilibration temperatures. It has been detected that due to variations in the physical state of mass spectrometers, the raw Δ_{47} values of the equilibrium CO₂ gas may drift overtime which results in drifting the slope and intercept of the EFT (Huntington et al., 2009; Passey et al., 2010). For correction of this drift, we used a MATLAB script that models deviations in the intercept and slope of the equilibrium gas lines as described by Passey et al., 2010.

In cases when there is no apparent drift in the reference gas line, a static correction of simple linear regression was used. All data values were normalized to acid extractions performed at 90°C using an acid temperature correction factor. An acid correction value of

0.082 was used following Henkes et al., 2013. Along with the samples, International standard NBS-19 and internal carbonate standards 102-GC-AZ01 were analyzed at regular intervals for monitoring precision and stability of the system. The standard analyzed showed the following results NBS-19 (n = 23) $\Delta_{47} = 0.414 \pm 0.018$ (mean $\pm 1\sigma$ standard deviation); 102-GC-AZ01 (n = 102) $\Delta_{47} = 0.710 \pm 0.015$ (reported on the ‘carbon dioxide equilibrium scale’). The $\delta^{13}\text{C}$ and $\delta^{18}\text{O}$ values of the samples were normalized to simultaneous analyses of NBS-19 ($\delta^{13}\text{C} = 1.95\text{‰}$ PDB, $\delta^{18}\text{O} = -2.20\text{‰}$ PDB) or an in-house carbonate standard calibrated to NBS-19. Corrected isotopic data was statistically treated using Kaleidagraph 4 (Synergy Software) and JMP 9 (SAS Institute Inc.).

4.4 Results and Discussion

The isotopic compositions ($\delta^{13}\text{C}$, $\delta^{18}\text{O}$) of the Ostrich eggshells are presented in Fig. 4.6 and Table 4.2.

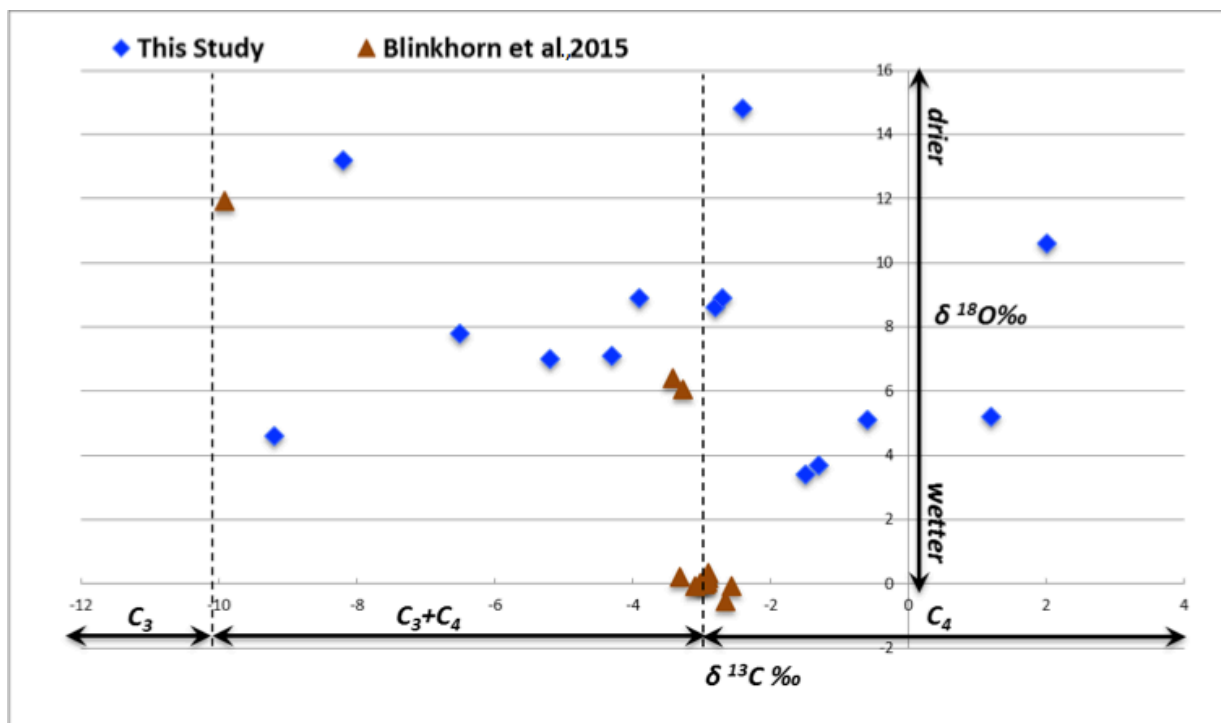


Figure 4.6 Stable oxygen and carbon isotope results of ostrich eggshells collected from Upper Paleolithic sites compared with Blinkhorn et al., 2015 illustrating the relationship between stable isotope values.

Table 4.2 Result of stable isotope studies from fossil ostrich eggshells collected from Upper Paleolithic sites of India (n= no. of times sample was run)

Site	Sample ID	Taxa	n	$\delta^{13}\text{C}_{\text{carb}}$ (‰, PDB)	$\delta^{18}\text{O}_{\text{carb}}$ (‰, PDB)
Chavni Baroda	OSI-001	Struthinoid	3	-3.9	8.9
Chavni Baroda	OSI-002	Struthinoid	3	-6.5	7.8
Chavni Baroda	OSI-003	Struthinoid	3	1.2	5.2
Anjar	OSI-004	Struthinoid	3	-8.2	13.2
Chandresal- 1	OSI-005	Struthinoid	3	-1.5	3.4
Chandresal- 1	OSI-006	Struthinoid	3	-0.6	5.1
Chandresal- 1	OSI-007	Struthinoid	3	-1.3	3.7
Chandresal- 2	OSI-008	Struthinoid	3	-4.3	7.1
Chandresal- 2	OSI-009	Struthinoid	3	-2.8	8.6
Chandresal -2	OSI-010	Struthinoid	3	-2.7	8.9
Nagda	OSI-011	Struthinoid	3	2	10.6
Runija	OSI-012	Struthinoid	3	-2.4	14.8
Khajurna	OSI-013	Struthinoid	3	-5.2	7.0
Africa	CHA-2013	Struthinoid	3	-9.2	4.6

Isotopic composition of ostrich eggshells can reveal the diet of ostriches which is an average of three to five days when nutrients have been sufficiently assimilated after the rainy season when breeding occurs (Johnson et al., 1998). Oxygen isotope data preserved in ostrich

eggshells might be affected by the physiological responses of the ostrich to environmental factors like humidity and a series of fractionation processes, as they are non-obligate drinkers (Johnson et al., 1998). Thus, this data indicates only a qualitative measure of palaeoclimate.

$\delta^{18}\text{O}$ results from Chavnibaroda, Chandresal-1, Chandresal-2, Khajurna showed an enriched value ranging from ~ 3 to 8‰ whereas the samples from Nagda, Runija and Anjar showed a measurement of $\delta^{18}\text{O}$ as high as 14.8‰ . Thus, it can be implied that these samples were from less humid conditions and arid conditions.

The carbon isotope results obtained from ostrich eggshells directly reflect isotopic composition of the diet. An average value of $\delta^{13}\text{C}$ of -9.5‰ indicated C_3 diet of ostriches and a value of 4.2‰ denoted C_4 diet of ostriches showing a preference for C_3 shrubs. Data obtained from samples signified a diet of ostriches having an equal proportion of C_3 and C_4 plants during Late Pleistocene era. The $\delta^{13}\text{C}$ values range from -0.6 to -6.5‰ indicated slight biases towards C_3 plants. Samples collected from Anjar site showed a pure C_3 diet with a value of -8.2‰ . Sample collected from Nagda showed a very high positive value of $\delta^{13}\text{C}$, which indicated C_4 vegetation in that area. Oxygen isotope results from Nagda, Runija and Anjar showed an increase in aridity beyond the usual range seen in ratite population of India (Blinkhorn et al., 2015). Both carbon and oxygen isotope analysis indicated that these result obtained are on an individual scale rather than population-wide.

Clumped isotope analysis data obtained from fossil ostrich eggshell revealed the relationship between calculated Δ_{47} values from ostrich eggshells and body temperature of ostriches as shown in Table 4.3 and Fig. 4.7. Earlier Ghosh et al., 2006 derived a relationship between Δ_{47} values of carbon dioxide extracted from calcite on reaction with phosphoric acid at temperatures varying between $0\text{-}50^\circ\text{C}$.

$$\Delta^{47} = 0.0592 \times 106 \times T^{-2} - 0.02$$

Fossil ostrich eggshells samples were analyzed on clumped isotope line. Analysis revealed a Δ_{47} value ranging between $0.647\text{-}0.684\text{‰}$. In order to calculate the body temperature using clumped isotope palaeothermometry, one sample was selected from each location as these samples were exposed to different diagenetic alterations and different burial environments. Body temperatures of ostriches were reported to vary between $37\text{-}42^\circ\text{C}$ (Schrader et al., 2009). The Indian ostrich samples showed a range from 26.1°C to 42.1°C for the body temperature of ostrich of that era. Interestingly, the sample collected from location

Chandresal-2 showed lower body temperature of ostriches. This temperature range signified that this sample might have gone under diagenetic alteration, as it is unlikely that samples are exposed to diagenetic fluids with such low temperatures. Samples collected from other remaining sites are within the error range of body temperature of modern ostriches. Thus, this technique has the potential for accurate reconstruction of body temperatures of ostriches.

Table 4.3 Δ_{47} measurements from fossil ostrich eggshells

Sample ID	N	Δ_{47} (‰), (Passey et al) (Acid correction 0.082)	Apparent Temperature ($^{\circ}$ C)
OSI-001	3	0.654	38.3
OSI-002	3	0.641	43.7
OSI-003	3	0.667	33.4
OSI-004	3	0.635	42.1
OSI-005	3	.660	36.2
OSI-006	3	0.662	35.4
OSI-007	3	0.686	26.4
OSI-008	3	0.684	27.1
OSI-009	3	0.675	30.5
OSI-010	3	0.678	29.3
OSI-011	3	0.664	34.3
OSI-012	3	0.659	36.6
OSI-013	3	0.647	41.2
CHA-2013	3	0.647	41.3

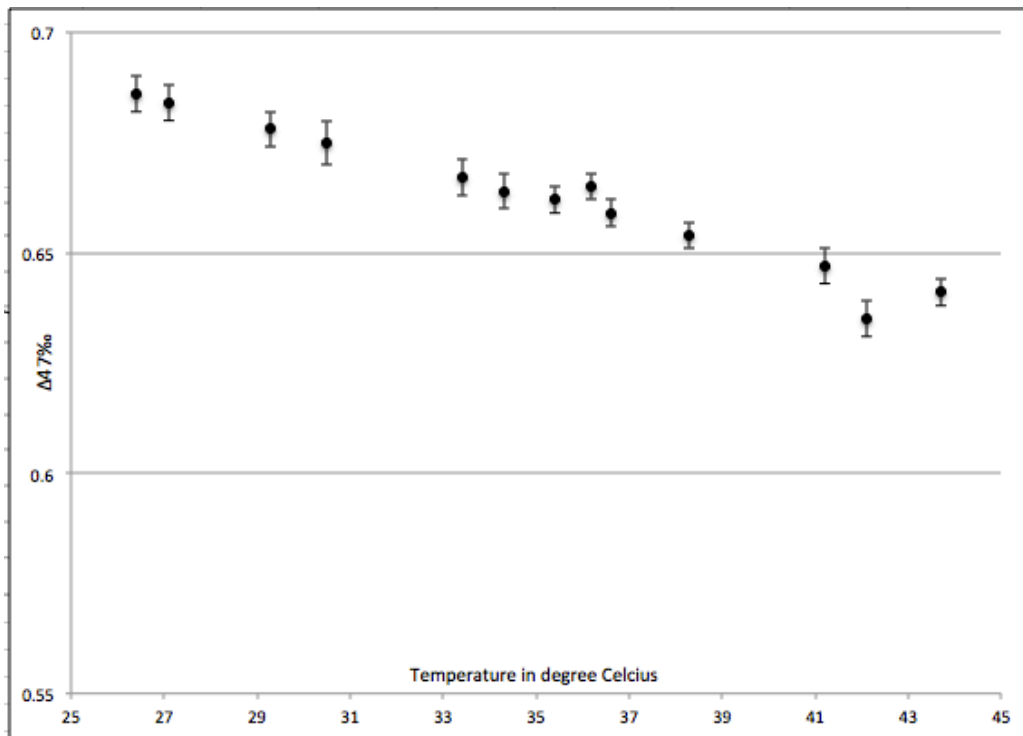


Figure 4.7 The relationship between calculated Δ_{47} values from ostrich eggshells and body temperature of ostriches. The X-axis shows the predicted body temperature of ostriches and Y-axis depicts the mean Δ_{47} values obtained from the extractions of carbon dioxide from eggshells

4.5 Conclusion

The stable O and C isotopes from inorganic carbonates in ostrich eggshells (OES) collected from various Upper Paleolithic sites of India was used to ascertain the variations in C₃ and C₄ vegetation since 25000-40000 years. The samples collected from Nagda indicated the dietary of ostriches to be of C₄ plants and other locations showed a combination of dietary of ostriches to be of C₃ and C₄ plants. Oxygen isotope data revealed the ecology of Late Pleistocene indicating less humid and arid conditions. Data obtained from the bond ordering of ¹³C- ¹⁸O has been used as a paleothermometer to measure the body temperature of ostriches of Late Pleistocene epoch. However, this is majorly a result of individual scale variation.

CHAPTER 5

TRIPLE OXYGEN ISOTOPE STUDIES IN BIOGENIC CARBONATES AND ITS APPLICATION IN ANIMAL PHYSIOLOGY

5.1 Background

5.1.1 Triple Oxygen Isotope Analysis

Conventional oxygen isotopes (^{16}O , ^{18}O) in meteoric waters present in atmospheric gases, sedimentary rocks and biogenic minerals are the core of research related to paleoclimate reconstructions, biogeochemical processes and hydrologic cycle (Cerling, 1984; Clayton, 1961; Grossman, 2012; Knauth and Epstein, 1976; Kohn, 1996; McCarroll and Loader, 2004; Urey et al., 1951). Changes in ($^{16}\text{O}/^{18}\text{O}$) ratios in water are used as an index to measure paleoclimate as these ratios are preserved in geologic materials, like ice cores, rocks, and minerals and are susceptible to a range of environmental parameters. The ease of the measurement of $^{18}\text{O}/^{16}\text{O}$ ratios in geological material and waters makes them a strong tool in the reconstruction of temperature, the isotopic composition of pore and sea water, the origin and amount of precipitation (Bony et al., 2008; Knauth and Epstein, 1976). However, the $^{16}\text{O}/^{18}\text{O}$ ratio is not well preserved, as an increase in this ratio in surface water may be altered by many reasons. These alterations could be due to a change in moisture source for precipitation or a decrease in elevation or due to increased influence of evaporation. These restrictions lower the use of ratios as paleoclimate proxies. To overcome this constraint, Triple oxygen isotope studies have been exploited to answer paleoclimate questions. It uses both the ratios $^{18}\text{O}/^{16}\text{O}$ and $^{17}\text{O}/^{16}\text{O}$. The $^{17}\text{O}/^{16}\text{O}$ can be used to differentiate between the different fractionation processes inside the hydrological cycle that are conserved in rock and mineral fossil. Atmospheric chemistry and cosmochemistry studies use the relative abundance of $^{18}\text{O}/^{16}\text{O}$ and $^{17}\text{O}/^{16}\text{O}$ as indicators of mass independent isotopic fractionations (Clayton and Mayeda, 1983; Thiemens et al., 1995; Luz et al., 1999; Hoag et al., 2005; Bao et al., 2009). It was assumed that the isotopic ratio $^{17}\text{O}/^{16}\text{O}$ convey no extra information to $^{18}\text{O}/^{16}\text{O}$ in the earth surface processes. It was contemplated on the basis of mass independent fractionation law that $^{17}\text{O}/^{16}\text{O}$ vary in a uniform and predictable way relative to $^{18}\text{O}/^{16}\text{O}$.

According to the fractionation law:

$$^{17}\alpha = ^{18}\alpha\theta \text{ or } \delta'^{17}\text{O} = \theta \Delta \delta'^{17}\text{O}, \text{ where } \delta' = \ln(\delta + 1)$$

$\alpha_{A-B} = R_A/R_B$ is the ratio of heavy isotope to light isotope in two minerals (A and B),

$$\delta = (R_{\text{sample}}/R_{\text{standard}} - 1)$$

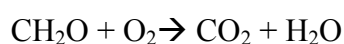
and θ is the mass-dependent fractionation exponent approximated to be 0.52 (Miller, 2002; Rumble et al., 2007; Kusakabe and Matsuhisa, 2008).

However, the assumption of a constant θ value is not correct when $^{18}\text{O}/^{16}\text{O}$ and $^{17}\text{O}/^{16}\text{O}$ ratios are calculated with very high precise techniques. Minor but computable variations in the $\delta^{17}\text{O}$ - $\delta^{18}\text{O}$ relationship have been observed in plant waters, carbonates, meteoric waters, silicates and ocean waters on high precision analysis of $^{17}\text{O}/^{16}\text{O}$. It differs as a function of mass dependent fractionation managed by kinetic effects like water-rock interactions, evapotranspiration, and diffusion during evaporation. (Landais et al., 2006; Landais et al., 2008, 2012a,b; Luz and Barkan, 2010; Barkan and Luz, 2011; Winkler et al., 2012; Levin et al., 2014; Pack and Herwartz, 2014; Passey et al., 2014; Schoenemann et al., 2014). In the past decade, triple oxygen isotope variations study in atmosphere and the hydrological cycle has advanced considerably. Common processes on earth such as phase changes in water and interactions between common rocks and water, their mass dependent fractionation slopes have been restrained by empirical observations and theoretical calculations. For example, the slopes that define diffusive fractionations (θ_{diff}) are described as $\ln^{17}\alpha_{\text{diff}}/\ln^{18}\alpha_{\text{diff}}$ and the slope that describes equilibrium isotopic fractionation ($\theta_{\text{eq}} = 0.529$) is the logarithmic ratio of the equilibrium fractionation factors, $\ln^{17}\alpha_{\text{eq}}/\ln^{18}\alpha_{\text{eq}}$ (Young et al., 2002; Barkan and Luz, 2005; Cao and Liu, 2011), and is usually smaller than θ_{eq} . Thus, the deviance from the equilibrium line, $\Delta^{17}\text{O}$ or ^{17}O -excess, could be used as an efficient method to differentiate equilibrium from kinetic isotope effects (Matsuhisa et al., 1978; Angert et al., 2004). Understanding of the interaction between $\Delta^{17}\text{O}$ in water and calcite and variation in $\Delta^{17}\text{O}$ in meteoric and plant waters helps in using the triple oxygen isotope system as a means in paleoclimate research.

All the fractionation processes mentioned above are mass-dependent fractionations (MDF). There is also mass-independent fractionation (MIF) processes. MIF is independent of the mass differences between isotopes, and can lead to large ^{17}O anomalies. These processes follow a relationship of $\alpha^{17} \approx \alpha^{18}$ (Thiemens et al., 1983, 1995). Anomalous triple oxygen

isotope compositions have been observed in meteorites and in the atmosphere, where the $\Delta^{17}\text{O}$ can be used as an indicator of MIF processes. A dominant origin of ^{17}O anomalies in the atmosphere due to photochemical reactions in the stratosphere, leading to an extremely ^{17}O -enriched O_3 and CO_2 , and ^{17}O -depleted O_2 . This study revealed that O_2 and CO_2 are good tracers for studying the stratospheric photochemical reactions and also the global carbon cycle (Yung, 1997; Young et al., 2014).

Variable triple oxygen isotope information is recorded in different earth materials and is valuable for studying natural processes. As a dominant constituent in the Earth-surface system, water is involved in most of the fractionation processes. It influences animals and plants, interacts with atmospheric gases and reacts with many kinds of minerals, for example, carbonates. Several ways to generate ^{17}O anomalies in waters are: 1) fractionation during transport of moisture from ocean to the inland continents (e.g., Meijer and Li, 1998; Luz and Barkan, 2010) 2) kinetic fractionation during evaporation of surface water, leaf water, and animal body water (e.g., Landais et al., 2006) and 3) biological respiration that incorporates ^{17}O anomalies in atmospheric O_2 into metabolic water through the reaction



(e.g., Gehler et al., 2011; Pack et al., 2013). These anomalies promise to record information about aspects of the hydrological cycle, climates, atmosphere, and physiology of animals both in the present day and the distant geological past. Triple oxygen isotopes analysis is performed to study the physiology and habitat of present or extinct animals, and to reconstruct the carbon cycle in the past.

5.2 Sample Details

Eggshells collected from various Paleolithic sites in India and a modern eggshell from China was analyzed as mentioned in Table 5.1. Along with the samples various international standards, NBS-19 and NBS-18 and internal references, 102-GCAZ01 and “Tank #2 CO_2 were also examined. These standards were examined in each session of analysis and act as reproducibility standards ($\Delta^{17}\text{O}$ and $\delta^{18}\text{O}$). They also serve as a basis for session-specific normalization to absolute d-values ($\delta^{18}\text{O}$).

Table 5.1 Ostrich eggshell sample collection sites and their respective states

Site	State & GPS Coordinates	Sample ID	Taxa
Chavni Baroda	Rajasthan (25° 26' 24" N, 75° 38' 24" E)	OSI-001	Struthinoid
Chavni Baroda	Rajasthan (25° 26' 24" N, 75° 38' 24" E)	OSI-002	Struthinoid
Chavni Baroda	Rajasthan (25° 26' 24" N, 75° 38' 24" E)	OSI-003	Struthinoid
Anjar	Gujarat (23° 6' 48.32" N, 70° 1' 39.88" E)	OSI-004	Struthinoid
Chandresal- 1	Rajasthan (25° 10' 48" N, 75° 49' 48" E)	OSI-005	Struthinoid
Chandresal- 1	Rajasthan (25° 10' 48" N, 75° 49' 48" E)	OSI-006	Struthinoid
Chandresal- 1	Rajasthan (25° 10' 48" N, 75° 49' 48" E)	OSI-007	Struthinoid
Chandresal- 2	Rajasthan (25°13'34.1"N 75°55'34.7"E)	OSI-008	Struthinoid
Chandresal- 2	Rajasthan (25°13'34.1"N 75°55'34.7"E)	OSI-009	Struthinoid
Chandresal -2	Rajasthan (25°13'34.1"N 75°55'34.7"E)	OSI-010	Struthinoid
Nagda	Rajasthan (25°10'53.3"N 75°48'45.5"E)	OSI-011	Struthinoid
Runija	Madhya Pradesh (23°09'39.4"N 75°16'02.6"E)	OSI-012	Struthinoid
Khajurna	Madhya Pradesh (26°44'33.6"N 78°47'45.6"E)	OSI-013	Struthinoid
China	Linyi, China (35.10 N 118.32 E)	CHA-2013	Struthinoid

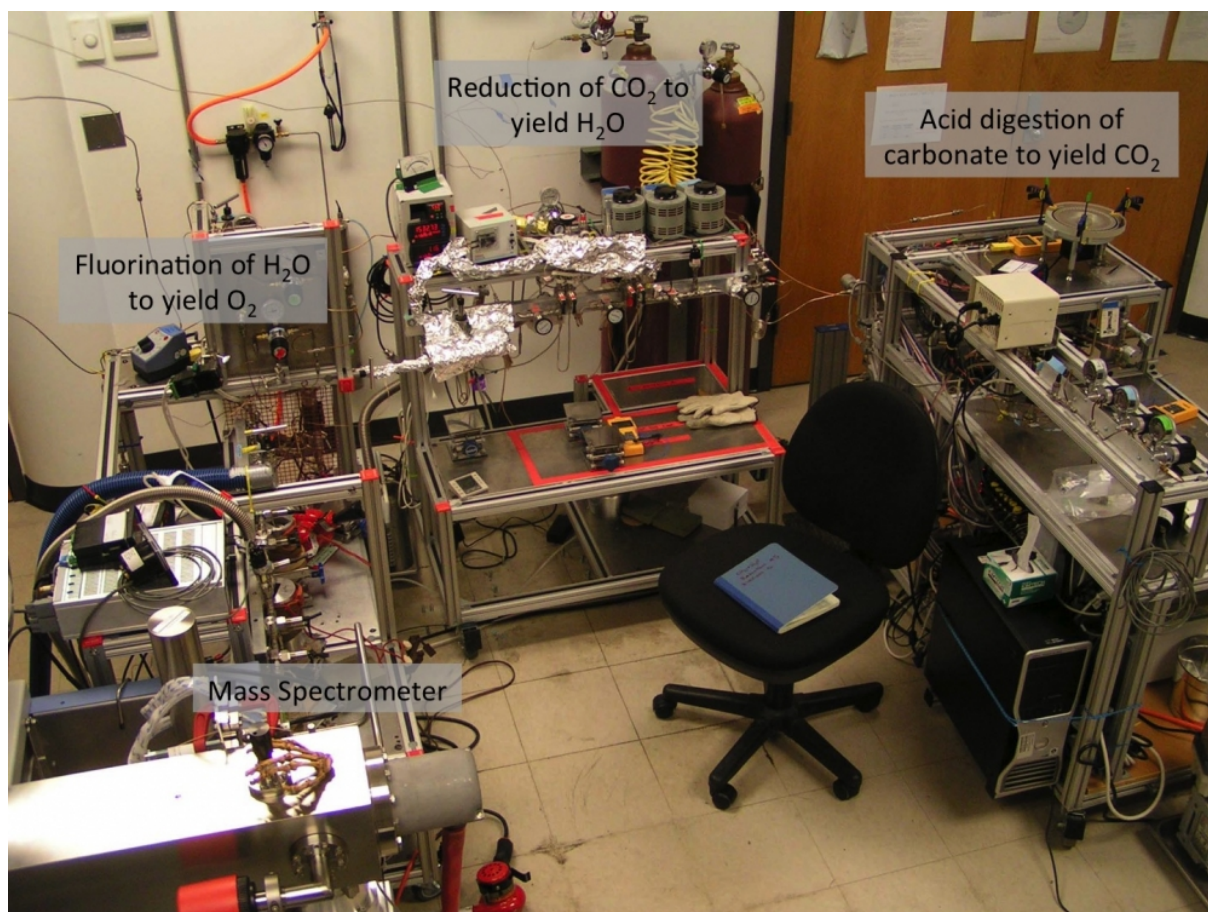


Figure 5.1 Autoline for triple oxygen isotope analysis at Johns Hopkins University

5.3 Experimental

The triple oxygen isotope analysis consists of extraction of CO_2 from carbonate, reduction of CO_2 to produce water, and finally, the fluorination of water to produce oxygen (Fig 5.1). The O_2 produced was then analyzed by extended-collection-time dual inlet mass spectrometry. This whole procedure of extraction of CO_2 from carbonate and introduction of O_2 in the mass spectrometer was completed in about three hours which was similar to the time required by the isotope characterization of the O_2 samples in the mass spectrometers as depicted in Fig 5.2.

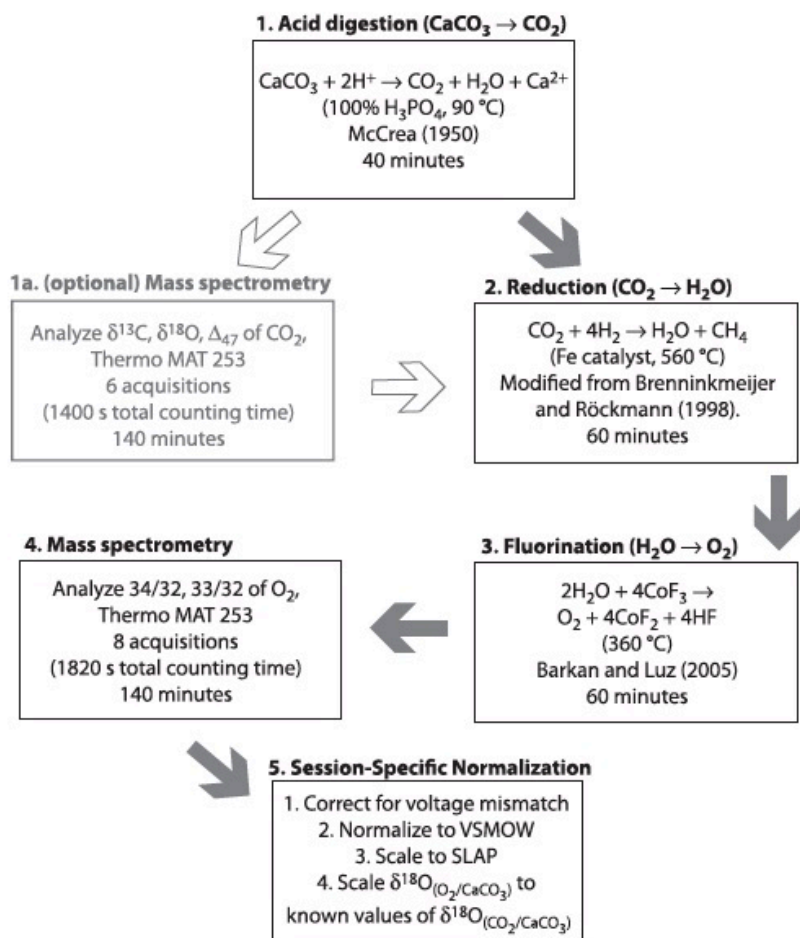


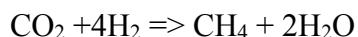
Figure 5.2 An overall analytical procedure used in this study (Passey et al. 2014)

5.3.1 Extraction of CO_2 from carbonate

Phosphoric acid digestion (McCrea, 1950) was used for extraction of CO_2 from carbonates. The carbonate clumped isotope thermometry extraction line was used for CO_2 extraction from carbonates (Passey et al., 2010; Henkes et al., 2014, Passey et al., 2014). Briefly, 8-10 mg of sample was crushed and stored in silver capsules. These samples were then loaded in autosampler and then reacted in 100% H_3PO_4 at 90°C. The evolved CO_2 was passed through multiple cryogenic traps and Gas Chromatography column at 20°C for purification. This CO_2 extraction line was directly connected to the reduction line.

5.3.2 Reduction of CO₂ to produce H₂O

In the reduction line, the oxygen from CO₂ is converted to O₂ in H₂O based on a Bosch-type reaction (Brenninkmeijer and Rockmann, 1998).



Reactants of these reactions were actively passed through a 560⁰ C reactor (having iron powder as the catalyst) via circulating loop system and the product H₂O was actively removed (Fig. 5.3). The unreacted CO₂ was passed multiple times through the reactor via circulating closed loop design system until the gas was totally reacted. It further allows the H₂O to later be effectively expelled into a CoF₃ reactor by a stream of helium. At the initiation of the reaction, the circulating loop encloses an excess of hydrogen with a pressure of 1600 mBar i.e. 1400 mbar of hydrogen and 200 mBar of CO₂. The system consists of two basic components as described in Fig 5.3. First one is the circulating loop, and the other one is a vacuum manifold for the insertion of CO₂ sample into the circulating loop and for ‘pre-reduction’ of the circulating loop. The ‘pre-reduction’ procedures comprised of following events. The names of the components are used as described in Fig 5.3. The circulating loop was injected with hydrogen gas from an external source (H₂ tank- 6.0 ultra high purity grade). This tank was purified of water and oxygen by passing through chemical traps (Restek Click one; Cat. # 22464, #22474). Then, the hydrogen gas was continuously circulated around the loop. The flow rate of the gas was about 20 ml/min using a peristaltic pump (Thermo Scientific FH10) with a Viton loop. This loop was coupled to the main circulating loop with multiple brass hose barb fittings. The gas moved through the reactor, which was a glassy carbon tube containing Fe powder (300 mg). A furnace kept at 560⁰C heated this powder. The reactor was coated with a quartz tube that was injected with helium to reduce oxidation of the external of the carbon tube and the diffusion of oxygen and other atmospheric gasses in the tube. The gas was passed through a 6-port, 2-way valve after leaving the reactor. This valve allowed the gas to pass through Trap 4, which was a water collection trap, maintained at 78⁰C or to bypass the trap. The circulating loop was warmed with heat tape in order to reduce the adsorption of water onto the inner surface of the loop.

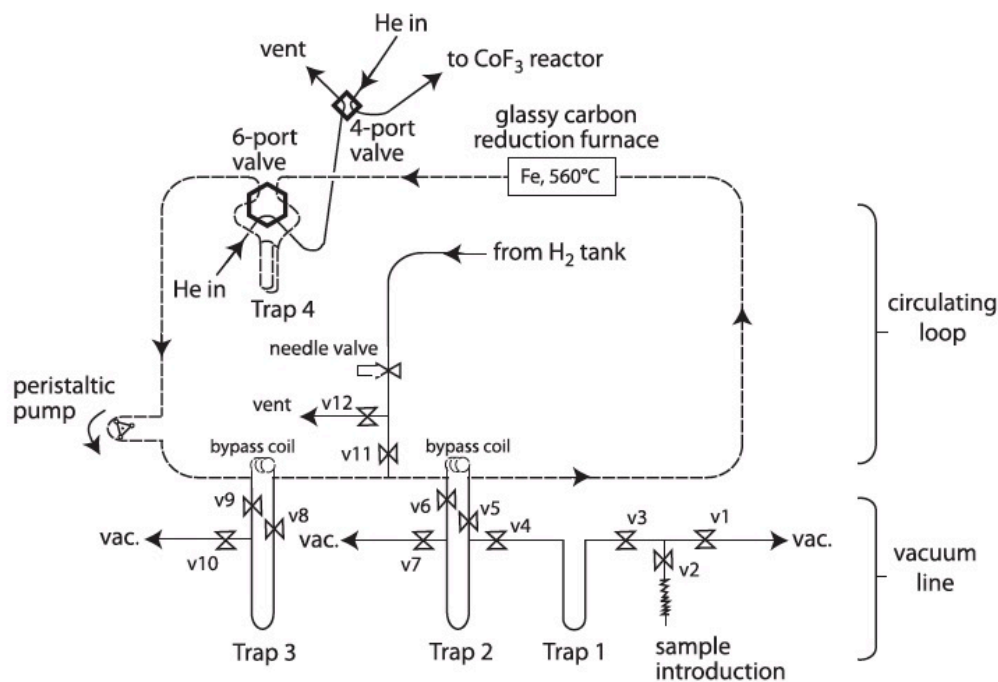


Figure 5.3 Diagram of the system used to transform oxygen into carbon dioxide to oxygen in the water and to introduce carbon dioxide samples into the circulating loop. (v- valve, vac- vacuum; Passey et al, 2014)

After recharging the circulating loop with hydrogen gas, the system was pre-reduced for 30-60 min, before introducing a new CO₂ sample. This pre-reduction was necessary to remove residual gas from the earlier sample or to remove water, which could be produced by reduction of contaminants oxygen, carbon dioxide or oxides in the reactor. Trap 3 collected the water and other condensable gasses formed during pre-reduction. These residuals were pumped before the analysis of next sample. During the pre-reduction, the pressure of hydrogen gas in the circulating loop decreased continuously (Fig 5.4), which indicated that contaminants were eliminated during this procedure. It may possibly also show the reaction of hydrogen gas with carbon to form methane or diffusion of hydrogen gas in the metal and hot glass carbon. CO₂ samples were introduced into the system via a port situated near Valve 2. Carbon dioxide was firstly purified cryogenically in Trap 1 and Trap 2 and then introduced into the reactor loop. On Trap 4, methanol slurry was placed maintained at 78⁰C. 6-port valve on which Trap 4 was located is designed in a way so that the gas in the loop flows via this trap. The carbon dioxide sample gas was then allowed in from Trap 2 into the circulating loop. The advancement of the reaction was examined using a pressure transducer. The reaction was regarded as done when the rate of pressure decrease equals to its baseline rate measured during the pre-reduction procedure. After the reaction, the 6-port orientation is changed so that helium gas flows through

Trap 4. The methanol slurry was upheld for few minutes on Trap 4 as helium carrier gas removed residual hydrogen gas out of Trap 4 and via a vent to atmosphere. After that, the arrangement of 4-port valve was modified so that the helium emission from Trap 4 was targeted into a flow-through CoF_3 reactor. Trap 4 was then heated using a hot air gun, which allowed the H_2O to be expelled into the CoF_3 reactor.

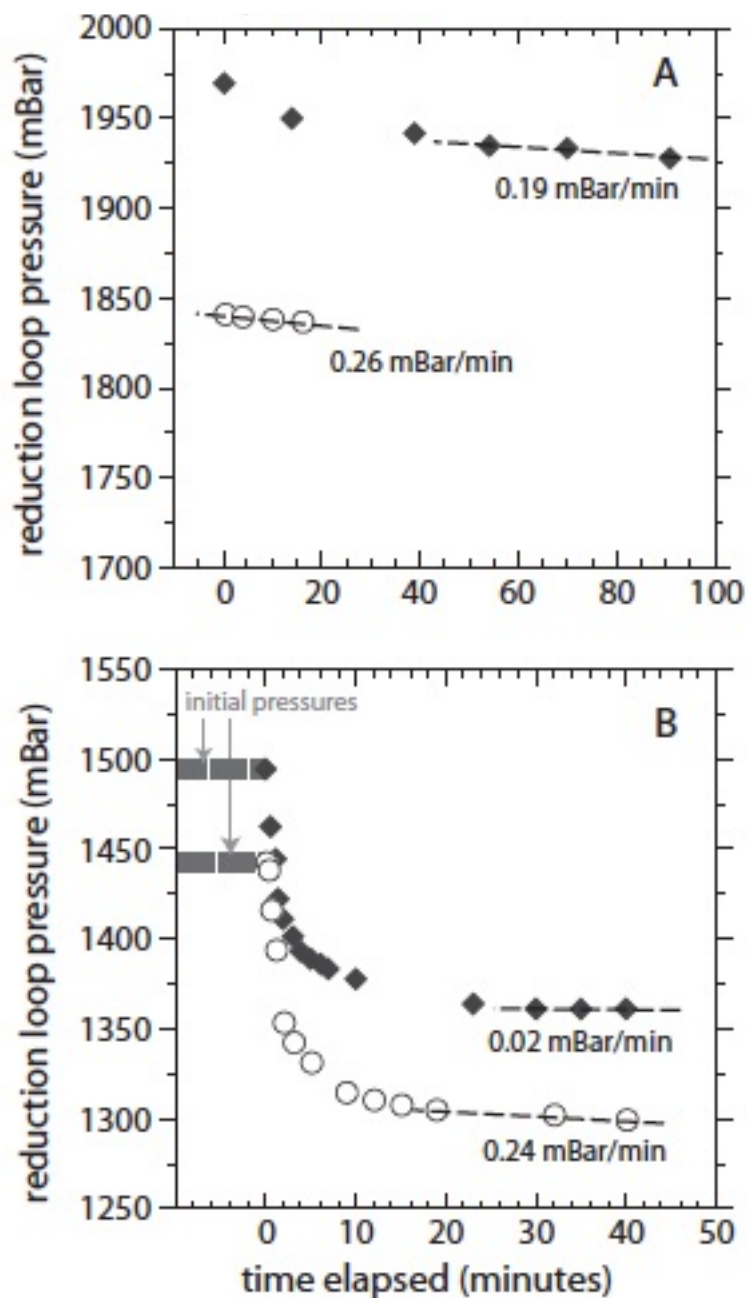


Figure 5.4 Reaction progress in the circulating loop of reduction line. (A) Before the introduction of each sample decrease in pressure during the 'pre-reduction' step performed. (B) The decrease in pressure following the introduction of sample carbon dioxide (Passey et al., 2014)

5.3.3 Fluorination of water to produce oxygen

The water was reacted with the mixture of HF + oxygen by passing through the CoF₃ reactor which was maintained at 370⁰C, similar in design to the extraction line of Barkan and Luz, 2005. The HF was entrapped in a liquid nitrogen trap at 196⁰C and the oxygen was collected in a trap with the molecular sieve. The helium carrier gas was expatriated and the trap was heated to transfer the oxygen gas to the trap with the molecular sieve. The oxygen gas was then expanded by heating, which minimized the isotope effects linked with desorption of oxygen from molecular sieves. After the expansion, the yield was calculated and gas was finally introduced into the mass spectrometer.

5.3.4 Isotopic analysis of oxygen and carbon dioxide

Thermo MAT 253 mass spectrometer was used to analyze the m/z 33/32, 34/32 ion ratios of oxygen at Johns Hopkins University. Dual-inlet mode was used to analyze the samples at a single intensity of 2500 Å. Seven acquisitions were conducted for each sample where each acquisition was comprised of 10 sample-reference gas measurement cycles. Mass spectrometry was also done on carbon dioxide produced by acid digestion method of carbonate samples. D₄₇, δ¹⁸O, and δ¹³C values were defined from measured 47/44, 46/44, and 45/44 ion ratios. For carbon dioxide gas six acquisitions were conducted, each comprised of 9-reference gas – sample gas cycles.

5.3.5. Data normalization

All oxygen data were normalized to concurrent analysis of SLAP2 (δ¹⁸O=-55.5%), and VSMOW2 (δ¹⁸O=0%, δ¹⁷O =0%). A reference frame was suggested by Schoenemann et al. (2013) where D¹⁷O_{SLAP2} =0%, which translates to δ¹⁷O_{SLAP2} =-29.6986490 when δ¹⁸O_{SLAP2}=-55.5% and λ = 0.528. The same CoF₃ extraction line was used for reacting oxygen, as used for unknown water samples. Thus, this is a straight, ‘real-time’ normalization to international standards set in the same approach as samples. The δ values of samples relative to VSMOW2 are measured as:

$$\delta_{SA-VSMOW2} = \{(\delta_{SA-REF}+1)/(\delta_{VSMOW2-REF}+1)\} - 1$$

A correction for the voltage difference between reference gas ion beams & sample ion beams was applied before normalization to VSMOW2 and scaling to SLAP2. Samples of

oxygen, initiating as carbon dioxide or CaCO₃ goes through an extra normalization step. This step corrects for slope <1 for regressions between measured δ¹⁸O (O₂/CaCO₃) and “known” values of δ¹⁸O (CO₂/CaCO₃).

Values of δ¹⁸O were normalized to internal standards calibrated to NBS-19 or to simultaneous analysis of NBS-19 for direct analysis of carbon dioxide. The relationship δ¹⁸O_{VSMOW} = 1.03091 * δ¹⁸O_{VPDB} + 30.91 was used to convert these values to the VSMOW scale (Coplen et al., 1983)

5.4 Results and Discussion

Following the approach of the ¹⁸O-body water model presented by Kohn (1996), we developed a new oxygen isotope mass balance model that includes all three isotopes of oxygen in the form of ¹⁸O/¹⁶O and ¹⁸O/¹⁷O ratios. The basic scenario for our model is the oxygen mass balance of outputs and inputs for an animal (Fig. 5.5).

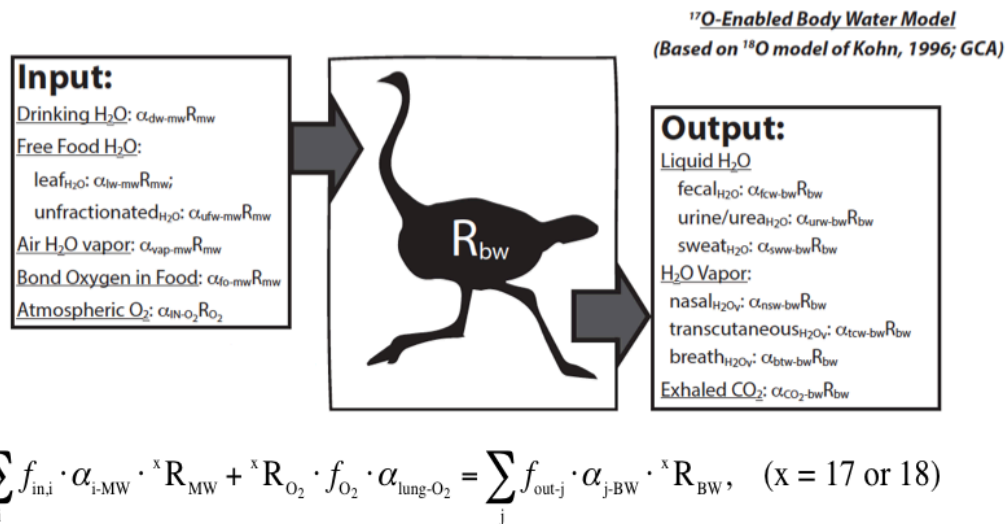


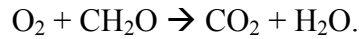
Figure 5.5 ¹⁷O-enabled body water model for animals based on ¹⁸O model of Kohn, 1996. The oxygen isotope output and input fluxes are in mass balance relationship. Inputs can be expressed in terms of fractionated meteoric water plus the term of atmospheric O₂. Outputs can be expressed in terms of fractionated body water. Fractionation factors (α) and fraction (f) are in light of previous work (Kohn, 1996; Barkan and Luz, 2005; Hofmann et al., 2012). Leaf water models are based on the ¹⁸O/¹⁶O model of Roden and Ehleringer (1999). The relationship between relative humidity and the oxygen isotope fractionation exponent λ is given by Landais et al., 2006

Animals interchange oxygen with the ecosystem mainly in the form of Oxygen, H₂O, CO₂ and chemically bound oxygen in food. Figure 5.5 shows that oxygen inputs for body water are drinking water, atmospheric O₂, free water in food, chemically bound oxygen in food, and inhaled air water vapor. These oxygen components are related to two main oxygen reservoirs: atmospheric O₂ and surface water. Oxygen outputs are described as liquid excreted water (urine and sweat), fecal water, CO₂, water vapor (nasal, breath, and transcutaneous water), and O in urea and uric acid. As the inputs and outputs oxygen isotope fluxes should be balanced to keep the animal body water at a steady state, it can be equated as:

$$\sum_i f_{in,i} \cdot {}^xR_i = \sum_j f_{out,j} \cdot {}^xR_j, \quad ({}^xR = {}^xO/{}^{16}O, \quad x = 17 \text{ or } 18)$$

where $f_{in,i}$ and $f_{out,j}$ are the fraction of moles for each input oxygen component (i) and output oxygen component (j).

Animals incorporate atmospheric O₂ into metabolic water through respiration:



Therefore, the metabolic H₂O constitutes part of the body water and strongly affects body water D¹⁷O signals because of the large ¹⁷O anomalies from atmosphere O₂. The atmospheric O₂ inputs can be expressed as:

$$R_{O_2} \cdot f_{O_2} \cdot \alpha_{lung-O_2},$$

where f_{O_2} is the molar fraction of O from O₂ relative to all oxygen input fluxes and α_{lung-O_2} is the fractionation factor between O₂ absorbed by the lungs and atmospheric O₂. All the other oxygen input fluxes are related to ambient meteoric water by specific fractionation factors and can be expressed by

$$R_{MW} \cdot f_{in,i} \cdot \alpha_{i-MW},$$

where R_{MW} is the oxygen isotope ratio of local meteoric water, $f_{in,i}$ is the fraction of input component i, α_{i-MW} is the fractionation factor between component i and the meteoric water. Similarly, all output oxygen components are related to animal body water. So the right side of the equation can be expressed in form of

$$R_{\text{BW}} \cdot f_{\text{out},j} \cdot \alpha_{j\text{-BW}}$$

Where R_{BW} is the oxygen isotope ratio of animal body water, $\alpha_{j\text{-BW}}$ is the fractionation factor between output component j and the body water. Finally, the isotopic mass balance equation can be expressed as:

$$\sum_i f_{\text{in},i} \cdot \alpha_{i\text{-MW}} \cdot {}^x R_{\text{MW}} + {}^x R_{\text{O}_2} \cdot f_{\text{O}_2} \cdot \alpha_{\text{lung-O}_2} = \sum_j f_{\text{out},j} \cdot \alpha_{j\text{-BW}} \cdot {}^x R_{\text{BW}}, \quad (x = 17 \text{ or } 18)$$

Specific and fractionation factors (a) and ranges of input or output fractions (f_i, f_j) for each component were obtained from previous studies (O'Neil and Adami, 1969; Majoube, 1971; Friedman and O'Neil, 1977; Epstein and Zeiri, 1988; Kohn, 1996; Roden and Ehleringer, 1999; Barkan and Luz, 2005; Landais et al., 2006).

The triple oxygen isotope compositions in animal body water were mainly controlled by ambient humidity, the fractional contribution of metabolic water, animal water use efficiency, and the fraction of evaporated water (like leaf water) consumed by animals. Variability in the relative contributions and isotopic compositions of these inputs can lead to a wide range in $D^{17}\text{O}$ of animal body water. The highest animal body water $D^{17}\text{O}$ values are expected for animals that live in humid climates, consume little evaporated water (leaf water) from food, and have poor water use efficiency (= high water economy index, WEI, the amount of water needed for per unit energy metabolized, e.g., ml/KJ). Conversely, the lowest body water $D^{17}\text{O}$ values are expected for animals that live in arid climates, consume a large amount of evaporated water from food, and have high water use efficiency (low WEI). There do not seem to be clear differences in WEI across broad taxonomic groups, such as birds, mammals, reptiles, and arthropods, and no clear correlations with body mass (Nagy and Peterson, 1988). For instance, typical values for desert-adapted animals are ≤ 0.15 mL/KJ and for humans are ≥ 0.3 mL/KJ.

The lower and upper limits of body water $D^{17}\text{O}$ were explored by running a “maximum evaporation body water model” and a “minimum evaporation body water model”, respectively. In the “maximum evaporation model”, the relative humidity (Rh) was assumed 0.2, fraction of evaporated leaf water relative to whole food water 0.4, and the WEI value 0.1 mL/KJ. Similarly, the limits for the “minimum evaporation model” were modeled by holding Rh at 0.8, the WEI value at 0.5 mL/KJ, and fraction of leaf water at 0.01 (Fig.5.6). This model is widely

applicable to both modern and fossil animals for determining variations in climate and animal physiology.

In order to analyze the isotopic compositions of parent waters for these carbonates, knowledge of the isotopic fractionation factors between the carbonate and its parent water is required. Egg white water was extracted from fresh chicken and duck eggs using a vacuum distillation method (unpublished data from Johns Hopkins University). Assuming there is no significant fractionation between egg white water and body H₂O, the distilled water is taken as the parent water for eggshell carbonate. By analyzing both the parent water and carbonates, the fractionation factors between carbonate and water were calculated under a constant temperature assuming ostrich body temperature, ~38-40 °C using equation given below

$${}^x\alpha_{\text{Carb-H}_2\text{O}} = \frac{1000 + \delta^x\text{O}_{\text{Carb}}}{1000 + \delta^x\text{O}_{\text{H}_2\text{O}}}, \quad (x = 17 \text{ or } 18)$$

The mean fractionation factors based on these experiments are ${}^{18}\alpha = 1.0380 \pm 0.0008$, and ${}^{17}\alpha = 1.0197 \pm 0.0004$, translating to a fractionation exponent of $l = 0.5245 \pm 0.0003$ (95% confidence interval). These calculated fractionation factors combine the carbonate-water fractionation, the so-called “acid” fractionation (as O₂ is analyzed ultimately produced from CO₂ derived from carbonate by acid digestion), and any other fractionations from this analytical method. Therefore, the triple oxygen isotope composition of carbonate parent water (body water) was calculated based on these fractionation factors and analyzed eggshell carbonate data (Table 5.2). The samples analyzed for comparisons were from climates varying from arid to humid and include species that intake a large amount of evaporated leaf water (ostrich and wild birds) to domestic animals that consume very little leaf water. The observed body water $d^{18}\text{O}$ and $D^{17}\text{O}$ values have a large range, from -6‰ to +10‰ and +0.02‰ to -0.15‰, which reflects the effects from different environments and physiologies. Comparison of the observed data with the body water model shows that all data fit within the modeled maximum and minimum range of $d^{18}\text{O}$ and $D^{17}\text{O}$ within error values (Fig. 5.6).

Table 5.2 Measured isotopic compositions of eggshells from India (carbonates) and calculated isotopic compositions of parent waters of the eggshells (carbonates). Values are given in units of per mil relative to the VSMOW-SLAP scale of Schoenemann et al. (2013), with $\lambda = 0.528$

Sample id	Species	n	Measured Values		Calculated values	
			$\delta^{18}\text{O}^b$ (O_2/CaCO_3)	D^{17}O^b (O_2/CaCO_3)	$\delta^{18}\text{O}$ H_2O	D^{17}O H_2O
OSI-001	Ostrich	3	44.01	-0.288	8.9	-0.244
OSI-002	Ostrich	3	43.38	-0.285	7.8	-0.238
OSI-003	Ostrich	3	40.92	-0.260	5.2	-0.219
OSI-004	Ostrich	3	48.52	-0.330	13.2	-0.279
OSI-005	Ostrich	3	37.34	-0.247	3.4	-0.202
OSI-006	Ostrich	3	40.40	-0.281	5.1	-0.242
OSI-007	Ostrich	3	38.49	-0.251	3.7	-0.217
OSI-008	Ostrich	3	42.18	-0.289	7.1	-0.248
OSI-009	Ostrich	3	43.27	-0.303	8.6	-0.263
OSI-010	Ostrich	3	43.20	-0.311	8.9	-0.266
OSI-011	Ostrich	3	46.02	-0.320	10.6	-0.276
OSI-012	Ostrich	3	49.86	-0.338	14.8	-0.284
OSI-013	Ostrich	3	41.93	-0.280	7	-0.236
CHA2013	Ostrich	3	28.42	-0.163	4.6	-0.131

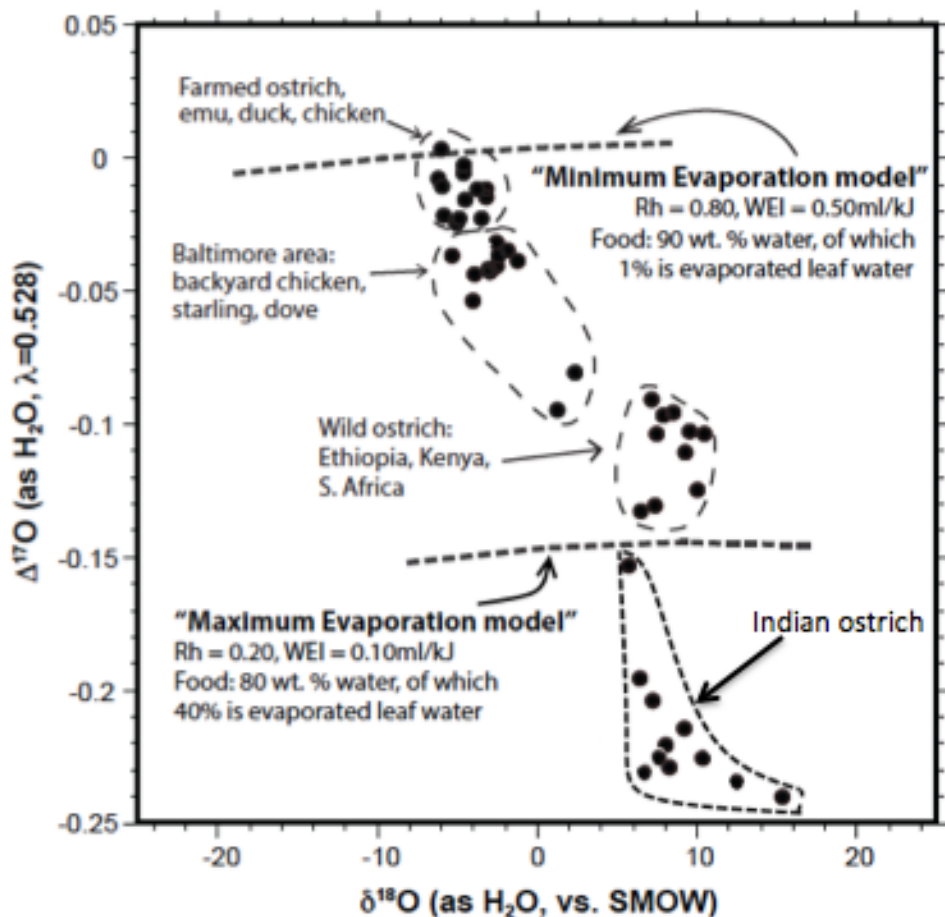


Figure 5.6 “Minimum Evaporation” and “Max Evaporation” model (dashed lines) predicted by the ^{17}O -enabled body water model. Actual measurements of body water isotopes from analysis of eggshells are shown in black circles.

The highest $d^{18}\text{O}$ values were from animals consuming lots of evaporated water and living in arid environments and the lowest are from animals consuming little evaporated water and living in humid environments (Fig 5.6). In contrast, the highest $D^{17}\text{O}$ values are from animals living in humid environments with high WEI and small intake of leaf water, while the lowest $D^{17}\text{O}$ values are from animals living in arid environments with low WEI and large intake of leaf water. Indian ostrich eggshell samples lie below the maximum evaporated model. Low $D^{17}\text{O}$ values and $d^{18}\text{O}$ values obtained indicate that ostriches were living in arid climates with low water economy index and they mostly consumed lots of evaporated water during that age.

5.5 Concluding Remarks

To conclude, this model extends oxygen isotope studies in biogenic minerals from $^{18}\text{O}/^{16}\text{O}$ as well as $^{17}\text{O}/^{16}\text{O}$ which could be widely used for studying animal physiology and palaeoclimate.

Furthermore, as the body water inherits information from atmospheric O₂, we can apply the model to fossil biominerals to reconstruct paleoatmospheric compositions. However, to refine and evaluate the body water model, we need more systematic data to address the uncertainties brought up by the complex animal physiology and various climate parameters.

CHAPTER 6

GENERAL DISCUSSION AND FUTURE DIRECTIONS

6.1 General Discussion

Research work conducted exhibits the advantage of blending molecular biology work with stable isotope profiling of ostrich fossils eggshells for studies in the field of paleobiology and archaeology. To the best of our knowledge, the work presented in this thesis determines the presence of aDNA in the fossil eggshells collected from various Upper Paleolithic sites of India. aDNA was first visualized using Confocal laser Scanning microscopy and then isolated and amplified using species-specific primers as described in Chapter 3. The results from this chapter provide the first genetic evidence of ostriches present in India. Stable isotope profiling of these eggshells were further done to reveal the insights into paleoecology, paleodietary and paleoenvironment (Chapter 4 and 5).

Fossil ostrich eggshells were collected from numerous localities in India. Morphological and compositional analysis of these eggshells was done using SEM, XRD and EBSD (Chapter 2). SEM studies demonstrated the ultrastructure of fossil eggshells and formation of the calcified cuticular layer. The presence of calcified cuticle layer in the eggshell is the basis for aDNA studies as it contains preserved biomolecules. EBSD accentuates the crystallographic structure of the ostrich eggshells with sub-micrometer resolution. It is a non-destructive tool for evaluating the extent of diagenesis in eggshell. EBSD analysis revealed the presence of dolomite in the eggshells. This research resulted in the complete recognition of the structure of ostrich eggshells as well as the nature and extent of diagenesis in these eggshells which is vital for genetic and paleoenvironmental studies.

Chapter 3 presents confocal microscopy and ancient DNA studies on these eggshells. Eggshells that have undergone diagenesis were not used as a substrate for aDNA analysis as known from EBSD analysis. aDNA from Indian eggshells have been extracted and amplified for the first time dating 25000 to 40000 years old. DNA in these fossil eggshells was found to be well preserved compared to other substrates due to the intracrystalline matrix of eggshell. To maximize the recovery of DNA from these eggshells, they were observed under CLSM. DNA hotspots were visualized using this microscopy technique. Many attempts were made to extract DNA from these samples and further an extraction protocol was optimized consisting of an

extra heating step modified from the protocol of Oskam et al., 2010. Since the copy number of DNA is traditionally low in ancient samples and aDNA is fragmented in nature, we optimized the amplification protocol targeting the mitochondrial hypervariable region (HVR) and 16SrRNA gene by using PCR primers designed to amplify short fragments, using multiple aliquots of the DNA extracts as a template for the PCR reactions. A fragment length of 43 bp and 23 bp, was obtained from 25,000 years old samples collected from Ravishankarnagar (and Runija respectively, which showed an identity of 92% and 100% with *Struthiocamelus* species. Alignments of partial 16SrRNA gene sequence of ratites (obtained from NCBI) and samples were done. Obtained sequences were submitted to NCBI GenBank (Accession No KU251475) and compared with published partial mitochondrial sequences. BLAST (NCBI) and multiple sequence alignment show similarity with *Struthio* species. To explore the phylogenetic relationship with our DNA sequences, a comparative study with published avian mtDNA sequences was done and the phylogenetic tree was constructed using MEGA 6.06 showing similarity with *Struthio camelus*.

Stable isotope profiling of eggshells reveals insights on paleodietary, paleoecology and paleoenvironment. Carbon and oxygen isotopes were analyzed after acid digestion of carbonate eggshells. The samples from a specific location indicated the dietary of ostriches to be of C₃ plants and other locations showed a paleodietary mixture of C₃ and C₄ plants. Oxygen isotope data shed some light on the ecology of Late Pleistocene indicating less humid and arid conditions. Bond order of ¹³C- ¹⁸O was used as a paleothermometer to calculate the body temperature of ostriches. Triple oxygen isotope model extends oxygen isotope studies in biogenic minerals from ¹⁸O/¹⁶O to include ¹⁷O/¹⁶O and which was used for studying animal physiology and climate. Indian ostrich eggshell samples lie below the maximum evaporated model. Low *D*¹⁷O values and *d*¹⁸O values showed that these birds were living in arid climates with low water economy index. They mostly consumed lots of evaporated water. Furthermore, as the body water inherits information from atmospheric O₂, this model was applied to fossil biominerals to reconstruct paleoatmospheric compositions.

6.2 Future Directions

This research has considerably advanced the knowledge about the biogeography of ostrich, their aDNA analysis, palaeodiet and paleoecology. However for further research work

- Next Generation Sequencing (NGS) advances could be employed for extraction and sequencing of smaller fragments.
- Proteins located in the carbonate material could be employed for species identification. This method is a fast process for species identification and may help in any protein composition difference in eggshells.
- Samples analyzed in these eggshells were from the western peninsular region of India. Additional sample analysis from other sites could have provided a greater understanding about their paaleodiet, paleoecology and paleoenvironment.

BIBLIOGRAPHY

1. Anderson, S., Bankier, A.T., Barrell, B.G., de Bruijn, M.H., Coulson, A.R., Drouin, J., Eperon, I.C., Nierlich, D.P., Roe, B.A., Sanger, F., Schreier, P.H., Smith, A.J., Staden, R., and Young, I.G. (1981). **Sequence and organization of the human mitochondrial genome.** *Nature* 290, 457-465.
2. Andrews, R.M., Kubacka, I., Chinnery, P.F., Lightowlers, R.N., Turnbull, D.M., and Howell, N. (1999). **Reanalysis and revision of the Cambridge reference sequence for human mitochondrial DNA.** *Nature genetics* 23, 147.
3. Angert A., Cappa C. D. and De Paolo D. J. (2004) **Kinetic ^{17}O effects in the hydrologic cycle: indirect evidence and implications.** *Geochimica et Cosmochimica Acta* 68, 3487-3495.
4. August, G.C., Ajithprasad, P., Sharma, B. (2011). **Tracking early humans in coastal western India: the Gujarat Palaeoanthropology Project.** *Antiquity Bulletin Project Gallery* 327, 85.
5. Ayliffe, L. K., & Chivas, A. R. (1990). **Oxygen isotope composition of the bone phosphate of Australian kangaroos: potential as a palaeoenvironmental recorder.** *Geochimica et Cosmochimica Acta* 54, 2603-2609.
6. Badam, G.L. (2005). **A note on the Ostrich in India since the Miocene.** *Man Environment* 30, 97-104.
7. Bao H., Fairchild I. J., Wynn P. M. and Spötl C. (2009) **Stretching the envelope of past surface environments: Neoproterozoic Glacial Lakes from Svalbard.** *Science* 323, 119-122.
8. Barkan, E., & Luz, B. (2005). **High precision measurements of $^{17}\text{O}/^{16}\text{O}$ and $^{18}\text{O}/^{16}\text{O}$ ratios in H_2O .** *Rapid communications in mass spectrometry* 19, 3737-3742.
9. Barkan E. and Luz B. (2011). **The relationships among the three stable isotopes of oxygen in the air, seawater, and marine photosynthesis.** *Rapid communications in mass spectrometry* 25, 2367-2369.

10. Bednarik, R.G. (1994). **A taphonomy of palaeoart.** *Antiquity* 68, 68-74.
11. Bednarik, R.G. (1993a). **About Palaeolithic ostrich eggshell in India.** *Indo-Pacific Prehistory Association Bulletin* 13, 34-43.
12. Bednarik, R.G. (1993b). **Palaeolithic art in India.** *Man Environment* 18, 33-40.
13. Berg, C., Blomqvist, A., Holm, L., Brandt, I., Brunstrom, B., Ridderstrale, Y., (2004). **Embryonic Exposure to Oestrogen Causes Eggshell Thinning and Altered Shell Gland Carbonic Anhydrase Expression in the Domestic Hen.** *Reproduction* 128, 455-461.
14. Biswas, A., Rao, V.R., Seth, S., Maulik, S.K. (2014). **Next generation sequencing in cardiomyopathy: towards personalized genomics and medicine.** *Molecular Biology Reports*, 3418-3419.
15. Blinkhorn, J., Achyuthan, H., Petraglia, M. D. (2015). **Ostrich expansion into India during the Late Pleistocene: Implications for continental dispersal corridors.** *Palaeogeography Palaeoclimatology Palaeoecology* 417, 80-90.
16. Bony S., Risi C. and Cimeux F. (2008). **Influence of convective processes on the isotopic composition ($\delta^{18}\text{O}$ and δD) of precipitation and water vapor in the tropics: Radiative-convective equilibrium and Tropical Ocean–Global Atmosphere–Coupled Ocean-Atmosphere Response Experiment (TOGA-COARE) simulations.** *Journal of Geophysical Research* 113, D19305.
17. Brooks, A.S., Hare, P.E., Kokis, J.E., Miller, G.H., Ernst, R.D., Wendorf, F. (1990). **Dating Pleistocene Archaeological Sites by Protein Diagenesis in Ostrich Eggshell.** *Science* 248, 60-64.
18. Bryant, J. D., & Froelich, P. N. (1995). **A model of oxygen isotope fractionation in body water of large mammals.** *Geochimica et Cosmochimica Acta* 59, 4523-4537.
19. Burk, R.L., Stuiver, M. (1981). **Oxygen isotope ratios in trees reflect mean annual temperature and humidity.** *Science* 211, 1417-1419.
20. Cann, R.L., Stoneking, M., and Wilson, A.C. (1987). **Mitochondrial DNA and human evolution.** *Nature* 325, 31-36.

21. Cao X. and Liu Y. (2011). **Equilibrium mass-dependent fractionation relationships from triple oxygen isotopes.** *Geochimica et Cosmochimica Acta* 75, 7435-7445.
22. Carrino, D.A. et al. (1996). **The avian eggshell extracellular matrix as a model for biomineralization.** *Connective Tissue Research* 35, 325-329
23. Cerling T.E. (1984). **The stable isotopic composition of modern soil carbonate and its relation to climate.** *Earth Planet Science Letters* 71, 229-240.
24. Chandrasekar, A., Kumar, S., Sreenath, J., Sarkar, B.N., Pralhad, B., Urade, Mallick, S., Bandopadhyay, S.S., Barua, P., Barik, S.S., Rao, V.R., (2009). **Updating Phylogeny of Mitochondrial DNA Macrohaplogroup M in India: Dispersal of Modern Human in South Asian Corridor.** *PloS ONE* 4, e7447.
25. Chaubey, G., Singh, M., Crivellaro, F., Tamang, R., et al. (2014). **Unravelling the distinct strains of Tharu ancestry.** *European Journal of Human Genetics* 22, 1404-1412.
26. Chauhan T, Kushwaha KPS, Chauhan V (2015). **Genetic Polymorphism of Eleven STR Loci in Rajput Population of Delhi, India.** *Forensic Research and Criminology International Journal* 1, 00031.
27. Clarke, S.J., Miller, G.H., Fogel, M.L., Chivas, A.R., Murray-Wallace, C.V. (2006). **The Amino Acid and Stable Isotope Biogeochemistry of Elephant Bird (*Aepyornis*) Eggshells from Southern Madagascar.** *Quaternary Science Reviews* 25, 2343-2356.
28. Clayton R. N. (1961). **Oxygen isotope fractionation between calcium carbonate and water.** *Journal of Chemical Physics* 34, 724-726.
29. Clayton R. N. and Mayeda T. K. (1983). **Oxygen isotopes in eucrites, shergottites, nakhlites, and chassignites.** *Earth Planet Science Letters* 62, 1-6.
30. Cooper, A. C., Lalueza-Fox, C., Anderson, S., Rambaut, A., Austin, J. and Ward, R., (2001). **Complete mitochondrial genome sequences of two extinct moas clarify ratite evolution.** *Nature* 409, 704-707.
31. Cooper, A. et al. (2001). **Complete mitochondrial genome sequences of two extinct moas clarify ratite evolution.** *Nature* 409, 704-707

32. Cooper, A., and Poinar, H.N. (2000). **Ancient DNA: do it right or not at all.** *Science* 289, 1139.
33. Cooper, R. G., Mahrose, K. M., Horbańczuk, J. O., Villegas-Vizcaino, R., Sebei, S. K., & Mohammed, A. F. (2009). **The wild ostrich (*Struthio camelus*): a review.** *Tropical animal health and production* 41, 1669-1678.
34. Coplen T. B., Kendall C. and Hopple J. (1983). **Comparison of stable isotope reference samples.** *Nature* 302, 236–238.
35. Cracraft, J. (1974). **Phylogeny and evolution of the ratite birds.** *Ibis* 116, 494-521.
36. Craig H. (1961). **Isotopic variations in meteoric waters.** *Science* 133, 1702–1703.
37. Crivellaro, F. (2001). **Human skeletal remains from R12, a Late Neolithic cemetery in the Northern Dongola Reach (Sudan): A descriptive anthropological study.** *Rivista di Archeologia*, 25, 57-66.
38. Cullity, B. D., & Weymouth, J. W. (1957). **Elements of X-ray Diffraction.** *American Journal of Physics* 25, 394-395.
39. Cusack, M., England, J., Dalbeck, P., Tudhope, A.W., Fallick, A. E., Allison, N. (2008). **Electron backscatter diffraction (EBSD) as a tool for detection of coral diagenesis.** *Coral Reefs* 27, 905-911.
40. Dawkins, R. (2004). **The ancestor's tale: a pilgrimage to the dawn of evolution.** New York: Houghton Mifflin. 688p.
41. DE Silva S, Tennekoon, K.H., Karunanayake, E.H., DE Silva W, Amarasinghe, I., Angunawela, P. (2011). **Novel sequence variants and common recurrent polymorphisms of BRCA2 in Sri Lankan breast cancer patients and a family with BRCA1 mutations.** *Experimental and Therapeutic Medicine* 2, 1163-1170.
42. Dennis K. J., Affek H. P., Passey B. H., Schrag D. P. and Eiler J. M. (2011). **Defining an absolute reference frame for ‘clumped’ isotope studies of CO₂.** *Geochimica et Cosmochimica Acta* 75, 7117–7131.
43. Der Sarkissian, C., Allentoft, M. E., Ávila-Arcos, M. C., Barnett, R., Campos, P. F., Cappellini, E., Raghavan, M., Hansen, A. J., et al. (2015). **Ancient genomics.**

Philosophical Transactions of the Royal Society of London B: Biological Sciences 370, 20130387.

44. Dettman, D. L., Fang, X., Garziona, C. N., & Li, J. (2003). **Uplift-driven climate change at 12 Ma: a long $\delta^{18}\text{O}$ record from the NE margin of the Tibetan plateau.** *Earth and Planetary Science Letters* 214, 267-277.
45. Dongmann, G., Nurnberg, H.W., Forstel, H., Wagener, K. (1974). **On the enrichment of H_2^{18}O in the leaves of transpiring plants.** *Radiation and Environmental Biophysics II*, 41-52.
46. Eckhardt, R.B., Wolpoff, M.H., and Thorne, A.G. (1993). **Multiregional evolution.** *Science* 262, 973-974.
47. Emslie, S.D., Patterson, W.P., (2007). **Abrupt Recent Shift in $\delta^{13}\text{C}$ and $\delta^{15}\text{N}$ Values in Adelie Penguin Eggshell in Antarctica.** *Proceedings of the National Academy of Sciences of the USA* 104, 11666-11669.
48. Epstein, S., & Zeiri, L. (1988). **Oxygen and carbon isotopic compositions of gases respired by humans.** *Proceedings of the National Academy of Sciences* 85, 1727-1731.
49. Farquhar, G.D., Ehleringer, J.R., Hubick, K.T. (1989). **Carbon isotope discrimination and photosynthesis.** *Annual Review of Plant Physiology and Plant Molecular Biology* 40, 503-537.
50. Felsenstein J. (1985). **Confidence limits on phylogenies: An approach using the bootstrap.** *Evolution* 39, 783-791
51. Feng, Q.L., Zhua, X., Lia, H.D., Kimb, T.N. (2001). **Crystal orientation regulation in ostrich eggshells.** *Journal of Crystal Growth* 233, 548-554.
52. Ferhi, A., Letolle, R. (1977). **Transpiration and evaporation as the principal factors in oxygen isotope variations of organic matter in land plants.** *Physiol. Veg.* 15, 363-370.
53. Fernandez, M.S., Passalacqua, K., Arias, J.I., Arias, J.L. (2004). **Partial Biomimetic Reconstitution of Avian Eggshell Formation.** *Journal of Structural Biology* 148, 1-10.

54. Fink, D. et al. (2006). **The “artificial ostrich eggshell” project: Sterilizing polymer foils for food industry and medicine.** *Solar Energy Materials & Solar Cells* 90, 1458-1470
55. Flanagan, L.B., Bain, J.F., Ehleringer, J.R., (1991). **Stable oxygen and hydrogen isotope composition of leaf water in C3 and C4 plant species under field conditions.** *Oecologia* 88, 394-400.
56. Fogel, M.L., Cifuentes, L.A. (1993). **Isotope fractionation during primary production.** In: Engel, M.H., Macko, S.A. (Eds.), *Organic Geochemistry Plenum*, New York, NY, pp. 73-98.
57. Forstel, H., (1978). **The enrichment of ^{18}O in leaf water under natural conditions.** *Radiation Environment Biophysics* 15, 323-344.
58. Fricke, H. C., Clyde, W. C., & O’Neil, J. R. (1998). **Intra-tooth variations in $\delta^{18}\text{O}$ (PO4) of mammalian tooth enamel as a record of seasonal variations in continental climate variables.** *Geochimica et Cosmochimica Acta* 62, 1839-1850.
59. Friedman, I., & O’Neil, J. R. (1977). **Compilation of stable isotope fractionation factors of geochemical interest** (Vol. 440). USGPO.
60. Fry, B. (2006). **Stable Isotope Ecology.** Springer, Los Angeles, USA.
61. Gaur, A., Chandra, S.S., Sreenivas, A., Singh, L. (2012). **DNA-based identification of a snake in a wine bottle using universal primers: A case of mistaken identity.** *Forensic Science International* 214, e51-e53.
62. Gehler, A., Tütken, T., & Pack, A. (2011). **Triple oxygen isotope analysis of bioapatite as tracer for diagenetic alteration of bones and teeth.** *Palaeogeography Palaeoclimatology Palaeoecology* 310, 84-91.
63. Gerstenberger, J., Hummel, S., Schultes, T., Hack, B., and Herrmann, B. (1999). **Reconstruction of a historical genealogy by means of STR analysis and Y-haplotyping of ancient DNA.** *European journal of human genetics: EJHG* 7, 469-477.

64. Grossman E.L. (2012). **Applying oxygen isotope paleothermometry in deep time. In *Reconstructing Earth's Deep-Time Climate***. (eds. L. Ivany and B. Huber) *The Paleontological Society Papers* 18, 39–67.
65. Haak, W. et al. (2010). **Ancient DNA from European early neolithic farmers reveals their near eastern affinities.** *PLoS Biology* 8,e1000536.
66. Hadly, E.A., Kohn, M.H., Leonard, J.A., and Wayne, R.K. (1998). **A genetic record of population isolation in pocket gophers during Holocene climatic change.** *Proceedings of National Academy of Sciences USA* 95, 6893-6896.
67. Hagelberg, E., Sykes, B., and Hedges, R. (1989). **Ancient bone DNA amplified.** *Nature* 342, 485.
68. Haile, J., Holdaway, R., Oliver, K., Bunce, M., Gilbert, M.T., Nielsen, R., Munch, K., Ho, S.Y., Shapiro, B., and Willerslev, E. (2007). **Ancient DNA chronology within sediment deposits: are paleobiological reconstructions possible and is DNA leaching a factor?** *Molecular biology and evolution* 24, 982-989.
69. Handt, O., Hoss, M., Krings, M., and Paabo, S. (1994). **Ancient DNA: methodological challenges.** *Experientia* 50, 524-529.
70. Harper, D., 2001. Ostrich. Online Entomology Dictionary. Accessed on: 29th September 2008. Available at: <http://www.etmonline.com/index>.
71. Harris, J.M., Leakey, M.G (2003). **The Dawn of Humanity in Eastern Africa** (161-166). Columbia University Press.
72. Henkes G. A., Passey B. H., Grossman E. L., Shenton B. J., Perez- Huerta A. and Yancey T. E. (2014). **Temperature limits for the preservation of primary calcite clumped isotope paleotemperatures.** *Geochimica et Cosmochimica Acta* 139, 362–382.
73. Henkes G.A., Passey B.H., Wanamaker Jr. A.D., Grossman E.L., Ambrose Jr. W.G., Carroll M.L. (2013). **Carbonate clumped isotope compositions of modern marine mollusk and brachiopod shells.** *Geochimica et Cosmochimica Acta* 106, 307–325.

74. Higham, T. (1994). **Radiocarbon Dating New Zealand Prehistory with Moa Eggshell: Some Preliminary Results.** *Quaternary Science Reviews* 13, 163-169.
75. Higuchi, R., Bowman, B., Freiberger, M., Ryder, O.A., and Wilson, A.C. (1984). **DNA sequences from the quagga, an extinct member of the horse family.** *Nature* 312, 282-284.
76. Hincke, M.T. et al. (2000). **Identification and localization of lysozyme as a component of the eggshell membranes and shell matrix.** *Material Biology* 19, 443-453.
77. Hoag K. J., Still C. J., Fung I. Y. and Boering K. A. (2005). **Triple oxygen isotope composition of tropospheric carbon dioxide as a tracer of terrestrial gross carbon fluxes.** *Geophysics Residual Letters* 32, L02802.
78. Hofmann, M. E., Horváth, B., & Pack, A. (2012). **Triple oxygen isotope equilibrium fractionation between carbon dioxide and water.** *Earth and Planetary Science Letters* 319, 159-164.
79. Hofreiter, M., Serre, D., Poinar, H.N., Kuch, M., and Paabo, S. (2001). **Ancient DNA.** *Nature reviews Genetics* 2, 353-359.
80. Hoss, M., Jaruga, P., Zastawny, T.H., Dizdaroglu, M., and Paabo, S. (1996). **DNA damage and DNA sequence retrieval from ancient tissues.** *Nucleic Acids Research* 24, 1304-1307.
81. Howell, N., Chinnery, P.F., Ghosh, S.S., Fahy, E., and Turnbull, D.M. (2000). **Transmission of the human mitochondrial genome.** *Human Reproduction Supplements* 2, 235-245.
82. Huntington K. W., Eiler J. M., Affek H. P., Guo W., Bonifacie M., Yeung L. Y., Thiagarajan N., Passey B. H., Tripathi A., DaeÅNron M. and Came R. (2009). **Methods and limitations of 'clumped' CO₂ isotope (D₄₇) analysis by gas-source isotope ratio mass spectrometry.** *Journal of Mass Spectrometry* 44, 1318–1329.
83. Huoponen, K., Schurr, T.G., Chen, Y., and Wallace, D.C. (2001). **Mitochondrial DNA variation in an aboriginal Australian population: evidence for genetic isolation and regional differentiation.** *Human immunology* 62, 954-969.

84. Ingman, M., Kaessmann, H., Paabo, S., and Gyllensten, U. (2000). **Mitochondrial genome variation and the origin of modern humans.** *Nature* 408, 708-713.
85. Jobling, M.A., and Tyler-Smith, C. (1995). **Fathers and sons: the Y chromosome and human evolution.** *Trends in genetic* 11, 449-456.
86. Jobling, M.A., and Tyler-Smith, C. (2003). **The human Y chromosome: an evolutionary marker comes of age.** *Nature reviews Genetics* 4, 598-612.
87. Johnson B. J., Miller G. H., Beaumont P. B., and Fogel M. L. (1997). **The determination of late Quaternary paleoenvironments at Equus Cave, South Africa, using stable isotopes and amino acid racemization in ostrich eggshell.** *Palaeogeogr. Palaeoclimatol. Palaeoecol.* 136,121–137.
88. Johnson, B.J. (1995). **The stable isotope biogeochemistry of ostrich eggshell and its application to late Quaternary paleoenvironmental reconstructions in South Africa.** Ph.D., Dissert. Univ. Colorado, Boulder, CO, 229 pp.
89. Johnson, B.J., Miller, G.H., Fogel, M.L., Beaumont, P.B. (1997). **The determination of the late Quaternary paleo- environments at Equus Cave, South Africa, using stable isotopes and amino acid racemization in ostrich eggshell.** *Palaeogeography Palaeoclimatology Palaeoecology* 136, 121-137
90. Johnson, B.J., Fogel, M.L., Miller, G.H. (1998). **Stable isotopes in modern ostrich eggshell: A calibration for paleoenvironmental applications in Semi-Arid Regions of Southern Africa.** *Geochimica et Cosmochimica Acta* 62, 2451-2461.
91. Jonnalagadda, M., Shantanu O., and Mushrif-Tripathy, V. (2011). **Population affinities of Parsis in the Indian subcontinent.** *International Journal of Osteoarchaeology* 21,103-110.
92. Juras, A., Mirosława, D., Alena, K., Helena, M., Raghavan, M., Kosicki, J.Z., Metspalu, E., Eske Willerslev, E., Janusz, P. (2014). **Ancient DNA reveals matrilineal continuity in present-day Poland over the last two millennia.** *Plos one*, e110839.
93. Knauth L. P. and Epstein S. (1976). **Hydrogen and oxygen isotope ratios in nodular and bedded cherts.** *Geochimica et Cosmochimica Acta* 40, 1095-1108.

94. Koch, P.L. (2008). **Isotopic Study of Viology of Modern and Fossil Vertebrates**, in: **Michener, R.H., Lajtha, K.** (Eds.), *Stable Isotopes in Ecology and Environmental Science, 2nd ed.*, Wiley-Blackwell, Chichester, UK, pp. 99-154.
95. Koch, P.L., Fogel, M.L., Tuross, N. (1994). **Tracing the diets of fossil animals using stable isotopes.** In: Lajtha, K., Michener, R.H. (Eds.), *Stable Isotopes in Ecology and Environmental*.
96. Kohn M. J. (1996). **Predicting animal $\delta^{18}\text{O}$: Accounting for diet and physiological adaptation.** *Geochimica et Cosmochimica Acta* 60, 4811-4829.
97. Krings, M., Geisert, H., Schmitz, R.W., Krainitzki, H., and Paabo, S. (1999). **DNA sequence of the mitochondrial hypervariable region II from the neandertal type specimen.** *Proceedings of the National Academy of Sciences of the United States of America* 96, 5581-5585.
98. Kumar, G., Narvare, G., Pancholi, R. (1988). **Engraved ostrich eggshell objects: New evidence of Upper Paleolithic art in India.** *Rock Art Research* 5, 98843-98853.
99. Kumar, G., Sahni, A., Narvare, G. and Pancholi, R. (1990). **Archaeological discoveries and a study of Late Pleistocene ostrich eggshell and eggshell objects in India.** *Man and Environment* 15, 30-40.
100. Kumar, S., Rajasekhara, R., Padmaja, K., Urade, B.P., Biswanath, S., Chandrasekar, A., Rao, V.R. (2009). **Reconstructing Indian-Australian Phylogenetic link.** *BMC Evolutionary Biology*, 9,193.
101. Kumar, S.S., Gaur, A., Shivaji, S. (2011). **Phylogenetic studies in Indian scleractinian corals based on mitochondrial cytochrome b gene sequences.** *Current Science* 101, 5.
102. Kumar. G. (1983). **Chronology: Upper Palaeolithic Culture.** *Archaeology of northwestern Malwa* (Ph.D. Thesis), 227-229. Ujjain: Vikram University.
103. Kusakabe, M. and Matsuhisa Y. (2008). **Oxygen three-isotope ratios of silicate reference materials determined by direct comparison with VSMOW-oxygen.** *Geochemical Journal* 42, 309-317.

104. Kushwaha, K.P.S. Gaur, J.R. Goyal M.K. & Rao, M.B. (1983). **Identification of Seminal & Vaginal acid phosphates using Iso-Electric focusing technique.** Paper presented in the *Annual Conference of Indian Academy of Forensic Sciences* held in November.
105. Kushwaha, K.P.S. Sangwan, S.K. Thukral, K. & Gaur, J.R. (1986). **Detection of ABO blood group factors in putrefied liquid blood in samples-A 20 months study.** Paper presented in the *Scientific meeting of Indian Academy of Forensic Sciences* held at Patiala
106. Lahr, M.M., Robert F., Simon, A., Huw, B., Crivellaro, F., Drake, N., et al. (2008). **DMP III: Pleistocene and Holocene palaeoenvironments and prehistoric occupation of Fazzan, Libyan Sahara.** *Libyan Studies*, 39, 263-294.
107. Landais A., Barkan E. and Luz B. (2008). **Record of $\delta^{18}\text{O}$ and ^{17}O -excess in ice from Vostok Antarctica during the last 150,000 years.** *Geophysics Research Letters* 35, L02709.
108. Landais A., Barkan E., Yakir D. and Luz B. (2006). **The triple isotopic composition of oxygen in leaf water.** *Geochimica et Cosmochimica Acta* 70, 4105-4115.
109. Landais A., Ekaykin A., Barkan E., Winkler R. and Luz B. (2012a). **Seasonal variations of d-excess and ^{17}O -excess in snow at the Vostok station (East Antarctica).** *Journal of Glaciology* 58, 725-733.
110. Landais A., Steen-Larsen H. C., Guillevic M., Masson-Delmotte V., Vinther B. and Winkler R. (2012b). **Triple isotopic composition of oxygen in surface snow and water vapor at NEEM (Greenland).** *Geochimica et cosmochimica acta* 77, 304-316.
111. Landais, A., Barkan, E., Yakir, D., & Luz, B. (2006). **The triple isotopic composition of oxygen in leaf water.** *Geochimica et cosmochimica acta* 70, 4105-4115.
112. Lee, K., Feinstein, J. and Cracraft, J. (1997). **The phylogeny of ratite birds: resolving conflicts between molecular and morphological data sets.** In *Avian Molecular Evolution and Systematics* (ed. Mindell, D.), Yale University Press, New Haven, pp. 173-208.

113. Levin N. E., Raub T.D., Dauphas N., Eiler J. M. (2014). **Triple oxygen isotope variations in sedimentary rocks.** *Geochimica et cosmochimica acta* 139, 173-189.
114. Levin, N. E., Cerling, T. E., Passey, B. H., Harris, J. M., & Ehleringer, J. R. (2006). **A stable isotope aridity index for terrestrial environments.** *Proceedings of the National Academy of Sciences* 103, 11201-11205.
115. Llamas, B., Holland, M.L., Chen, K., Cropley, J.E., Cooper, A., and Suter, C.M. (2012). **High-resolution analysis of cytosine methylation in ancient DNA.** *PloS one* 7, e30226.
116. Longinelli, A. (1984). **Oxygen isotopes in mammal bone phosphate: a new tool for paleohydrological and paleoclimatological research.** *Geochimica et Cosmochimica Acta* 48, 385-390.
117. Luz B. and Barkan E. (2010). **Variations of $^{17}\text{O}/^{16}\text{O}$ and $^{18}\text{O}/^{16}\text{O}$ in meteoric waters.** *Geochimica et cosmochimica acta* 74, 6276-6286.
118. Luz B., Barkan E., Bender M. L., Thiemens M. H. and Boering K. A. (1999). **Triple isotope composition of atmospheric oxygen as a tracer of biosphere productivity.** *Nature* 400, 547-550.
119. Luz, B., & Kolodny, Y. (1985). **Oxygen isotope variations in phosphate of biogenic apatites, IV. Mammal teeth and bones.** *Earth and Planetary Science Letters* 75, 29-36.
120. Luz, B., Cormie, A. B., & Schwarcz, H. P. (1990). **Oxygen isotope variations in phosphate of deer bones.** *Geochimica et Cosmochimica Acta* 54, 1723-1728.
121. Magee, J.W., Miller, G.H., Spooner, N.A., Questiaux, D.G., McCulloch, M.T., Clark, P.A. (2008). **Evaluating Quaternary Dating Methods: Radiocarbon, U-Series, Luminescence and Amino Acid Racemisation Dates of a Late Pleistocene Emu Egg.** *Quaternary Geochronology* 4, 84-92.
122. Majoube, M. (1971). **Fractionnement en oxygene-18 et en deuterium entrel'eau et sa vapeur.** *Journal of Chemical Physics* 58, 1423-1436.

123. Marshall, J.D., Brooks, J.R., Lajtha, K. (2008). **Sources of Variation in the Stable Isotopic Composition of Plants**, in: Michener, R.H., Lajtha, K. (Eds.), *Stable Isotopes in Ecology and Environmental Science*, 2nd ed., Wiley-Blackwell, Chichester, UK, pp. 22-60.
124. Matsuhisa Y., Goldsmith J. R. and Clayton R. N. (1978) **Mechanisms of hydrothermal crystallization of quartz at 250°C and 15 kbar.** *Geochimica et cosmochimica acta* 42, 173-182.
125. McCarroll D. and Loader N. J. (2004). **Stable isotopes in tree rings.** *Quaternary Science Reviews* 24, 771-801.
126. McCrea J. M. (1950). **On the isotopic chemistry of carbonates and a paleotemperature scale.** *Journal of Chemical Physics* 18, 849–857.
127. Meijer, H. A. J., & Li, W. J. (1998). **The use of electrolysis for accurate $\delta^{17}\text{O}$ and $\delta^{18}\text{O}$ isotope measurements in water.** *Isotopes in Environmental and Health Studies* 34, 349-369.
128. Mellars, P. (2006). **Why did modern human populations disperse from Africa ca. 60,000 years ago? A new model.** *Proceedings of National Academy of Sciences USA* 103, 9381-9386
129. Miller, G.H., Beaumont, P.B., Deacon, H.J., Brooks, A.S., Hare, P.E., Jull, A.J.T., (1999a). **Earliest Modern Humans in Southern Africa Dated by Isoleucine Epimerization in Ostrich Eggshell.** *Quaternary Science Review* 18, 1537-1548.
130. Miller, G.H., Beaumont, P.B., Jull, A.J.T., Johnson, B. (1992). **Pleistocene Geochronology and Palaeothermometry from Protein Diagenesis in Ostrich Eggshells: Implications for the Evolution of Modern Humans.** *Philosophical Transactions of the Royal Society B* 337, 149-157.
131. Miller, G.H., Fogel, M.L., Magee, J.W., Gagan, M.K., Clarke, S.J., Johnson, B.J., (2005). **Ecosystem Collapse in Pleistocene Australia and a Human Role in Megafauna Extinction.** *Science* 309, 287-290.
132. Miller, G.H., Hart, C.P., Roark, E.B., Johnson, B.J. (2000). **Isoleucine epimerization in eggshells of the flightless Australian birds, Genyornis and Dromaius.** In

- Perspectives in amino acid and protein geochemistry ed. [161-181] [Goodfriend GA, Collins MJ, Fogel ML, Macko SA, Wehmiller JF, Oxford, MA] (Oxford University)
133. Miller, G.H., Magee, J.W., Johnson, B.J., Fogel, M.L., Spooner, N.A., McCulloch, M.T., Ayliffe, L.K. (1999b). **Pleistocene Extinction of *Genyornis newtoni*: Human Impact on Australian Megafauna.** *Science* 283, 205-208.
134. Miller, M. F. (2002). **Isotopic fractionation and the quantification of $\delta^{17}O$ anomalies in the oxygen three-isotope system: an appraisal and geochemical significance.** *Geochimica et Cosmochimica Acta* 66, 1881-1889.
135. Misra, V. N. (2001). **Prehistoric human colonization of India.** *Journal of Biosciences* 26, 491-531.
136. Mohabey, D.M. (1989). **Avian Egg Shells from Pleistocene of Kachchh.** *Journal of Geological Society of India* 33, 477-481.
137. Mullis, K.B., and Faloona, F.A. (1987). **Specific synthesis of DNA in vitro via a polymerase-catalyzed chain reaction.** *Methods in Enzymology* 155, 335-350.
138. Muruganathan, A., Karunanayake, E.H., Tennekoon, K.H. (2010). **Cloning and Characterisation of Alkali myosin light chain gene (MLC-3) of cattle filarial parasite *setaria digitata*.** *The IIOAB Journal* 1, 1-10.
139. Mushrif-Tripathy, V. (2014). **Maxillary Sinusitis from India: A Bio-cultural Approach.** *Korean Journal of Physical Anthropology* 27,11-28.
140. Mushrif-Tripathy, V., Ajithprasad, P., Madellal, M., Mateos, J.L., Rajesh, S.V., Rondelli, B., Saiz, J.C., Lancelotti, C., Gadekar, C., Granero, J.G. (2014). **Osteological Study of a Human Skeleton Excavated from Vaharvo Timbo, District Patan, Gujarat.** *Man and Environment XXXIX* 1, 45-51.
141. Nagy K. A. and Peterson C. C. (1988). **Scaling of water flux rate in animals.** *University of California Publications in Zoology* 120, 1-172.
142. Navidi, W., Arnheim, N., and Waterman, M.S. (1992). **A multiple-tubes approach for accurate genotyping of very small DNA samples by using PCR: statistical considerations.** *American Journal of Human Genetics* 50, 347-359.

143. Newsome, S.D., del Rio, C.M., Bearhop, S., Phillips, D.L. (2007). **A Niche for Isotopic Ecology.** *Frontiers in Ecology and the Environment* 5, 429-436.
144. Nys, Y., Gautron, J., Garcia-Ruiz, J.M., Hincke, M. **Avian eggshell mineralization: biochemical and functional characterization of matrix proteins.** *Comptes Rendus Palevol* 3, 549-562 (2004).
145. O'Neil, J. R., & Adami, L. H. (1969). **Oxygen isotope partition function ratio of water and the structure of liquid water.** *The Journal of Physical Chemistry* 73, 1553-1558.
146. Orlando, L., Bonjean, D., Bocherens, H., Thenot, A., Argant, A., Otte, M., and Hanni, C. (2002). **Ancient DNA and the population genetics of cave bears (*Ursus spelaeus*) through space and time.** *Molecular Biology and Evolution* 19, 1920-1933.
147. Oskam, C.L. et al. (2010). **Fossil avian eggshell preserves ancient DNA.** *Proceedings of Royal Society B.* 277, 1991-2000.
148. Oskam, C.L., Bunce, M. (2012). **DNA Extraction from Fossil Eggshell**, in: [Shapiro B, Hofreiter M. (Eds.)] [65-70] *Ancient DNA: Methods and Protocols*, Humana Press.
149. Ostrom, P.H., Fry, B. (1993). **Sources and cycling of organic matter within modern and prehistoric food webs.** In: Engel, M.H., Mackom, S.A. (Eds.). *Organic Geochemistry: Principles and Applications*, Plenum, New York, NY, pp. 785-798
150. Paabo, S. (1985). **Molecular cloning of Ancient Egyptian mummy DNA.** *Nature* 314, 644-645.
151. Paabo, S. (1989). **Ancient DNA: extraction, characterization, molecular cloning, and enzymatic amplification.** *Proceedings of National Academy of Sciences USA* 86, 1939-1943.
152. Paabo, S. et al. (2004). **Genetic analyses from ancient DNA.** *Annual Review of Genetics* 38, 645-679
153. Pack A. and Herwartz D. (2014). **The triple oxygen isotope composition of the Earth mantle and understanding $\Delta^{17}\text{O}$ variations in terrestrial rocks and minerals.** *Earth and Planetary Science Letters* 390, 138-145.

154. Pack, A., Gehler, A., & Süssenberger, A. (2013). **Exploring the usability of isotopically anomalous oxygen in bones and teeth as paleo-CO₂-barometer.** *Geochimica et Cosmochimica Acta* 102, 306-317.
155. Passey B. H., Hu H., Ji H. Montanari S., Li S, Henkes G. A., Levin N. E. (2014) **Triple oxygen isotopes in biogenic and sedimentary carbonates.** *Geochimica et Cosmochimica Acta* 141, 1-25.
156. Passey B. H., Levin N. E., Cerling T. E., Brown F. H. and Eiler J.M. (2010) **High-temperature environments of human evolution in East Africa based on bond ordering in paleosol carbonates.** *Proceedings of National Academy of Science USA* 107, 11245–11249.
157. Patnaik, R., Sahni. A., Cameron. D., Pillans. D., Chatrath. P., Simons. E., Williams. M., Bibi. F. (2009). **Ostrich-like eggshells from a 10.1 million-yr-old Miocene ape locality, Haritalyangar, Himachal Pradesh, India.** *Current Science* 96, 1485-1495.
158. Patrinos, G.P., Smith, T.D., Howard, H., AlMulla, F., Chouchane, L., Hadjisavvas, A., Hamed, S.A., Li, X.T., Marafie, M., Ramesar, R.S. and Ramos, F.J., Shrestha, T.R. (2012). **Human variome project country nodes: Documenting genetic information within a country.** *Human mutation*, 33, 1513-1519.
159. Pérez-Huerta, A., Cusack, M. (2009). **Optimising electron backscatter diffraction (EBSD) of carbonate biominerals—resin type and carbon thickness.** *Microscopy and Microanalysis* 15, 197-203.
160. Pérez-Huerta, A., Dauphin, Y., Cuif, J. P., & Cusack, M. (2011). **High resolution electron backscatter diffraction (EBSD) data from calcite biominerals in recent gastropod shells.** *Micron* 42, 246-251.
161. Pickford, M., Senut, B. (2000). **Geology and paleobiology of the central and southern Namib Desert, southwestern Africa.** *Geological Survey of Namibia* 18, 1-155
162. Prakash, S., Mishra, A., Shrestha, T.R., Awasthi, N., Pradhan, I., Dewangan, H., Mishra, A., Manandhar, K.D. (2015). **Evolutionary perspective of Indian subcontinent Populations.**

163. Raghavan, M., Skoglund, P., Graf, K.E., Metspalu, M., Albrechtsen, A., Moltke, I., Rasmussen, S., Stafford Jr, T.W., Orlando, L., Metspalu, E. and Karmin, M. (2014). **Upper Palaeolithic Siberian genome reveals dual ancestry of Native Americans.** *Nature* 505, 87- 91.
164. Raghavan, M., Steinrücken, M., Harris, K., Schiffels, S., Rasmussen, S., DeGiorgio, M., Albrechtsen, A., Valdiosera, C., Ávila-Arcos, M.C., Malaspinas, A.S. and Eriksson, A. (2015). **Genomic evidence for the Pleistocene and recent population history of Native Americans.** *Science* 349, 3884.
165. Rai, N. et al. (2014). **Relic excavated in western India is probably of Georgian Queen Ketevan.** *Mitochondrion* 14, 1-6
166. Rao, M.B., Kushwaha, K.P.S. & Gaur, J.R. (1981). **Examination of species of origin, sex & age from the fragments of burn bones.** Paper presented in the *Bienial Conference of Forensic Science* held at Jaipur.
167. Rao, M.B. Goyal, M.K. Kushwaha, K.P.S. Gaur, J.R. (1984). **Experimental study on the development states of maggots for the estimation of time since death.** Papers presented in the *International meeting of Forensic Science at United Kingdom* in August.
168. Rasmussen, M., Li, Y., Lindgreen, S., Pedersen, J.S., Albrechtsen, A., Moltke, I., Metspalu, M., Metspalu, E., Kivisild, T., Gupta, R., Bertalan, M., Nielsen, K., Gilbert, M.T., Wang, Y., Raghavan, M., Campos, P.F., Kamp, H.M., Wilson, A.S., Gledhill, A., Tridico, S., Bunce, M., Lorenzen, E.D., Binladen, J., Guo, X., Zhao, J., Zhang, X., Zhang, H., Li, Z., Chen, M., Orlando, L., Kristiansen, K., Bak, M., Tommerup, N., Bendixen, C., Pierre, T.L., Gronnow, B., Meldgaard, M., Andreasen, C., Fedorova, S.A., Osipova, L.P., Higham, T.F., Ramsey, C.B., Hansen, T.V., Nielsen, F.C., Crawford, M.H., Brunak, S., Sicheritz-Ponten, T., Villems, R., Nielsen, R., Krogh, A., Wang, J., and Willerslev, E. (2010). **Ancient human genome sequence of an extinct Palaeo-Eskimo.** *Nature* 463, 757-762.
169. Richards, P.D.G., Richards, P.A., Lee, M.E. (2000). **Ultrastructural characteristics of ostrich eggshell: outershell membrane and the calcified layers.** *Journal of South African Veterinary Association* 71, 97-102.

170. Roberts, P. et al. (2014). **Continuity of mammalian fauna over the last 200,000 y in the Indian subcontinent.** *Proceedings of National Academy of Sciences USA* 111, 5848-5853.
171. Roden, J. S., & Ehleringer, J. R. (1999). **Observations of hydrogen and oxygen isotopes in leaf water confirm the Craig-Gordon model under wide-ranging environmental conditions.** *Plant physiology* 120, 1165-1174.
172. Rondelli, B., Lancelotti, C., Madella, M., Pecci, A., Balbo, A., Perez, J.R., Inserra, F., C. Gadekar, C., Ontiveros M.A.C., Ajithprasad, P. (2014). **Anthropic activity markers and spatial variability: an ethnoarchaeological experiment in a domestic unit of Northern Gujarat (India).** *Journal of Archaeological Science* 41,482-492.
173. Rumble D., Miller M. F., Franchi I. A. and Greenwood R. C. (2007). **Oxygen three isotope fractionation lines in terrestrial silicate minerals: An inter-laboratory comparison of hydrothermal quartz and eclogitic garnet.** *Geochimica et Cosmochimica Acta* 71, 3592-3600.
174. Sahni, A., Kumar, G., Bajpai, S., Srinivasan, S. (1989). **A review of Late Pleistocene ostriches (Struthio sp.) in India.** *Man and Environment* 25, 41-47.
175. Sahni, A., Kumar. G., Bajpai. S., Srinivasan. S. (1990). **Ultrastructure and taxonomy of ostrich eggshells from Upper Palaeolithic sites of India.** *Journal of Paleontological Society of India* 34, 91-98.
176. Saitou N., Nei M. (1987). **The neighbor-joining method: A new method for reconstructing phylogenetic trees.** *Molecular Biology and Evolution* 4, 406-425.
177. Sauer, E.F.G., Sauer, E.M. (1978). **Ratite eggshell fragments from Mio-Pliocene continental sediments in the district of Ouarzazate, Morocco.** *Palaeontology* 161, 1-54.
178. Schoenemann S. W., Schauer A. J. and Steig E. J. (2013). **Measurement of SLAP2 and GISP d17O and proposed VSMOW-SLAP normalization for d17O and 17Oexcess.** *Rapid Communications in Mass Spectrometry* 27, 582–590.
179. Schoenemann S. W., Steig E. J., Ding Q., Markle B. R. and Schauer A. J. (2014) **Triple water-isotopologue record from WAIS Divide, Antarctica: controls on**

- glacial-interglacial changes in ^{17}O excess of precipitation.** *Journal of Geophysical Research: Atmospheres* 119, 8741-8763.
180. Sibley, C. G. and Ahlquist, J. E. (1990a). **Phylogeny and Classification of Birds.** A Study in Molecular Evolution, Yale University Press, New Haven, pp. 976.
181. Sibley, C. G. and Ahlquist, J. E. (1990b). **The phylogeny and relationships of the ratite bird as indicated by DNA/DNA hybridization.** In *Evolution Today* (eds Scudder, G. C. E. and Reveal, J. L.), Hunt Institute for Botanical Documentation, Carnegie Mellon University, Pittsburgh, pp. 301-335.
182. Singh, A., Gaur, A., Shailaja, K., Satyare B.B., Singh, L. (2004). **A novel microsatellite (STR) marker for forensic identification of big cats in India.** *Forensic Science International* 141, 143-147.
183. Singh, C.S., Gaur, A., Sreenivas, A., Singh, L. (2012). **Species Identification from Dried Snake Venom.** *Journal of Forensic Sciences* 57, 826-828.
184. Singh, U. (2008). **A History of Ancient and Early medieval India: from the Stone Age to the 12th century.** Pearson Education India.
185. Sirocko, F., Seelos, K., Schaber, K., Rein, B., Dreher, F., Diehl, M. & Degering, D. (2005). **A late Eemian aridity pulse in central Europe during the last glacial inception.** *Nature* 436, 833-836.
186. Smith, C.I., Chamberlain, A.T., Riley, M.S., Cooper, A., Stringer, C.B., and Collins, M.J. (2001). **Neanderthal DNA. Not just old but old and cold?** *Nature* 410, 771-772.
187. Stern, L. A., Johnson, G. D., & Chamberlain, C. P. (1994). **Carbon isotope signature of environmental change found in fossil ratite eggshells from a South Asian Neogene sequence.** *Geology* 22, 419-422.
188. Stidham, T.A. **Extinct ostrich eggshell (Aves: Struthionidae) from the Pliocene Chiwondo Beds, Malawi: implications for the potential biostratigraphic correlation of African Neogene deposits** Laboratory for Human Evolutionary Studies, Museum of Vertebrate Zoology, and Museum of Paleontology, University of California, Berkeley, CA 94720, USA. *Journal of Human Evolution* 46, 489-496 (2004).

189. Tamura K., Nei M., and Kumar S. (2004). **Prospects for inferring very large phylogenies by using the neighbor-joining method.** *Proceedings of National Academics of Sciences USA* 101, 11030-11035
190. Tamura K., Stecher G., Peterson D., Filipski A., Kumar S. (2013). **MEGA6: Molecular Evolutionary Genetics Analysis version 6.0.** *Molecular Biology of Evolution* 30, 2725-2729.
191. Tennekoon, K.H., Indika, W.L., Sugathadasa, R., Karunanayake, E.H., Kumarasiri, J., Wijesundera, A. (2012). **LEPR c.668A>G polymorphism in a cohort of Sri Lankan women with pre-eclampsia/pregnancy induced hypertension: a case control study.** *BMC Research Notes*, 12, 25.
192. Thangaraj, K., Gyaneshwar, C., Thomas, K., Reddy, A.G., Singh, V., Rasalkar, A., Singh, L., (2005). **Reconstructing the origin of Andaman Islanders.** *Science* 308, 996.
193. Thangaraj, K., Gyaneshwar, C., Thomas, K., Reddy, A.G., Singh, V., Rasalkar, A., Singh, L., (2006). **Response to Comment on reconstructing the origin of Andaman Islanders.** *Science* 311, 470.
194. Thangaraj, K., Singh, L., Reddy, A.G., Rao, V.R., Sehgal, S.C., Underhill, P.A., Pierson, M., Frame I.G., Hagelberg E., (2003). **Genetic Affinities of the Andaman Islanders, a Vanishing Human Population.** *Current Biology* 13, 86-93.
195. Thanseem. I., Thangaraj. K., Chaubey, G., Singh, V.K., Bhaskar, L.V.K.S., Reddy, B.M., Reddy, A.G., Singh, L. (2006). **Genetic Affinities Among the Lower Castes and Tribal Groups of India: Inference from Y Chromosome and Mitochondrial DNA.** *BMC Genetics* 42, 148.
196. Thiemens M. H., Jackson T., Zipf E. C., Erdman P. W. and van Egmond C. (1995). **Carbon dioxide and oxygen isotope anomalies in the Mesosphere and Stratosphere.** *Science* 270, 5238.
197. Thiemens, M. H., & Heidenreich, J. E. (1983). **The mass-independent fractionation of oxygen: A novel isotope effect and its possible cosmochemical implications.** *Science* 219,1073-1075.

198. Thomas, M.G., Skorecki, K., Ben-Ami, H., Parfitt, T., Bradman, N., and Goldstein, D.B. (1998). **Origins of Old Testament priests.** *Nature* 394, 138-140.
199. Tiwari, S. K. (2000). **Riddles of Indian rockshelter paintings.** Sarup & Sons. 229-238
200. Torroni, A., Huoponen, K., Francalacci, P., Petrozzi, M., Morelli, L., Scozzari, R., Obinu, D., Savontaus, M.L., and Wallace, D.C. (1996). **Classification of European mtDNAs from an analysis of three European populations.** *Genetics* 144, 1835-1850.
201. Trimby, P., Grellet-Tinner. (2011). **The Hidden Secrets of Dinosaur Eggs Revealed Using Analytical Scanning Electron Microscopy.** *Infocus* 24, 5-21.
202. Urey H. C., Lowenstam H. A., Epstein S., and McKinney C. R. (1951). **Measurement of paleotemperatures and temperatures of the Upper Cretaceous of England, Denmark, and the southeastern United States.** *Geological Society of America Bulletin* 62, 399-416.
203. Vernesi, C., Caramelli, D., Dupanloup, I., Bertorelle, G., Lari, M., Cappellini, E., Moggi-Cecchi, J., Chiarelli, B., Castri, L., Casoli, A., Mallegni, F., Lalueza-Fox, C., and Barbujani, G. (2004). **The Etruscans: a population-genetic study.** *American Journal of Human Genetics* 74, 694-704.
204. Vigilant, L., Stoneking, M., Harpending, H., Hawkes, K., and Wilson, A.C. (1991). **African populations and the evolution of human mitochondrial DNA.** *Science* 253, 1503-1507.
205. von Schirnding, Y., van der Merwe, N.J., Vogel, J.C. (1982). **Influence of Diet and Age on Carbon Isotope Ratios in Ostrich Eggshell.** *Archaeometry* 24, 3-20.
206. Wakankar, V.S. (1984). **Bhimbetka and dating of Indian rock paintings, in Rock Art of India** (K.K. Chakravarti, ed.), 44-46. Arnold Heinemann. New Delhi
207. Wellman-Labadie, O., Lakshminarayanan, R., Hincke, M.T. (2008a). **Antimicrobial properties of avian eggshell- specific C-type lectin-like proteins.** *FEBS Letters* 582, 699-704.

208. Wellman Labadie, O., Picman, J., Hincke, M. (2008b). **Anti- microbial activity of cuticle and outer eggshell protein extracts from three species of domestic birds.** *British Poultry Science* 49, 133-143
209. Wickramasinghe L.J.M., Bandara, I.N., Vidanapathirana, D.R., Tennakoon, K.H., Samarakoon, S.R., Wickramasinghe, N. (2015). **Pseudophilautus dilmah, a new species of shrub frog (Amphibia: Anura: Rhacophoridae) from a threatened habitat Lookandura in Sri Lanka.** *Journal of Threatened Taxa* 5, 7089-71.10.
210. Winkler R., Landais, A., Sodemann H., Dümbgen L., Prié F., Masson-Delmotte V., Stenni B. and Jouzel J. (2012). **Deglaciation records of $\delta^{17}O$ -excess in East Antarctica: reliable reconstruction of oceanic normalized relative humidity from coastal sites.** *Climate of the Past* 8, 1-16.
211. Young E. D., Galy A. and Nagahara H. (2002). **Kinetic and equilibrium mass-dependent isotope fractionation laws in nature and their geochemical and cosmochemical significance.** *Geochimica et Cosmochimica Acta* 66, 1095–1104.
212. Young, E. D., Yeung, L. Y., & Kohl, I. E. (2014). **On the $\delta^{17}O$ budget of atmospheric O_2 .** *Geochimica et Cosmochimica Acta* 135, 102-125.
213. Yung, Y. L., Lee, A. Y., Irion, F. W., DeMore, W. B., & Wen, J. (1997). **Carbon dioxide in the atmosphere: Isotopic exchange with ozone and its use as a tracer in the middle atmosphere.** *Journal of Geophysical Research: Atmospheres (1984–2012)*, 102(D9), 10857-10866.